Lawrence Berkeley National Laboratory

Lawrence Berkeley National Laboratory

Title

Indoor Measurements of Environmental Tobacco Smoke Final Report to the Tobacco Related Disease Research Program

Permalink

https://escholarship.org/uc/item/9sp2m2bq

Authors

Apte, Michael G.
Gundel, Lara A.
Dod, Raymond L.
et al.

Publication Date

2004-03-02

eScholarship.org Powered by the California Digital Library
University of California

LBNL-49148

Indoor Measurements of Environmental Tobacco Smoke

Final Report to the Tobacco Related Disease Research Program

Michael G. Apte, Lara A. Gundel, Raymond L. Dod, Marion L. Russell, Brett C. Singer, Michael D. Sohn, Douglas P. Sullivan, Gee-Minn Chang[1], and Richard G. Sextro

March 24, 2004

Lawrence Berkeley National Laboratory, 1 Cyclotron Rd., Berkeley CA, 94720

[1]University of California, Berkeley, 94720

Abstract

The objective of this research project was to improve the basis for estimating environmental tobacco smoke (ETS) exposures in a variety of indoor environments. The research utilized experiments conducted in both laboratory and 'real-world' buildings to 1) study the transport of ETS species from room to room, 2) examine the viability of using various chemical markers as tracers for ETS, and 3) to evaluate to what extent re-emission of ETS components from indoor surfaces might add to the ETS exposure estimates.

A three-room environmental chamber was used to examine multi-zone transport and behavior of ETS and its tracers. One room (simulating a smoker's living room) was extensively conditioned with ETS, while a corridor and a second room (simulating a child's bedroom) remained smoking-free. A series of 5 sets of replicate experiments were conducted under different door opening and flow configurations: sealed, leaky, slightly ajar, wide open, and under forced air-flow conditions. When the doors between the rooms were slightly ajar the particles dispersed into the other rooms, eventually reaching the same concentration. The particle size distribution took the same form in each room, although the total numbers of particles in each room depended on the door configurations. The particle number size distribution moved towards somewhat larger particles as the ETS aged. We also successfully modeled the inter-room transport of ETS particles from first principles – using size fractionated particle emission factors, predicted deposition rates, and thermal temperature gradient driven inter-room flows, This validation improved our understanding of bulk inter-room ETS particle transport.

Four chemical tracers were examined: ultraviolet-absorbing particulate matter (UVPM), fluorescent particulate matter (FPM), nicotine and solanesol. Both (UVPM) and (FPM) traced the transport of ETS particles into the non-smoking areas. Nicotine, on the other hand, quickly adsorbed on unconditioned surfaces so that nicotine concentrations in these rooms remained very low, even during smoking episodes. These findings suggest that using nicotine as a tracer of ETS particle concentrations may yield misleading concentration and/or exposure estimates. The results of the solanesol analyses were compromised, apparently by exposure to light during collection (lights in the chambers were always on during the experiments). This may mean that the use of solanesol as a tracer is impractical in 'real-world' conditions.

In the final phase of the project we conducted measurements of ETS particles and tracers in three residences occupied by smokers who had joined a smoking cessation program. As a pilot study, its objective was to improve our understanding of how ETS aerosols are transported in a small number of homes (and thus, whether limiting smoking to certain areas has an effect on ETS exposures in other parts of the building). As with the chamber studies, we examined whether measurements of various chemical tracers, such as nicotine, solanesol, FPM and UVPM, could be used to accurately predict ETS concentrations and potential exposures in 'real-world' settings, as has been suggested by

several authors. The ultimate goal of these efforts, and a future larger multiple house study, is to improve the basis for estimating ETS exposures to the general public.

Because we only studied three houses no firm conclusions can be developed from our data. However, the results for the ETS tracers are essentially the same as those for the chamber experiments. The use of nicotine was problematic as a marker for ETS exposure. In the smoking areas of the homes, nicotine appeared to be a suitable indicator; however in the non-smoking regions, nicotine behavior was very inconsistent. The other tracers, UVPM and FPM, provided a better basis for estimating ETS exposures in the 'real world'. The use of solanesol was compromised - as it had been in the chamber experiments.

Introduction

Environmental tobacco smoke (ETS) is a common contaminant in indoor air. In those indoor environments where cigarette smoking occurs; ETS is a significant contributor to the measured concentrations of respirable suspended particles (RSP) (Spengler *et al* 1981; NRC 1986). A survey of the activity patterns of Californians found that, on average, residents of this state spend 87% of the time indoors and 62% of the time indoors at home (Jenkins *et al.,* 1992). Total exposure to a specific pollutant within a given setting can be estimated from the product of the pollutant concentration and exposure time in that setting. Due to the long potential exposure times, ETS in indoor air is a major source of contaminant exposure of the general population. ETS exposures have been associated with increased risk of lung and heart diseases (see, for example, NRC 1986; DHHS 1986; Wald *et al.,* 1986; Wells 1988), and more recently, ETS has been classified as a Class A carcinogen by the U.S. Environmental Protection Agency (USEPA 1992). Based on estimates of population exposure and lung cancer risk, ETS is calculated to cause approximately 3000 cases of lung cancer per year (USEPA 1992). This calculation estimate would place ETS exposure as the leading cause of lung cancer for the non-smoking population in the U.S.

The major source of ETS is sidestream smoke emitted from the burning end of a cigarette between puffs, and depending upon the smoking rate, combustion during smoldering accounts for half, or more, of the tobacco burned in a cigarette. ETS is a complex mixture of particle- and vapor-phase constituents, many of which were also present in mainstream smoke (Baker *et al.,* 1990; NRC 1986), although the distribution of some species between the two phases differs markedly for sidestream vs. mainstream smoke. For example, nicotine has been reported to be mainly in the vapor phase for sidestream smoke, while it is mostly in the particulate phase in mainstream smoke (Eudy *et al.* 1985; Eatough *et al.* 1986, 1989).

Indoor concentrations of ETS in most buildings, and the resulting ETS exposures of the general population are not well-quantified, however, inhibiting an understanding of the relationship between the inferred health consequences and the detailed causal mechanisms. A comprehensive review of the status of knowledge up to the mid-1980's regarding the effects of ETS, conducted by the National Research Council (NRC 1986), pointed out several critical gaps in our understanding of the relationships among exposure, dose and health effects in non-smokers exposed to ETS: a) research progress has been handicapped by a lack of clear definition of the physicochemical nature of ETS; b) reliable information is needed on the quantity, fate and transport of ETS chemicals in the indoor environment; and c) a number of factors, including room size, temperature, relative humidity, air exchange rate, and smoking rate are important in the interpretation of exposure data (NRC 1986). In addition, aging of ETS may affect the particle size and chemical characteristics of ETS (DHHS 1986). Extensive research efforts at Lawrence Berkeley National Laboratory and other institutions have begun to address these critical gaps in knowledge, but significant issues remain to be investigated.

Particle-phase ETS is an important, possibly dominant, source of non-smoker exposure to chemicals associated with adverse health effects. Many of the carcinogens identified in both mainstream and sidestream tobacco smoke, for example polycyclic aromatic hydrocarbons (PAH) and tobacco-specific N-nitrosamines, are concentrated in the tar or particle phase (Hoffmann and Wynder 1986; Hecht and Hoffmann 1988). Deposition of particles in the lung - and hence the dose of the particle phase chemical species to specific lung regions - is strongly affected by the size distribution of the particles breathed into the lung (NRC 1986; see also Nazaroff *et al.* 1993, and the summary in the next section).

Assessment of ETS particle exposure requires that concentrations of ETS particles, or their surrogates be measured with enough specificity to distinguish these species from other constituents in indoor air. The particle size distribution of ETS particles is approximately the same as that of many other indoor particles (e.g. particles that have infiltrated from outdoors, cooking, and woodsmoke). Thus chemical rather than size characteristics of ETS particles must be employed for a positive identification of ETS. Alternatively, various chemical tracers have been proposed (or used) to help identify ETS particles or tobacco combustion processes, for example nicotine, as discussed below.

Recent investigations of ETS exposure (LaKind *et al.* 1999; Phillips *et al.* 1999) have used more specific candidate tracers such as Ultraviolet Particulate Matter (UVPM), Fluorescent Particulate Matter (FPM) and solanesol, in addition to nicotine. Indoor environmental conditions such as building design and ventilation are important determinants of dynamic behavior of both ETS and any potential tracers, in addition to the time history of smoking. A recent review (Daisey, 1999) also cautioned that the validity of tracer measurements depends on understanding the dynamic behavior of each tracer and understanding both ETS emission characteristics and building ventilation. ETS exposure assessment in office buildings and homes has been based primarily on measurements of chemical tracers. The use of these tracers in actual home or building environments needs to be examined in light of the following criteria for tracer effectiveness:

1. Tracers must be conservative, that is, remain in constant ratio to the ETS constituent of interest. Exposures to ETS aerosols are generally regarded as the source of the health effects; thus a tracer must reflect changes in ETS particle mass as the ETS particles dilute, age, and move between rooms, even in the presence of other sources of particles. Conservative tracers must also be chemically stable over the time necessary to both collect and analyze tracer samples.

2. The analytical procedures for tracers must have the appropriate sensitivity and selectivity, again depending on the ETS constituent of interest.

3. The analytical methods for the tracers must also be cost effective. This is especially important for large-scale exposure studies where many tracer samples will be processed. The main issue is balancing precision and accuracy with analysis cost.

Nicotine, as noted above, is largely in the gas phase for ETS, which means that differences between gas-phase and particle-phase behavior in indoor environments must be accounted for. Nicotine has been widely used in various studies of ETS exposure (see, for example, Hammond and Leaderer, 1987; Daisey 1999). On the other hand, the behavior of nicotine in well-controlled chamber experiments is complicated and doesn't exhibit the first-order decay properties generally observed for particles (Van Loy et al, 1997**;** Van Loy, 1998; Van Loy et al, 2001, Piade, 1999).

The objective of this work is to examine several of the commonly used ETS tracers in both a controlled laboratory environment and a small-scale pilot study in actual homes. The ETS tracers used in this study are UVPM, FPM, particle mass (PM 3.5), solanesol and nicotine. The first four of these tracers are constituents of ETS particles and thus should behave *physically* like particle-phase ETS. The key question in these cases is whether the tracers are stable and suitably specific to distinguish ETS particles from other sources of particulate matter in the environment.

Methods

Our approach for this work was first to examine the behavior of the ETS tracers in a laboratory environment where most of the important parameters could be controlled and many of the potentially confounding issues, such as the presence of non-ETS aerosols could be reduced or eliminated and effects of ETS-room surface interactions could be explored. We deployed a variety of instruments for the laboratory-based studies to examine both size- and time-resolved ETS behavior. For the last phase of this study, based in part on the results of the chamber studies, we investigated ETS tracer behavior in a three-house pilot study. In addition to providing a limited field data set, this pilot study was intended to test the approach and methodology for application to a larger field study. The results of this pilot study are presented in Appendix A.

Test space description

Chamber layout and construction

A 50 m^3 multizone environmental chamber was constructed within a temperature controlled single-story building at Lawrence Berkeley National Laboratory (LBNL). The chamber was designed to mimic conditions of a multi-room residential or office building where ETS might be generated in one room and transported to others. The layout of the chamber, shown in Figure 1, consisted of three rooms, a smoking room (SR), a connecting corridor (COR), and a non-smoking room (NSR). The chamber was built using wood frame construction with taped and painted gypsum wallboard walls and ceiling, and a high-quality nylon carpet laid over plywood sub-flooring in all three chamber rooms. The entry and interconnecting doors were standard solid core wood design; however, magnetic refrigerator door seals (and accompanying steel flanges for the door openings) were added to the entire door perimeters to ensure near airtight sealing when the doors were fully closed. Low volatile organic compound (VOC) emitting paints and sealants were used throughout the chamber in order to minimize the buildup of

unwanted VOCs in the chambers. A plastic (PVC) membrane vapor barrier was placed behind the gypsum wallboard on the interior walls between the SR and the other two chambers to retard any diffusion of ETS components through the wall materials between rooms. Fully closed, the baseline air exchange rate (λ_v) of the chamber and its composite sub-rooms was approximately 0.01 h^{-1}.

Four 10- cm-diameter axial mixing fans were placed in each room, mounted at a height of approximately 1.5m above the floor, at about 1.5m along the diagonals between corners. The fan axes were horizontal and were oriented in opposing directions in order to enhance the mixing within each room. The fan speed was controlled using a Variac transformer at a speed just high enough to achieve uniform mixing of gases, based upon previous chamber experiments.

Each chamber room was equipped with a set of small- and large-diameter sampling ports, each with a plug to close the ports not in use. The large sampling ports were just large enough to permit the insertion of a 47mm particle sampling filter holder, while the small ports allowed for the insertion of nicotine sampling sorbent tubes into the chamber.

Chamber ventilation

Each chamber room was equipped with independent 10- cm-diameter inlet and exhaust ventilation ports, each with a fully sealing-slide valve at the chamber wall. The inlet ports were connected to a HEPA-filtered room air system, supplying particle-free air into the chamber. This supply system had a maximum flowrate of approximately 7 m^3 min^{-1}. The exhaust ports were vented directly through the roof of the building under a protective rain cover. Under full-flow condition it is possible to ventilate the entire chamber at a λ_v of up to 8.5 h^{-1}.

Cigarette smoking machine

A self-sealing sliding drawer containing the cigarette smoking apparatus was built into the exterior wall of the SR, approximately 1.5 m up from the floor for ease of access and replacement of cigarettes in the smoking machine without entering the SR. The inside flange of the drawer was fitted with magnetic refrigerator door seals. The smoking apparatus consisted of an automatic smoking machine (Arthur D. Little model ADL II) with the inlet fitted to a custom made 12-cigarette carousel. This system was capable of smoking 12 cigarettes sequentially without interruption. The mainstream cigarette smoke was removed from the smoking machine via polyethylene tubing and vented outdoors. The smoking rate of the machine was one 35-ml puff per minute, with a puff stroke designed to emulate a smoking puff flow profile.

Measurement and analytical techniques

The measurements and instrumentation used are summarized in Table 1. The sampling rates and averaging times are indicated in the table.

Environmental parameters

Temperature, relative humidity, and pressure difference

Air temperature and relative humidity were measured continuously at the center of each chamber room at 1.8m above the floor. Additional measurements included the air temperature outside the chamber in the room in which the chamber is housed, and the surface temperature of each chamber room wall and ceiling. Pressure differences (sensitive to 0.1 Pa) between outside the chamber and the SR and outside the chamber and the COR were measured. These data were stored as 10-minute averages on a central data logging system. Differential pressure between the SR and COR was then calculated based upon these data.

Chamber ventilation and inter-room transport measurement

Chamber ventilation and inter-room air flow was monitored using a near-real-time sulfur hexafluoride (SF_6) monitoring system consisting of a multi-port sequential sampling valve and a gas chromatograph (GC, Hewlett Packard Model 5890) with an electron capture detector. Sampling ports were connected via 3-mm-ID copper tubing into the center of the SR, COR, and NSR, at a height of approximately 1.8m from the floor. A fourth sampling port was connected to the real-time particle sampling system manifold as discussed below. The system was set to sample and advance from one port to the next every 60 seconds. In order to avoid lag time in the sample line, all four ports were sampled continuously, each at a rate of 1 L min^{-1} and vented out of the building when not being measured by the GC. The SF_6 concentration at each site was logged every four minutes. SF_6 concentrations outside the chamber were measured prior to and just after the multizone experiments in order to determine background concentrations.

An aliquot of three to five cm^3 of pure SF_6 was injected into the SR just prior to the start of cigarette smoking. The initial SF_6 concentration was typically 160 ppb (10^{-3}mL m^{-3}). SF_6 concentrations outside of the chamber were very low with respect to the concentrations in the chamber, and have been neglected in the modeling discussed below. The time dependent transport of SF_6 from the SR to the COR and NSR was calculated using related Equations 1 and 2:

$$q_{12} = \frac{\left[V_1 \frac{dC_1}{dt} + q_1 C_1 \right]}{(C_2 - C_1)}, \qquad (1)$$

and

$$q_{12} = \frac{\left[V_2 \frac{dC_2}{dt} - q_2 C_2 \right]}{(C_1 - C_2)} \qquad (2)$$

Where …

C_1 = SF_6 concentration average for the COR and NSR (mL m^{-3});

C_2 = SF_6 concentration in the SR (mL m^{-3});

q_1 = flow rate between COR+NSR and outside the environmental chamber (m^3 h^{-1});

q_2 = flow rate between SR and outside the environmental chamber (m^3 h^{-1});

q_{12} = flow rate between SR and COR+NSR (m^3 h^{-1});

t = time (h);

V_1 = COR+NSR volume (m^3); and

V_2 = SR volume (m^3).

These equations apply to the time period after injection of SF_6 when the source term is zero. We have also assumed that the SF_6 concentration outside the chamber is essentially zero. During an experiment, there were no significant changes in the environmental conditions of the chamber (as monitored by T and RH measurements in each room) so the various flows (q_1, q_2 and q_{12}) should remain nearly constant over that time. The average interroom flow rate, q_{avg}, for each experiment could be calculated by averaging the q_{12} values derived from Equations 1 and 2. These values were, in turn, computed from the SF_6 measurements described earlier using the time series data until the ratio C_1/C_2 reached 0.8 (this flow rate computation method becomes inaccurate as the tracer concentration ratio of the rooms approaches unity). The flow rates described as q_1 and q_2 were dominated by the flow of the particle and gas measurement instrument sampling pumps used in the experiments discussed below. The baseline λ_v of the chamber was about 0.01 h^{-1} (equivalent to 2.5 L min^{-1}).

ETS and ETS tracer characterization

Gas- and particle-phase ETS tracers, as well as direct measurement of ETS particle mass, were used to characterize the ETS concentration in the chamber rooms. Additionally, the particle size distribution in each room was measured.

ETS particle mass concentration

Total ETS particle mass was measured gravimetrically. Particles were collected on pre-cleaned and pre-weighed 47-mm-diameter Teflon-coated glass fiber filters (Fiberfilm T60A20, Gelman/Pallflex). Before use, filters were cleaned by sequential Sohxlet extraction in dichloromethane followed by methanol for 8 hr each. Due to the low air exchange rate of the environmental chamber and to the very infrequent opening of the space, the infiltration of ambient particulate matter (PM) into the chamber was negligible. Thus, the dominant source of particulate matter in the chamber was the ETS generated during experiments. For this reason, it was not necessary to use a size selective inlet for particle sampling in the chamber experiments. The filter samples contained only respirable suspended particulate matter (RSP) with maximum particle aerodynamic diameter less than 1.5 μm.

The filter samples in each chamber were collected on the open-face filters using a three-channel medium volume air sampling system. This LBNL-built system was capable of sampling at rates up to 85 L min^{-1} while maintaining a constant flow rate as filter loading changed the pressure drop on the sampling system. Each sampling channel was equipped with a dry test meter for monitoring the total sample volume and a pressure gauge for correcting the sample volume to equivalent volume at standard pressure. The average sampling rate across all three chambers during the multizone experiments was 63 L min^{-1}, an overall contribution to the chamber λ_v of about 0.004 h^{-1}.

Gravimetric analysis was conducted using a microbalance (Cahn Model 21 Automatic Electrobalance) with 0.1-microgram resolution. Before weighing each filter was exposed to an ionizing antistatic device (alpha particles emitted from ^{210}Po) in the microbalance chamber to eliminate electrostatic charges. The filters were not conditioned or measured in a humidity-controlled environment because neither the filter media nor the ETS samples is hygroscopic. Mass concentrations in air were calculated (in units of $\mu g\ m^{-3}$) from the observed net mass (sample – tare) and the pressure corrected sample air volume.

Particle size

A system of three particle sizing instruments (Particle Measurements systems LAS-X optical particle counter (OPC) , Thermo Systems Inc. Differential Mobility Particle Sizer (DMPS), and California Measurements Systems PC2 Quartz Crystal Microbalance Cascade Impactor (QCM), Table 1) were used to monitor both particle number and mass, size distributions in the range of 0.01 μm to > 3 μm. Particle samples were drawn from the center of each chamber at a height of approximately 1.8m via clean 13-mm ID flexible copper tubing. These sample lines were connected to an isokinetic manifold via 19mm ID motor-actuated ball valves. Using the three-instrument array, the size-segregated particle concentrations of each room sample were measured in sequence from this manifold

The duration of the room sampling sequence was dictated by the DMPS which required approximately 17 minutes for a complete 34-step scan of the particle size distribution from 0.01μm to 0.45μm. The DMPS software (Thermo Systems Inc, Version 2.8) was modified to add control to select and sequence the chamber room valves and coordinate sample start and finish times for the other two particle size instruments. A 3-minute sample line purge was used at the beginning of each DMPS scan to ensure that the sample from each chamber was uncontaminated by the previous sample. Thus each room measurement took 20 minutes and a complete cycle of all three rooms took one hour.

The California Measurements, Inc. modified the QCM to our specifications, in order to run under automatic control of a personal computer, receiving start and stop signals from the DMPS control computer. The sampling time was controlled by repeatedly polling each stage for the QCM crystal frequency changes with mass loading – the end of sampling was triggered when the 0.1 μm stage had collected a sufficient sample mass for quantitation (approximately a 40 Hz frequency shift). Depending upon the concentration of ETS particles in the chamber room being measured the 10-stage (0.05μm to 25μm) QCM sampling time took from less than one minute up to the full 17 minutes required for

the DMPS. During pre-smoking measurements chamber particle concentrations were often below the QCM's limit of detection (LOD) for a 17-minute sample. During periods of higher ETS particle concentrations the QCM collected up to four samples in the 17-minute periods.

The OPC was set to collect a particle size spectrum (0.09 μm to >3.5 μm) into 16 size bins each minute. The data were written to disk with a time stamp synchronized to the QCM at the completion of each scan. To prevent exceeding the maximum particle count rate of the OPC, it was necessary to dilute the sample concentration in the sampling manifold during the high-ETS concentration periods. The dilution system consisted of particle-filtered room air (taken from outside the chamber) supplied to the sampling manifold at a constant rate through a mass flow controller. The flow rate was set to dilute the SR sampling line by approximately 6 fold. The SF_6 concentration was monitored in the particle-sampling manifold using the tracer gas system discussed above. The ratio of SF_6 concentrations in the SR and the sampling manifold was used to determine the exact sample dilution factor.

Size Segregated ETS Particle Emission Factor Calculations

The ETS particle emission factor during smoking of one cigarette in each of the transport experiments was calculated using a single-equation mass-balance model technique, previously described by Traynor *et al.,* 1982. This model has been used successfully to predict indoor air pollution levels as well as to quantify indoor air quality parameters that can affect such levels. The model is repeated here for completeness.

The mathematical expression for a change in the average indoor gaseous or particulate pollutant concentration in the chamber is:

$$\frac{dC}{dt} = P\lambda_v C_o + \frac{S}{V} - (\lambda_v + k)C \qquad (3)$$

where

$C(t)$ = SR pollutant concentration at time t (μg m^{-3})
$C(0)$ = SR pollutant concentration before smoking (μg m^{-3})

C_o = Pollutant concentration outside multizone chamber(μg m^{-3})
P = fraction of an outdoor pollutant species that penetrates the building shell (unitless)
λ_v = air-exchange rate (h^{-1})
t = time (h)
S = indoor pollutant source strength (μg h^{-1})
V = volume (m^3)
k = net rate of removal processes other than air exchange (h^{-1})

In the case of particles, size-dependent particle dynamics can influence apparent emissions if t is large relative to particle coagulation or differential particle penetration and deposition time constants. By choosing a value for t that is sufficiently short, or by

considering total particle mass, particle emission factors can be accurately assessed using this model.

The air-exchange rate, λ_v, was calculated from the decay in pollutant concentrations after the cigarette smoking is finished (i.e., $S = 0$; also note that for CO and SF_6, $k = 0$ as they are non-reactive gases). λ_v was computed using both cigarette-generated CO concentrations in the chamber and SF_6 that was injected at the beginning of each experiment. Assuming C_o, P, λ_v, S, and k were constant over the period of interest, we can solve Equation 3 for $C(t)$, the chamber pollutant concentration at time t:

$$C(t) = \frac{P\lambda_v C_o + S/V}{\lambda_v + k}[1 - e^{-(\lambda_v + k)t}] + C(0)e^{-(\lambda_v + k)t} \qquad (4)$$

Equation 4 describes the spatial average concentration of a pollutant in a given volume, where C(0) is the pollutant concentration at t = 0.

Solving Equation 4 for S, dividing it by the cigarette consumption rate, R (cigarettes h^{-1}), and letting T equal the duration of cigarette combustion, we obtain the pollutant emission rate, E (μg cig^{-1}):

$$E = \frac{S}{R} = \frac{V}{R}(\lambda_v + k)\frac{C(T) - C(0)e^{-(\lambda_v + k)T}}{1 - e^{-(\lambda_v + k)T}} - \frac{VP\lambda_v C_o}{R} \qquad (5)$$

In the case of the experiments discussed here it is assumed that C_o is negligible relative to C(T) and can be ignored. Likewise, the effect of ventilation and particle deposition losses during the short period of cigarette combustion ($T-T_0$) are quite small, estimated to be about 1% based upon the 0.17 hour cigarette burn time and average air exchange rate of the SR with door sealed. Thus, for calculation of the *per cigarette* total ETS pollutant emission rate in this study Equation 5 can be simplified to:

$$E = \frac{S}{R} = V[C(T) - C(0)] \qquad (6)$$

As discussed in detail below, particle C(0) and C(T) were measured in each experiment gravimetrically, and size resolved in real time using the DMPS, OPC, and QCM. The emission rate was then parsed into 34 bins by percentage of calculated total particle mass from 0.009 to 0.42 μm, and final bin for particles > 0.5 μm. It was assumed that the ETS particle density was constant across the entire size range based upon an observation that the major constituent in ETS particulate matter is condensed hydrocarbons. The percentage of total particle mass in size bin j was calculated as follows:

$$M_i = \frac{V_i N_i}{\sum_{i=1}^{i=35} V_i N_i} \qquad (7)$$

Where:

M_i = proportion of mass in size bin *i*,

V_j = calculated volume of mean particle size in bin *i* based upon median particle diameter of bin *i*,

N_i = DMPS-measured count of particles in size bin *i.*

The particle mass emitted in each size bin was then calculated as:

$$E_i = E\, M_i, \qquad (8)$$

Where:

E_i = the ETS particle emission rate in size bin *i*.

Since the measured C(T) is based upon a 15-30 minute gravimetric filter sample which took place just after smoking was completed, it underestimates the true peak value due to ventilation and depositional losses in the SR. A correction factor was used to account for this difference, based upon OPC data which were collected every minute during the same sampling period. A value (*c*) reflecting the ratio of the peak total OPC particle count to the value at the midpoint of the filter sampling period was calculated. This correction was applied as follows:

$$E_{ci} = cE_I \qquad (9)$$

Particulate ETS tracers

Preparation of filter extracts: Ultraviolet particulate matter (UVPM), fluorescent particulate matter (FPM) and solanesol were determined from methanol extracts of the filter-collected ETS particles after mass determination. Filters were transferred collection side down to individual 50 mL Erlenmeyer flasks and extracted in 2.5 mL of spectroscopic grade (high purity, glass distilled) methanol by sonication at 30ºC for 10 min. Each extract was transferred to a filtration flask, and the filter re-extracted with a second 2.5 mL aliquot of methanol. For any sample for with residual color a third 2.5 mL extraction was performed. For those cases where heavy filter loading was determined in advance (those weighing more than about 0.7 mg) the filters were extracted twice, first using 4.0 mL of spectroscopic grade methanol followed by a second 3.5 mL methanol extraction.

The extracts were pooled with two 0.5 mL rinses of the flask and filtered through unlaminated Teflon filters (0.5 micrometer pore size, FHUP04700, Millipore Corp.). Some extracts were reduced in volume by rotary evaporation of the methanol before tracer determination. Final extract volumes were determined using calibrated glass

syringes before transfer to amber glass vials with Teflon-lined septa. Extracts were stored at -20ºC.

UVPM: The UVPM method is based on the ultraviolet absorbance of ETS. We adapted and improved the UVPM method that was introduced by Ogden et al. (1990). The optimal wavelength of 325 nm was chosen after scanning the spectra of ETS extracts (in methanol) between 200 and 500 nm using both a spectrometer (Perkin-Elmer UV/Vis Lambda 2 with Perkin-Elmer Computerized Spectroscopy Software (PECSS) version 4 software), and the diode array detector of a high performance liquid chromatograph (Hewlett-Packard 1090M). Standard or micro-quartz microcuvettes were used in the spectrometer, after they had been cleaned with sulfuric acid and rinsed with deionized water and methanol. ETS extracts absorbed continuously with increasing intensity as the wavelength decreased. Fresh and archived (Gundel et al., 1997) ETS extracts gave identical spectra. Both instruments were calibrated at UV wavelengths of 205, 225, 250 and 325 nm with ETS extracts from many experiments in the smoking room of the environmental chamber. The correlation coefficients (r^2) between the HPLC and spectrometer signals averaged 0.97.

UVPM was determined routinely from the absorbance of methanol extracts at 325 nm because we found that this wavelength provided the optimal combination of selectivity for ETS, reproducibility, lamp stability and minimal filter/solvent blank interference. In a separate set of chamber experiments (Gundel et al., 2000; Alevantis et al., 2001) we found that diesel exhaust and woodsmoke could contribute to UVPM. These sources of interference were not present during our chamber studies, but they could have contributed to UVPM measured in the pilot (residential) field study described in Appendix A.

The HPLC-based measurement of UVPM was developed as a simpler and faster alternative to the use of the spectrometer. We found that UVPM, FPM and solanesol could be determined from the same chromatogram, if desired. We devised two HPLC procedures that used different chromatographic conditions, depending on whether or not solanesol was to be determined along with UVPM and FPM. More details are given below for FPM and solanesol methods. When solanesol was being analyzed, chromatographic conditions were adjusted so that the major UV absorbing and fluorescing components of the extract were retained only briefly on the analytical column (Vydac 201TP5215 analytical column, 5 μm particle size, 2mm ID, 201TP C_{18}), using an isocratic mobile phase of HPLC grade acetonitrile and methanol (80 and 20% by volume, respectively) at 0.3 mL min^{-1}. The UVPM peak eluted between 1 and 3 minutes, while the solanesol was detected later, as explained below. The other chromatographic procedure was used for samples that were expected to have solanesol concentrations below the limit of detection, such as filter extracts collected from the non-smoking room before smoking. In this alternate procedure the same mobile phase passed through only a guard column (Vydac 201GCC52T, 5 μm particle size, 2mm ID, 201TP C_{18}), at 0.3 mL min^{-1}. Each method used scopoletin used as an absorbance standard: For each extract the broad absorbance peak due to ETS was converted to 'scopoletin equivalents' (SE), using absorbance at 325 nm. To calibrate each HPLC procedure, SE were also determined from extracts of known ETS mass concentration, and response factors derived. UVPM

values for extracts were calculated by applying the response factor to the product of SE and the extract volume.

FPM: Fluorescent particulate matter was determined during the same chromatographic analysis as UVPM and solanesol. We adapted and improved the method outlined by Ogden et al. (1990). Fluorescence was excited at 225 and monitored at 355 nm using a fluorescence detector (Hewlett Packard HP1046A) that followed the diode array detector. Scopoletin was used as a fluorescence standard for the HPLC, to normalize for any change in lamp output or drift during the set of analyses. Archived extracts of known ETS mass concentration were used to generate FPM calibration curves.

Solanesol: Solanesol was determined from methanol extracts of ETS; this method was based on the best available information from the literature (Ogden and Maiolo, 1992). Solanesol is a long chain unsaturated alcohol that can be detected by its ultraviolet absorbance at 205 nm when it is separated chromatographically from the other major UV absorbing components of ETS. When the analytical column was used for simultaneous determination of UVPM, FPM and solanesol, solanesol eluted from the column at 8 min using 20% methanol in acetonitrile at 0.3 mL min^{-1}.

We found that solanesol standards degraded (oxidized) when exposed to ambient light for a few hours. ETS extracts were protected from light and stored in the freezer at –20ºC to preserve them before analysis. Re-analysis of archived ETS extracts indicated that the solanesol in them degraded within a month of storage. Solanesol's reactivity, both in any realistic smoking environment where ETS will be present in lighted rooms for several hours and during sample processing, makes it an unreliable ETS marker, as discussed below.

The chromatograms data from ETS tracer analyses were integrated using the Hewlett Packard HP 1090M Chemstation software. The tracer mass quantification data, and the gravimetric data analyses of each filter were logged in a MS Excel spreadsheet, along with sample volumes, pressure, and temperature, and sample start and end times. Standard sample volumes (m^3) and mass and tracer concentrations ($\mu g\ m^{-3}$) for each filter were calculated.

Nicotine

Gas-phase nicotine was sampled onto glass tubes containing Tenax TA sorbent and subsequently were thermally desorbed onto a gas chromatograph equipped with a flame ionization or nitrogen specific detector. The sample analysis protocol was adapted from the method of Hodgson and Girman (1989). The sorbent tubes, containing Tenax-TA, were pre-conditioned by heating at 300ºC for 30 min with a He purge to remove all VOC. For collection of ETS, chamber air was mechanically pulled through the glass tubes at 2 L min^{-1} using calibrated mass flow controllers; the open end of the sorbent tube was approximately 30 cm from the chamber wall. After sampling, the tubes were capped, placed in storage tubes and analyzed on the same day or stored in the freezer for analysis within three days. Samples were wrapped in foil and stored out of direct light in order to protect them from degradation.

Nicotine sampling ports that allowed for a 30 cm sampling probe to be inserted were located roughly mid-way along a wall in each chamber at a height of about 1.5m. Nicotine samples were collected at different times in the three chamber rooms depending upon the experimental phase and point in the experiments. In general, during the chamber-conditioning phase (see below) samples (or duplicate samples) were collected only in the smoking room prior to each weekday-smoking period, while a sample was collected in all three chambers post smoking. During the experimental phase samples were collected before, during, and after smoking in a sequence that is discussed in the protocol description section below.

The loaded sorbent tubes were thermally desorbed into a GC (Hewlett Packard 5890 II) containing a 15-m DB-Wax column with 0.53 mm internal diameter and 1μm film thickness. Temperature programming of the GC column was used to resolve nicotine from other semivolatile and volatile organic compounds. Nicotine quantitation was confirmed by daily calibrations using standards that produced peak areas bounding the range of masses observed during the day's samples. The nicotine solutions standards were applied to sorbent tubes from ethyl acetate solution injected via a hypodermic syringe.

During the course of these experiments the desorption unit and detector were upgraded. With each upgrade, we confirmed the equivalence of the new method for sample recovery and mass quantitation. Initially, samples were thermally desorbed onto the GC column using a UNACON Model 810A (Envirochem, Inc.) unit that concentrated the sample as it passed through sequential traps of decreasing internal diameter. Each sample was quantified with a Hewlett Packard flame ionization detector (FID) with output to a HP 3396-II peak integrator. About midway through the experiments, the UNACON was replaced with a Chrompack CP4020 TCT short path thermal desorption unit. This instrument desorbed the sample onto a cryogenically cooled hollow section of the chromatographic column, and then injected it directly onto the column by rapid heating of the "cold trap." At this time the FID was replaced with a HP nitrogen-phosphorous detector. We also added HP Chemstation software to control the analytical system and perform quantitation peak integration. A series of validation checks indicated that there were no systematic changes brought on by this upgrade that altered the detection limits, sensitivity, accuracy, or reproducibility of the nicotine measurements.

The gas chromatograpy data from nicotine sample analyses were analyzed using the Helwett Packard Chemstation software. The nicotine mass quantification for each sample tube was recorded, along with sample flowrates, start times and end times. Standard sample volumes (m^3) and nicotine concentrations ($\mu g\ m^{-3}$) were calculated for each sample.

Carbon monoxide

Carbon Monoxide (CO) was measured continuously in the SR using a Gas Filter Correlation Infrared gas analyzer (Thermo Environment, Model 48). No CO data were collected in the COR or NSR. A gas sample was drawn directly from the SR using the

CO instrument's internal pump, protected from contamination by particles using an inline filter. These data were stored as 10-minute averages on a central data logging system. The CO data were used as one means to assess the air exchange rate, $\lambda_{v,}$ of the smoking room. They were in close agreement with the SF_6 decays so have not been tabulated in this report, but the calculated SR air exchange rate from the CO data were used in a number of analyses, as discussed below.

Modeling

Nicotine modeling

One of the hypotheses we wanted to examine in this work is that ETS and/or ETS tracers may behave differently in environments where smoking occurs regularly and where smoking is infrequent or non-existent. Modeling of the both short-term and long-term behavior of nicotine in the environmental chamber was conducted. The Van Loy model for nicotine (Van Loy et al., 1997) was used prior to any experiments as an aid in planning a chamber-conditioning scenario for the SR. After the conditioning phase, and then again after the experimental phase, the Van Loy model was used to compare simulations of the SR nicotine concentrations to those that were observed. A statistical approach to assessing the factors influencing the nicotine concentration in the SR was also investigated.

The Van Loy Model

Recently Van Loy et al. (Van Loy 1998; Van Loy et al. 1997; 2001) examined the behavior of nicotine both in a bare stainless steel chamber and in the same chamber containing common indoor surface materials such as painted wallboard and carpet. This work showed that the sorption and desorption processes were non-linear and were dependent upon the previous nicotine 'exposure history' of the materials. We used the Van Loy nicotine model to devise a chamber conditioning procedure that emulated ETS behavior in a room where smoking occurred regularly.

The model, based on the principle of mass conservation, utilizes both a coupled surface sorption/bulk diffusion model and a surface sorption dynamics model to simulate the physical behavior of nicotine removal from the bulk room air to room surfaces and then into the bulk of the surface materials (i.e., painted wallboard and floor carpeting). This model attempts to simulate the nonlinear equilibrium partitioning and adsorption/desorption kinetics in the gas and sorbed phases of nicotine surface interactions. The reader is referred to Van Loy (1998) for the details of this simulation approach. This model is complicated due to the nonlinear equilibrium partitioning and the bulk diffusion mechanism. Simulations using this model were accomplished using Fortran software developed by Van Loy (routine "expsim.for", Van Loy, 1998).

The values initially used for the equilibrium and kinetic parameters in the simulations presented here were derived from Van Loy (1998) and Van Loy et al. (2001), although bulk diffusion was ignored in the latter paper. These parameters include nicotine and respirable particle emission rates, particle deposition velocity, sorbent thickness,

adsorption and desorption rates, and exponential coefficients for nicotine-carpet and nicotine-painted wallboard interactions. The values for these coefficients are as follows. The nicotine emission rate was 5.0 mg cig^{-1}, and the SR volume was 14.9 m^3. Painted wallboard parameters for surface area, adsorption rate constant (k_{aw}), desorption rate constant (k_{dw}) , bulk diffusion coefficient (D_w), and sorbent thickness were 30.4 m^2, 0.03 m h^{-1}, 2.2E-05 h^{-1}, 4.8E-12 m^2 h^{-1}, and 0.0125 m, respectively. Similarly the carpet parameter values for surface area, adsorption rate constant (k_{ac}), desorption rate constant (k_{dc}), bulk diffusion coefficient (D_c), and sorbent thickness were: 6.1 m^2, 0.13 m h^{-1}, 6.7E-06 h^{-1}, 4.17E-12 m^2 h^{-1}, and 0.0024 m, respectively. As discussed below, these initial values were subsequently rejected for a set that provided a better fit to measured data.

Subsequent to data collection in the laboratory phase of this study a simpler mass balance model was adopted which assumed linear partitioning at equilibrium and no bulk diffusion, as described in Van Loy et al. (2001), and a single pair of lumped surface adsorption and desorption coefficients to describe the overall nicotine behavior in the SR. This model is as follows:

$$\frac{dC_n}{dt} = \frac{E_n(t)}{V} - \lambda_v C_n - \frac{S}{V}\left(k_{an} C_n - k_{dn} M_n\right). \qquad (10)$$

Where C_n and E_n denote nicotine concentration (μg m^{-3}) and emission factor (μg h^{-1}), respectively. Additionally, V, λ, S, k_{an}, k_{dn}, and M_n denote chamber volume (m^3), air exchange rate (h^{-1}), chamber internal surface area (m^2), lumped nicotine adsorption coefficient (m h^{-1}), lumped nicotine desorption coefficient (h^{-1}), and total sorbed nicotine mass (μg), respectively. Simulations using this simpler model were accomplished using macro programming in Microsoft Excel spreadsheets with time steps of 0.01 hour throughout the modeled time period.

Multivariate modeling

In addition to the physical modeling of nicotine behavior discussed above, a multivariate regression approach was taken to identify the factors influencing the nicotine concentration in air. A dataset was constructed containing a time-series of measured nicotine values in the smoking room (C_{nic}, μg m^{-3}); the elapsed time since the first cigarette was smoked (t); the time since the last cigarette was smoked ($t_{last,}$ hours), the number of cigarettes smoked in the last 0-4h (n_4), 4-24h (n_{24}), 24-48h (n_{48}), 48-72h (n_{72}), 72-96h (n_{96}), 96-120h (n_{120}), 120-144h (n_{144}), and 144-168h (n_{168}); and the average air exchange rate (air changes per hour, ach) in the smoking room during the last 0-24h (λ_{24}), and 24-168h (λ_{168}). This dataset contained entries for each of these parameters for a series of 192 chamber measurements spanning almost two months.

The statistical relationship between C_{nic} and the independent variables listed above were assessed using a General Linear Model (Proc GLM, SAS, 1989). A log-transformation of nicotine concentrations was used in the modeling, as the data appear to more closely resemble a log-normal distribution. A number of combinations of covariates were

considered in the model and a final simplified model which contained the essential covariates was adopted. The general form of this model is:

$$\log(C_{nic}) \sim \alpha_1 t + \alpha_2 t^2 + \alpha_3 t_{last} + \alpha_4 n_4 + \alpha_5 n_{24} + \ldots + \alpha_i \lambda_n \,. \qquad (11)$$

Mass transport modeling

Predicting airflow and mass transport in multi-room systems

Air flow was modeled in the this study using a multizone, airflow model called COMIS (Feustel and Rayner-Hooson, 1990; Feustel, 1999). Feustel and Deris (1992) provide a list of similar multizone software packages. COMIS predicts the steady-state flow of air and the dynamic transport of pollutants between interior zones that are inter-connected by flow pathways such as doors, cracks, fans, and ductwork. The code also includes similar connections between the chamber rooms and outside. The mass flow is driven through pathways by pressure gradients induced by wind, thermal buoyancy, and the operation of mechanical flow systems. Dynamic pollutant transport is treated using a first-order conservation of mass model that assumes that the pollutant transports with the bulk airflow. COMIS has been used, and its predictions experimentally validated, for airflow and pollutant transport in multi-story low- and high-rise residences (Feustel et al., 1985; Sextro et al., 1999), small office buildings (Feustel, 1990), controlled experimental test houses (Haghighat and Megri, 1996), and single-family houses (Zhao et al., 1998).

Detailed aerosol transport was simulated using a multizone aerosol dynamics model called MIAQ4 (Nazaroff and Cass, 1989; Nazaroff et al., 1990). MIAQ4 simulates a size- and chemically-resolved evolution of particles in indoor environments. It tracks the effects of inter-room airflow, ventilation, filtration, emission, coagulation, and deposition onto indoor surfaces. As input to the model, it uses the airflow predictions from the COMIS model, the building description, and an aerosol emission profile. The model has been used to study the concentration and fate of particles from cigarette smoke in single- and two-chamber experimental studies (see e.g., Nazaroff and Cass, 1989; Nazaroff et al., 1993; Miller et al., 1997), and the concentration of particulate matter in museums (Nazaroff et al., 1990).

Experimental Protocol

Chamber conditioning phase

Based on the Van Loy model, a chamber conditioning strategy was developed to simulate smoking behavior in the SR under low ventilation conditions and a weekly pattern of daily smoking for five days followed by no smoking for two days. The simulations were used to identify a smoking pattern resulting in steady-state airborne nicotine levels after several weeks of intensive smoking. These simulations predicted near-equilibrium in the SR baseline nicotine concentrations after 6 weeks, using an average λ_v of 0.01 h^{-1} and Van Loy's parameter values (see Figure 2) for nicotine interactions with painted wallboard and carpet.

During a six-week period 36 cigarettes were machine-smoked each weekday in the SR. No smoking was conducted on the weekends. After six weeks the smoking rate was lowered to 6 cigarettes per weekday. Conditioning continued at this rate for an additional 3 weeks prior to the first experiment. The COR and NSR remained isolated with the connecting doors closed and sealed. Particle mass and nicotine concentrations were measured daily in each room during the conditioning phase.

After the start of the experimental phase the SR continued to be conditioned with 6 cigarettes per weekday. The exception was on one day per week when an ETS transport experiment was conducted. Two different conditioning protocols were used on the experimental days. Initially (MZ01-MZ02) one cigarette was smoked during an ETS transport test. In the evening of that day the SR door was closed and the remaining 5 cigarettes were smoked within about 40 minutes. From MZ03-MZ12 a full 24 hours was allowed to elapse after the single cigarette used for the ETS transport experiment was smoked. Then, on the day following the experiment eleven cigarettes were chain-smoked in the SR within about 90 minutes to making up for the five missed on the previous day.

Experimental phase

Experiments were designed to investigate the inter-room transport of ETS constituents from the SR to the COR and NSR under both natural and forced-mechanical transport conditions. Three natural ventilation settings were investigated to encompass the range of normal conditions in a home: SR door closed; SR door open 1.0 cm, 2.5 cm (measured as the closest distance between the inside edge of the door and the doorframe), and SR door wide open (set 90° from closed position). One forced ventilation setting was investigated: SR door open 1.0 cm with a pressure drop of 0.6±0.2 Pa across doorway created by supplying HEPA-filtered external room air into the SR while venting chamber air from a port in the NSR. During all experiments the door between the COR and NSR was set in the wide-open position. The chamber layout is shown in Figure 1.

A door opening and measurement protocol was developed for all experiments (Figure 3). Background measurements of particle mass and tracer concentrations (filters), particle size distribution (DMPS, OPC, and QCM), and nicotine were made in all three rooms with all chamber doors closed and sealed. After these measurements were completed one cigarette was machine-smoked under remote control in the closed SR. At the same time a bolus of pure SF_6 sufficient to raise the SR concentration to about 150 ppb was injected into the airstream of a mixing fan in the SR. Within abour 5-minutes after the cigarette smoking was complete the SR air was considered well mixed and peak ETS concentration measurements were begun. The COR was entered from the outside briefly, the NSR door was opened wide, and the SR door was opened to the required setting and locked into its preset position by a barrel bolt that was set into the floor. Door opening was conducted slowly and carefully to avoid excessive mechanical air movement and inter-room pumping. Filter and nicotine samples in the three chamber rooms were then collected again at the following times: one hour after smoking; 4-hours after smoking; and 20-24 hours after smoking. A 24-hour integrated particle filter measurement was made outside the chamber during each experiment.

During all experiments real-time monitoring of CO concentrations in the SR and SF_6 concentrations in all three chamber rooms was conducted. The DMPS, OPC, and QCM were set to operate continually, rotating between the three chamber rooms in a 60-minute cycle, starting at the time of the initial measurement and running continuously for the full duration of each experiment. The particle monitoring system was timed so that the SR peak ETS concentration was monitored just after smoking, but before the SR door was opened.

Due to the need to continue to condition the SR during the experimental time period, the schedule of transport experiments had an effect on initial ETS concentrations, and the age of the ETS at the beginning of each experiment. For experiments MZ01-MZ07 the experiments were conducted on Thursdays, and therefore the residual ETS from the previous days' conditioning was still present in the SR. For these experiments the initial background ETS in the SR was elevated (but always measured), and the ETS after smoking the single cigarette for the experiment was a mixture of aged and fresh components. For experiments MZ08-MZ12 the routine was changed to conducting the experiment on Monday, after a two-day weekend when no conditioning took place. The initial ETS concentration in the SR in these experiments was quite low which allowed an assessment of ETS transport behavior when only fresh ETS was present.

Results and Discussion

Chamber Conditioning

Figure 4 depicts the smoking room nicotine and RSP concentrations during the conditioning phase of the study. The ETS concentrations developed during the conditioning phase were very high, as expected from smoking 36 cigarettes over 8 hours in a very tight room. For the first 6 weeks of conditioning nicotine concentration range was 10 to 320 $\mu g\ m^{-3}$ (average=170±100 $\mu g\ m^{-3}$) in the morning prior to smoking (19 measurements), while the peak concentration after 36 cigarettes ranged from 800 $\mu g\ m^{-3}$ to 1660 $\mu g\ m^{-3}$ (average=900±100 $\mu g\ m^{-3}$, 21 measurements). These concentrations during chamber conditioning are approximately an order of magnitude higher than typical of indoor ETS levels, but served to accelerate the conditioning process.

RSP was also measured in the SR prior to and after most smoking days during the conditioning phase. The RSP concentration range was 1 to 2500 $\mu g\ m^{-3}$ (average=1100±800 $\mu g\ m^{-3}$) in the morning prior to smoking (16 measurements), while the peak concentration after 36 cigarettes ranged from 16,000 $\mu g\ m^{-3}$ to 21,200 $\mu g\ m^{-3}$ (average=19,900±1300 $\mu g\ m^{-3}$, 20 measurements).

During these conditioning weeks, where the COR and NSR doors were never opened, their nicotine and RSP levels were lower than the SR (Figure 5) by about 2 orders of magnitude. At the end of the conditioning period the nicotine levels in the COR and NSR were about 10 $\mu g\ m^{-3}$. Note that the nicotine levels did vary and that there is some evidence that ETS did infiltrate into the COR and NSR during this period, probably through small amounts of leakage between the rooms that occurred over the long-term conditioning period.

Inter-room air flow and mass transport

A list of the experimental conditions for the ETS inter-room transport experiments is provided in Table 2. Replicate tests were conducted under the following natural transport conditions: SR door sealed; SR door open 1 cm, 2.5 cm, and wide open. In addition the multizone chamber was operated under a forced flow regime with the SR door open 1 cm. Based upon the SF_6 tracer calculations (Equations 1 and 2) the average inter-room air flow between the SR and the NSR were 0, 1.0±0.2, 5.5±0.8, and 59±12 $m^3\ h^{-1}$, for the sealed, 1.0 cm, 2.5 cm and wide open conditions, respecively. The forced flow inter-room air flow was 150±13 $m^3\ h^{-1}$. The measured gas and particle decay rates for periods when no smoke was being generated are also presented in Table 2.

Gas-phase ETS tracers

Measured gas-phase ETS tracers were CO and nicotine. CO was only measured in the SR, and used primarily for quantifying the air exchange rate of the SR using the tracer decay method. Each cigarette smoked in the SR increased the CO concentration by approximately 3 ppm.

Table 3 and Figure 6 show nicotine data for all measurement periods for all of the multizone ETS transport experiments. The peak SR nicotine concentrations (corrected for pre-smoking background) for all tests ranged from 6 to 220 μg m^{-3} with an average of 110±60 μg m^{-3}. The net nicotine concentration change in the SR over the roughly 24 hours during which a single cigarette was smoked, for the 1 cm, 2.5 cm, wide open, and 1 cm forced door conditions were 6±6, 31±37, 57±8, and 74±20 μg m^{-3}, respectively. Similarly, the nicotine concentration change in the NSR over the same period for the 1 cm, 2.5 cm, wide open, and 1 cm forced door conditions were, 0±0, 1±1, 5±2, and 1±0 μg m^{-3}, respectively. Overall uncertainty in the nicotine measurements including measurement and quantitation error is approximately ±20%.

Particle-phase ETS tracers

Table 3 and Figure 7 present RSP data for all measurement periods for all of the multizone ETS transport experiments. Propagated error calculations (including gravimetric and sample volume measurements) indicate that the uncertainty for RSP measurements is approximately 3% (these are depicted in the error bars shown in Figure 7). The SR peak concentration (minus pre-smoking RSP concentrations), due to sidestream emissions from a single cigarette ranged from 440 to 630 μg m^{-3} for all tests, with an average of 510±60 μg m^{-3}. The RSP concentrations in the NSR increased over 4 hours after the door opening in all scenarios. The increases for the 1 cm, 2.5 cm, wide open, and 1 cm forced flow conditions were, 13±1, 88±17, 82±16, and 64±23 μg m^{-3}, respectively. After 20 hours, due to ventilation, particle deposition, and other mechanisms the NSR RSP increases for the 1 cm, 2.5 cm, wide open, and 1 cm forced door conditions decreased to 15±5, 27±2, 21±6, and 13±2 μg m^{-3}, respectively. As shown in Figure 7, the COR and NSR RSP concentrations were very similar.

Figure 8 and Table 3 contain UVPM data that parallel the RSP data above. Propagated error (including gravimetric and sample volume measurements, and HPLC quantitations)

indicate that the uncertainties for UVPM measurements are approximately ±30% for the SR and ±50% for the COR and NSR (these are depicted in the error bars shown in Figure 8). The SR peak concentration (minus pre-smoking UVPM concentrations), due to sidestream emissions from a single cigarette ranged from 160 to 640 μg m^{-3} for all tests, with an average of 450±160 μg m^{-3}. The UVPM concentrations in the NSR increased over 4 hours after the door opening in all scenarios. The increases for the 1 cm, 2.5 cm, wide open, and 1 cm forced flow conditions were, 15±4, 95±1, 65±4, and 73±9 μg m^{-3}, respectively. After about 20 hours these UVPM increases were 17±8, 30±25, 13±4, and 10±3 μg m^{-3}, respectively.

In similar fashion the FPM data (Figure 9 and Table 3) were as follows. Error calculations indicate that the uncertainty for FPM measurements are approximately 40% for the SR and ±80% for the COR and NSR (these are depicted in the error bars shown in Figure 9). The peak SR FPM concentration increases ranged from 400-to 720 μg m^{-3} with a mean of 530±99 μg m^{-3}. After 4 hours the NSR level increases for the 1 cm, 2.5 cm, wide open, and 1 cm forced door conditions were 15±0, 110±19 , 53±10, and 63±4 μg m^{-3}, respectively. Again, after about 20 hours increases in the NSR were 12±3, 21±15, 14±7, and 10±2 μg m^{-3}, respectively.

During chamber conditioning (phase 1) solanesol comprised an average of 0.85 ± 0.20 % of particulate ETS mass when determined in filter samples collected in the SR immediately after smoking, but only 0.14 ± 0.07 % of ETS mass when determined from filter samples collected the morning after smoking. Solanesol, as an unsaturated fatty alcohol, could oxidize as the ETS aged overnight. Solutions of solanesol in methanol also appeared to degrade, probably by oxidation to one or more polar compounds in the presence of light on the lab bench in a matter of hours. During the multi-zone chamber experiments ETS particles in the SR typically contained less than 0.1% solanesol, with a maximum of 0.5%. ETS in the COR and NSR apparently contained less than 0.1 % solanesol. Thus this study shows that solanesol could not be used as a quantitative ETS tracer under the current conditions and/or with our sampling and analytical methods.

Figure 10 shows how UVPM and FPM correlated with RSP for all the rooms together (upper left) and in each room individually, with no distinction of different times after smoking. The data for all rooms together and the smoking room showed slopes of close to 1.0 and r^2 above 0.9. This is reassuring since data from the smoking room were used to establish the quantitative relationship between the tracer instrumental responses and ETS concentration, by assuming that all RSP was due to ETS when only ETS was present.

The relationship between tracer concentrations and RSP in both the non-smoking room and the corridor differed from the smoking room. The ratio of UVPM to RSP was about 0.8 for the COR and NSR. The ratio of FPM to RSP was about 0.7 for the COR and NSR. A Student's t-test was used to compare the distribution of UVPM to RSP and FPM to RSP ratios for measurements collected in the SR vs. those collected in the COR and NSR. The hypothesis that the difference in the means of these distributions was zero was

rejected with a probability of greater than 99.5%. In other words, the UVPM/RSP and FPM/RSP ratios in the SR and in the COR/NSR were significantly different.

The disproportionate reduction of tracer response as the ETS moved into the COR and NSR could be due to several processes. 1) Coagulation of ultrafine ETS particles during aging could reduce UVPM and FPM if the optically active ETS components were concentrated on the surfaces of the ultrafine particles. However, this process would not be limited to the COR and NSR and would occur faster in the SR where particle number concentrations were much higher at the start of each experiment. 2) Particle deposition to the walls would not explain selective reduction of tracer response, since RSP would be reduced proportionately. 3) The longer sampling times used during sampling in the COR and NSR, compared to the SR for the first four hours, leading to higher evaporation of absorbing and fluorescing ETS components during sampling. 4) ETS particles in the COR and NSR had enhanced evaporation of optically active components due to higher adsorption to the walls, compared to the conditioned walls of the SR. If enhanced loss of absorbing and fluorescing components of ETS is occurring due to either or both of the latter two processes, a significant fraction of ETS is both semi-volatile and optically active.

Figure 11 shows how nicotine correlated with RSP for all the rooms together (upper left) and in each room individually, with no distinction between different times after smoking. The data for all rooms together and the smoking room showed slopes of 0.2 and r^2 of 0.7 and 0.6, respectively. Nicotine was always much lower in the NSR and the COR than in the SR. The ratio of nicotine to RSP was about 0.04 and 0.06 for the NSR and COR, with r^2 of 0.5 and 0.3, respectively. These results are consistent with the rapid adsorption of nicotine to the unconditioned walls of the COR and NSR as the ETS moved between rooms as expected from Van Loy's results and modeling (Van Loy 1997, 1998, and 2001).

Our results suggest that UVPM and FPM could trace ETS concentrations more accurately than nicotine when measurements are made in environments with varying or unknown conditioning (as would be the case for an unknown smoking history). This can be verified by observing that the slope of UVPM to RSP is roughly 1.0 in the SR and 0.8 in the COR and NSR indicating about a 20% reduction of PM tracer specificity through transport and loss mechanisms. In contrast the slope of nicotine to RSP is about 0.2 in the SR, dropping to about 0.05 in the COR and NSR. This is a 400% reduction in nicotine specificity of RSP. This reduction of specificity for nicotine, if it holds true in real-world environments suggests a potential for significant underestimation of exposure in the case where nicotine is used in non- or lightly-conditioned environments connected to rooms where smoking is occurring.

ETS particle size distribution and transport dynamics

Table 3 presents the number size distribution geometric mean (GM) and geometric standard deviation (GSD) for each experiment, room, and measurement period. The particle size distribution data were measured using the three sizing instrument systems,

the DMPS and the QCM (measuring aerodynamic diameter), and the OPC (measuring optical diameter). The count size distribution was calculated from the bin width-normalized DMPS particle counts, assuming a lognormal particle size distribution which was reasonable given the right-skewed form of the untransformed data.

Figure 12 presents the peak-corrected particle size resolved ETS emission factors per cigarette calculated from single cigarettes smoked in each of the 12 experiments as described in Equation 9.

The initial particle size distribution in the SR prior to smoking was quite variable, ranging from 0.05 to 0.37 μm, depending primarily upon the age of the ETS in the environmental chamber. In experiments MZ01, 02, 05, and 07, when initial concentrations in the SR were elevated due to aged ETS and DMPS data were available, the GM particle size ranged from 0.31 to 0.37 μm (GSD 2.6-3.1). In experiments MZ03, 05, 08, and 10-12 where very little residual ETS or ambient particles remained in the SR the GM of the initial particle size distribution ranged from 0.05 to 0.10 μm (mean GM = 0.07±0.02 μm), with GSD range of 1.7 to 2.2.

At peak ETS concentration in the SR during each natural flow experiment (MZ01-MZ10) the measured particle size GM ranged from 0.10 to 0.14 μm with GSD ranging from 1.7 to 1.9. After 4 hours the GM particle diameter increased, due to particle coagulation, by an average of 0.04 μm (GM size range 0.14 to 0.22 μm). After 20-24 hours the SR GM particle size ranged from 0.15 to 0.20 μm, a net increase in particle diameter of 0.05 to 0.07 μm. The initial particle size distribution in the SR prior to smoking does not appear to have influenced the post smoking size distribution, largely due to the great increase in particle number after smoking.

After roughly 4 hours from the time that the SR door was opened the GM of the particle size distribution when the door was open 2.5 cm and "wide open" was very slightly larger in the SR than in the COR or NSR, with the SR GM being about 0.01 μm larger, although the differences were not statistically significant (Student's t-test, $p=0.17$). In the case of the 1.0 cm door opening the transport of ETS from the SR to the COR/NSR was considerably slower, leading to a smaller amount of fresh ETS in the COR and NSR after 4 hours. The data from MZ10 indicate that the GM at 4 hours for the SR, COR and NSR were 0.14 μm, 0.09 μm, and 0.08 μm, respectively. Assuming the same variance for the GM estimates as were calculated for the wider door openings, the GM of the SR particle size distribution was statistically different from that of the COR or NSR (z-test, $p<0.005$). For corroboration of this observation the OPC particle size data for the COR and NSR in test MZ09 indicate a major left-shift compared to the SR data at 4 hours. It is likely that this difference is due to the lower particle concentrations in the COR and NSR during the 1.0 cm door opening conditions leading to lower particle coagulation rates. After 20-24 hours post SR door opening in all natural flow experiments the particle size GM were virtually identical (Student's t-test $p>.05$) in the SR, COR, and NSR, most likely due to complete mixing between all of the chamber rooms at that point.

ETS tracer effectiveness

Modeling

In order to better understand the behavior of the ETS tracers we have attempted to model our experiments and compare our observations against model predictions. The two areas considered important for understanding ETS tracer behavior were nicotine dynamics in the SR and inter-room transport of bulk air and particle-phase ETS.

Nicotine Modeling

The importance of accounting for the nicotine behavior in the three-zone chamber system began with an interpretation of the work of Van Loy et al. as discussed above. The Van Loy model was employed to develop a conditioning scheme that would lead to a steady-state baseline nicotine concentration. Once data were collected from the conditioning phase of the study it became clear that nicotine behavior in the SR was not fully consistent with the Van Loy Model. What follows are three different approaches that were taken to model the SR nicotine data. The first approach employed the Van Loy model assuming two interior surfaces, painted wallboard and paint, with different adsorption and desorption coefficient values selected to optimize the fit to the data. Second, a model was developed using a pair of lumped surface adsorption and desorption parameters, linear sorption dynamics and no bulk diffusion term, as described in Equation 10. Third, the multivariate statistical approach described in equation 11 was employed.

Figure 13 shows measured and Van Loy Model-predicted nicotine concentrations in the SR during the conditioning phase of the Multi Zone ETS experiments. The model parameters given in the figure represent optimal values from fitting the model to the measured data. This set of coefficients is not unique, and similar fits to the data can be achieved with very different values. The simulation follows the measured data better during the first half of the conditioning sequence when 36 cigarettes per day were smoked in the SR. Figure 14 shows measured vs. Van Loy Model-predicted SR nicotine concentrations. A least-squares regression fit to the entire dataset fits relatively poorly ($R^2 = 0.56$) while a fit to the data for the initial 6 weeks of conditioning at 36 cigarettes per weekday is slightly better ($R^2 = 0.70$).

The second modeling approach, using lumped sorption parameters and linear dynamics with no bulk diffusion was found to describe the measured data better. Figure 15 shows the measured and modeled nicotine concentrations using this approach. Optimal values for k_{an} and k_{dn} were found to be 0.5 m h^{-1} and 1.0 x 10^{-5} h^{-1}, respectively. By the end of the conditioning period the predicted sorbed nicotine mass in the SR was 4.1 x 10^6 μg. During the conditioning period 1260 cigarettes were smoked in the chamber with estimated sidestream nicotine source strength of 5 mg cig^{-1}, for a total of 6.3 x 10^6 μg emitted. Thus, according to this model about 65% of the emitted nicotine remained sorbed to the SR surface at the end of the conditioning period. Figure 16 shows measured vs. predicted SR nicotine concentrations for this analysis. The least-square regression fit for this approach is somewhat better than for the Van Loy model ($R^2 = 0.80$).

Finally, a statistical approach to SR nicotine modeling using GLM regression was attempted. Table 4 supplies the SAS GLM output for the model described in Equation 11. Statistically significant ($p < 0.05$) parameters include t, t^2, t_{last}, n_4, λ_{24}, and marginally, λ_{168} ($p=0.13$). Figure 17 shows the relationship between measured and GLM regression-predicted nicotine concentrations. Of all approaches, the GLM method provides the best predictive power ($R^2 = 0.88$). However, the model parameters do not relate to physical properties or mechanisms such as sorption dynamics or mass balance, so that these results are not strictly generalizable to other environments. Nonetheless, the results can be interpreted. The key factors controlling nicotine levels in the SR were the total number of cigarettes ever smoked in the SR (an interpretation of elapsed time), the elapsed time since the last cigarette was smoked, the number of cigarettes smoked recently, and the recent average air exchange rate. This suggests that the smoking history and recent smoking and ventilation events play equal parts in creating the current nicotine concentration.

Mass Transport Modeling

We explored whether well-mixed-zone models of airflow, gas, and aerosol transport could describe SF_6 and ETS transport in the three-room experimental chamber. The intent was not to validate the models, rather, we have only attempted to record the degree to which the computer models could characterize the experimental setup.

Modeling of experiment MZ04

We first developed an airflow model to describe the SF_6 tracer measurements. Inputs to the COMIS model include the chamber dimensions (Figure 1), the size of the door opening between the SR and COR (2.5 cm in MZ04), the temporal temperature measurements in each room, and the overall leakage of the chamber to the outside which is derived by fitting an exponential decay model to the decay portion of several SF_6 time series.

Figure 18 shows the average temperatures and airflow between the rooms. Large airflow is predicted between the COR and NSR because the door between them is open, despite the small temperature differences between the rooms. In contrast, flow between rooms SR and COR is less than 2% of the flow between COR and NSR because the door between them is open 2.5 cm. These predictions attest to the degree that opening size between rooms can dramatically affect airflow.

Figure 19 shows the SF_6 concentrations in each room. The concentration in each room is set to values taken from the data before the doors are opened. This is to ensure that the total mass released in the experiment corresponded with the total mass modeled. Thus any incomplete mixing at the beginning of the experiment is ignored. The predicted SF_6 concentrations agree well with the data, yet with noticeable differences after t=340 minutes after the SR door was opened. We attribute the differences to mass losses during the experiment from pumps used for particle measurements exhausted air, and SF_6, from the chamber. Figure 19 also illustrates the high degree of communication between rooms

COR and NSR. With an open door, the two room could be treated a single well-mixed room.

The airflow predictions in conjunction with ETS emission profiles have been used to predict ETS transport in the MZ04 experiment. ETS emission factors were based on the average of those measured in experiments MZ01-MZ12 (Figure 12).

Figure 20 shows the total mass ETS transport modeled using MIAQ4, allowing the program to select parameter values for particle deposition as a function of particle diameter. We fit the model predictions to the data by adjusting the turbulence intensity factor in MIAQ4, as suggested by Nazaroff and Cass (1989). The parameter describes particle deposition velocities through surface boundary layers (Nazaroff and Cass, 1989). A value of 1.2 s^{-1} best fit the MZ04 ETS data. Chen et al., (1992) found intensity factors reported in the literature ranging from 0.03 s^{-1} for unstirred chambers, to greater than 10 s^{-1} for mechanically mixed chambers. In the MZ04 experiment, mixing fans were operated to ensure that each room was well-mixed.

These simulations show the extent to which the transport of ETS constituents can be understood from basic physical phenomena. Thermal gradients driving airflow were all that was needed to understand the air transport in the case of the conservative tracer SF_6. In the case of ETS particles, adding the particle deposition terms enabled an accurate prediction of particle flows. Such modeling becomes much more difficult for non-conservative air contaminants with complicated dynamic behavior and surface interaction components – nicotine would be one such contaminant.

Summary

This project focused on investigating the factors affecting particle-phase ETS in indoor environments, with the goal of providing a better link between estimates of particle-phase ETS concentrations in indoor air and the quantification of exposures and dose. Here we report our results for the laboratory study where we examined the behavior of ETS under well-controlled conditions, while (a) assessing the effectiveness of several chemical tracers for ETS and (b) evaluating re-emission of ETS components from indoor surfaces.

The laboratory-based experiments were conducted in a 50 m^3 three-room chamber. The chamber contained a "smoking room" (SR, to simulate a living room), a "corridor" (COR), and a "non-smoking room" (NSR, to simulate a child's bedroom). The walls and ceilings of the chambers were constructed of painted gypsum wallboard, and the interior walls of the NSR were lined with plastic sheeting prior to installation of the wallboard to reduce the diffusion of nicotine (or other gas-phase species) into the wallboard from the neighboring rooms. The floors were covered with a nylon carpet, typical of that used in residences. The chamber air exchange rate was about 0.02 h^{-1}, not typical of residences.

The laboratory work was conducted in two phases. In the first phase the SR was conditioned with cigarette smoke. The rationale for the conditioning phase was based on observations of Van Loy et al. (1997) who examined the behavior of nicotine in chamber that contained common indoor surface materials such as painted wallboard and carpet.

They found that sorption and desorption of nicotine are non-linear and also dependent upon the previous nicotine 'exposure history' of the materials. We used the Van Loy nicotine model to devise a chamber conditioning procedure that simulated ETS behavior in a room where smoking occurs regularly.

All smoking was done using a smoking machine, drawing one 35 cm^3 puff per minute. The sidestream smoke was emitted directly into the chamber, while the mainstream smoke -- the smoke drawn through the smoking machine -- was vented outdoors. During the conditioning phase, which lasted for 6 weeks, 36 cigarettes were machine-smoked in the SR each weekday. The other rooms remained isolated with the connecting doors closed. Particle and nicotine concentrations were measured in the SR daily throughout this period.

In the second phase, a series of 5 types of experiments was conducted to observe the movement and inter-room mixing of ETS constituents from the SR, through the COR, and into the NSR. To measure the air exchange rate, sulfur hexafluoride (SF_6) tracer gas was injected into the SR. The subsequent concentration changes of SF_6 due to mixing were monitored continuously in the three chamber rooms. The inter-room transport rate varied from 0 to 160 $m^3\ hr^{-1}$ in these experiments.

Particle number and mass size distributions were monitored on a one-hour cycle in all three rooms over a 20-hr period after smoking one cigarette. Meanwhile, particulate matter was collected on filters for gravimetric determination of respirable suspended particles (RSP). These samples contained only respirable suspended particles (RSP) since the dominant source of particles in these experiments is ETS, which is mainly composed of sub-micron particles. Chemical characterization focused on determination of tracers for ETS, including nicotine and the particle-bound tracers UVPM, FPM and solanesol from all three rooms at several times during each experiment.

a) Effects of mixing on ETS characteristics

With the doors between the SR and COR open 2.5 cm (and NSR door wide open), ETS particles reached the same concentrations in all three rooms within about 18 hours after smoking one cigarette, while the SF_6 concentrations, a surrogate for non-reactive gas-phase ETS species, equilibrated after only six hours. The difference is due to the deposition losses of the particles. With wider door openings or forced ventilation, the particles reached the same concentrations in all rooms more rapidly. The particle size distribution took the same form in each room, although the total numbers of particles in each room depended on the door configurations. The particle number size distribution moved towards somewhat larger particles (from about 1.0 μm, doubling to about 2.0 μm) as the ETS aged. Also of interest is that we were able to model inter-room transport of ETS particles from first principles –particle size dependent emission factors and deposition rates, thermal temperature gradient driven inter-room flows were combined to produce reasonable estimates of total ETS particle behavior when compared with chamber experimental data. This examination ensures our understanding of bulk inter-room ETS particle transport.

The results indicated that inter-room mixing affected individual ETS constituents differently, depending upon both the chemical identity of the ETS constituent and whether it was in the gas or particle phase.

b) Markers for assessing ETS exposures

Nicotine transport to the corridor or the non-smoking room air was significantly attenuated due to surface sorption phenomena, even when ETS particles were easily detected. The rate of sorption onto and into chamber surfaces dominated the mass transfer dynamics. Airborne nicotine was virtually unseen in the COR or NSR, even when the door openings allowed for free air exchange between the rooms.

Particulate-bound solanesol was unstable during the aging of ETS in the presence of the chamber lights and in the field study. Because solanesol was not detected in constant ratio to ETS RSP mass under realistic chamber conditions, it was not a satisfactory conservative tracer for ETS.

Our results suggest that UVPM and FPM could trace ETS concentrations more accurately than nicotine when measurements are made in environments with low smoking, varying smoking rate, or unknown smoking exposure history. This can be verified by observing that the slope of UVPM to RSP is roughly 1.0 in the SR and 0.8 in the COR and NSR indicating about a 20% reduction of PM tracer specificity through transport and loss mechanisms. In contrast the slope of nicotine to RSP is about 0.2 in the SR, dropping to about 0.05 in the COR and NSR. This is a 400% reduction in nicotine specificity of RSP. This reduction of specificity for nicotine, if it holds true in real-world environments suggests a potential for significant underestimation of exposure in the case where nicotine is used in non- or lightly-conditioned environments connected to rooms where smoking is occurring.

c) Deposited ETS as a source of pollutant emissions

The nicotine data from the phase 1 conditioning experiments are consistent with the results of Van Loy *et al.* (1997) and Piade et al. (1999). In our experiments nicotine was observed to sorb readily into the surfaces of the SR, and then to be re-emitted at a lower rate. However, the Van Loy model did not accurately predict the behavior of nicotine for the conditions and materials used in this multi-zone chamber study ($R^2 = 0.56$), although it did perform better for the initial heavy smoking conditioning period ($R^2 = 0.70$). The second modeling approach, using lumped sorption parameters and linear dynamics with no bulk diffusion was found to describe the measured data better ($R^2 = 0.80$). According to this model about 65% of the emitted nicotine remained sorbed to the SR surface after 6 weeks of frequent, heavy smoking. A third, statistical approach, not generalizable to other environments, but useful in providing insight into the factors dominating nicotine behavior, gave the best predictive power ($R^2 = 0.88$). In this model, key factors controlling nicotine levels in the SR were the total number of cigarettes ever smoked in

the SR (an interpretation of elapsed time), the elapsed time since the last cigarette was smoked, the number of cigarettes smoked recently, and the recent average air exchange rate. This suggests that the smoking history and recent smoking and ventilation events all play important parts in creating the current nicotine concentration.

It is clear from the multizone chamber experiments (Phase 2) that some ETS constituents readily deposit on surfaces, and then are re-emitted as a source of indoor pollution over a long period of time. For example in an experiment with the SR door open 2.5 cm the nicotine concentration in the SR dropped by only 40% during the 4 hours, while the SF_6 levels in the SR dropped by almost 60% of its peak value. The reason for this difference is the re-emission of nicotine from the surfaces back into the bulk air of the room.

Conclusions

In conclusion, these results show that:

(1) The dynamic behavior of nicotine in chamber studies of ETS is a function of sorption and desorption processes,
(2) In contrast to ETS particles, nicotine sorbs quickly and strongly to the surfaces of rooms where smoking does not occur regularly,
(3) Interpretation of exposure data derived from nicotine concentrations alone can be complicated and misleading
(4) Other tracers, such as UVPM and FPM can represent ETS behavior more accurately, although the effects of confounders in real-world environments may be important, and
(5) Efforts are needed to further develop cost effective and reliable ETS tracer methods. Our results suggest that UV absorbance and fluorescence techniques might be promising approaches.

Acknowledgements

We would like to thank the participants of the ETS Field Study; Marcia Brown-Machen and Tina Benitez of the Tobacco Prevention Program, Berkeley Department of Health and Human Services; and S. Katharine Hammond and Charles Perino of the School of Public Health at the University of California, Berkeley. We would also like to thank Bill Riley, Derek Shendell, and Tracy Thatcher for their reviews of this manuscript. This work was supported by funds from the California Tobacco-Related Disease Research Program, Grant Number 6RT-0307. The study was additionally supported by the U.S. Department of Energy under Lawrence Berkeley National Laboratory contract number DE-AC03-76SF00098

References

Alevantis, L. and Fisk, W.J. 2001. Effectiveness of Smoking Rooms in Relation to AB13, Progress Report to TRDRP, Year 2, 2001.

Baker, R.R. and C.J. Proctor, The origins and properties of environmental tobacco smoke, *Environment International* 16:231-245, 1990.

Chen, B.T., Yeh, H.C. and Cheng, Y.S. 1992. Evaluation of an environmental reaction chamber. Aerosol Science and Technology, 17:9-24.

Daisey, JM. (1999) "Tracers for assessing exposure to environmental tobacco smoke: What are they tracing?,"Environmental Health Perspectives, 107(SUPP2):319-327.

DHHS. 1986. *The health consequences of involuntary smoking: a report of the Surgeon General*, U.S. Department of Health and Human Services, Centers for Disease Control, Office on Smoking and Health, Rockville, MD.

Eatough, D.J., C.L. Benner, H. Tang, V. Landon, G. Richards, F.M. Caka, E.A. Lewis, L.D. Hansen and N.L. Eatough, (1989) "The chemical composition of environmental tobacco smoke III. Identification of conservative tracers of environmental tobacco smoke," Environment International 15:19-28.

Eatough DJ (1993) "Assessing Exposure to environmental tobacco smoke", in Modeling of Indoor Air Quality and Exposure. ASTM STP 1205, Niren Nagda, Ed., American Society for Testing and Materials, Philadelphia, 42-63.

Eatough, D.J., C.L. Benner, R.L. Mooney, D. Bartholomew, D.S. Steiner, L.D. Hansen, J.D. Lamb, and E.A. Lewis (1986) "Gas and particle phase nicotine in environmental tobacco smoke," Paper No. 86-68.5, Proceedings of the 79th Annual Meeting of the Air Pollution Control Association, Pittsburgh: APCA.

Eudy, L.W., F.A. Thome, D.L. Heavner, C.R. Green and B.J. Ingebrethsen (1985) "Studies on the vapor-particulate phase distribution of environmental nicotine by selected trapping and detection methods," Presented at the 39th Tobacco Chemists' Research Conference, Montreal, Canada, 1985.

Feustel, H.E. 1999. COMIS - An international multizone air-flow and contaminant transport model. Energy and Buildings, 30(1):3-18.

Feustel, H.E. and Dieris, J. 1992. A survey of airflow models for multizone structures. Energy and Buildings, 18:79-100.

Feustel, H.E. 1990. Measurements of air permeability in multizone buildings. Energy and Buildings, 14(2):103-116.

Feustel, H. E., Rayner-Hooson, A. (1990) COMIS Fundamentals, Lawrence Berkeley National Laboratory, CA-USA, LBNL-28560.

Feustel, H.E., Zuercher, C.H., Diamond, R., Dickinson, B., Grimsrud, D. and Lipschutz, R.. 1985. Temperature- and wind-induced air flow patterns in a staircase. Computer modeling and experimental verification. Energy and Buildings, 8:105-122.

Gundel, L.A., Fisk, W.J., Apte, M.G.; Sullivan, D.; Faulkner D.; Shpilberg, V. 2000. Real-time monitoring of environmental tobacco smoke in the presence of other combustion sources, presented at the annual meeting of the International Society for Exposure Analysis, Asilomar, CA, October 2000.

Gundel, L.A.; Hansen A.D.A.; Apte, M.G. 1997. Real-time monitoring of ETS by ultraviolet absorption, presented at the 1997 annual meeting of the American Association for Aerosol Research.

Haghighat, F, and Megri, A.C., 1996. A comprehensive validation of two airflow models - COMIS and CONTAM. Indoor Air, 6(4):278-288.

Hodgson, A.T. and Girman, J.R. 1989. Application of a Multisorbent Sampling Technique for Investigations of Volatile Organic Compounds in Buildings. Design and Protocol for Monitoring Indoor Air Quality, ASTM STP 1002, N.L. Nagda and J.P. Harper, Eds., American Society for Testing and Materials, Philadelphia, PA, pp. 244-256.

Hammond SK, Leaderer BP (1987) "Diffusion monitor to measure exposure to passive smoking," *Environmental Science and Technology*; 21:494-497.

Hecht, S.S., and D. Hoffmann, Tobacco-specific nitrosamines, an important group of carcinogens in tobacco and tobacco smoke. Carcinogenesis 39:875-884, 1988.

Hoffmann, D. and E.L. Wynder, Chemical constituents and bioactivity of tobacco smoke. In D.G. Zaridze and R. Peto, Eds., *Tobacco: A Major International Health Hazard*, Lyon, France: IARC Publications, Vol. 74, 1986.

Jenkins, P.L., T.J. Phillips, E.J. Mulberg and S.P. Hui (1992) "Activity patterns of Californians: Use of and proximity to indoor pollutant sources," *Atmospheric Environment*, 26(A):2141-2148.

La Kind JS, Jenkins RA, Naiman DQ, Ginevan ME, Graves CG, Tardiff, RG (1999) "Use of Environmental Tobacco Smoke Constituents as Markers for Exposure," *Risk Analysis*; 19(3):359-373.

Miller, S.L, Lieserson, K, Nazaroff, W.W. 1997. Nonlinear least-squares minimization applied to tracer gas decay for determining airflow rates in a two-zone building. *Indoor Air*, 7:64-75.

Nazaroff, W.W., Hung, W.Y., Sasse A.G., and Gadgil, A.J. 1993. Predicting regional lung deposition of environmental tobacco smoke particles. *Aerosol Science and Technology*, 19(3),243-254.

Nazaroff, W.W., Ligocki, M.P., Ma, T., and Cass, G.R. (1990). Particle deposition in museums: Comparison of modeling and measurement results. *Aerosol Sci. Technol*., 13(3):332-348.

Nazaroff, W.W., and Cass, G.R. 1989. Mathematical modeling indoor aerosol dynamics. *Env. Sci. Technol*., 23(2):157-166.

NRC (1986) *Environmental Tobacco Smoke: Measuring Exposures and Assessing Health Effects*, National Research Council, Washington, DC: National Academy Press.

Ogden M.W. and Maiolo, K.C. 1992. Determination of solanesol by gas and liquid chromatography, *LC/GC* 10, 459-463, 1992

Ogden, M.W., Maiolo, K.C.; Oldacker, G.B., Conrad, F.W. 1990. Tracers for assessment of environmental tobacco smoke in indoor environments, Indoor Air 90, Proceedings of the 5th International Conference on indoor Air Quality and Climate, Toronto, 2, 415-420.

Phillips K, Howard DA, Bentley MC, Alvan G (1999) "Assessment of Environmental Tobacco Smoke and Respirable Suspended Particle Exposures for Nonsmokers in Basel by Personal USEPA (1992). *Respiratory Health Effects of Passive Smoking: Lung Cancer and Other Disorders*, EPA/600/6-90/006F, U.S. Environmental Protection Agency, Washington, DC.

Piade, J.J., D'Andres, S., and Sanders, E.B. 1999 Sorption Phenomena of Nicotine and Ethenylpyridine Vapors on Different Materials in a Test Chamber*, Environ. Sci. Technol*., 33:2046-2052.

SAS 1989. SAS/STAT user's guide, Version 6, 4th ed., SAS Institute, Cary NC.

Sextro, R.G., Daisey, J.M., Feustel, H.E., Dickerhoff, D.J., and Jump, C. 1999. Comparison of modeled and measured tracer gas concentrations in a multizone building. 8th Int. Conf. on Indoor Air Quality & Climate, Indoor Air 99.

Spengler, J.D., D.W. Dockery, W.A. Turner, J.M. Wolfson, and B.J. Ferris, Long-term measurements of respirable sulphates and particles inside and outside homes, *Atmospheric Environment*. 15:23-30, 1981.

Traynor GW, DW Anthon and CD Hollowell, 1982. Technique for determining pollutant emissions from a gas-fired range. Atmos. Environ. 16:2979

USEPA (1992). *Respiratory Health Effects of Passive Smoking: Lung Cancer and Other Disorders*, EPA/600/6-90/006F, U.S. Environmental Protection Agency, Washington, DC.

Van Loy M.D., W.J. Riley, Daisey, J.M. and Nazaroff, W.W. 2001. Dynamic behavior of semivolatile organic compounds in indoor air. 2. Nicotine and phenanthrene with carpet and wallboard. Environ Sci. Technol. 35(3):560-567.

Van Loy M.D. 1998. Dynamic Behavior of Semivolatile Organic Compounds in Indoor Air. Ph.D. Dissertation, University of California at Berkeley, LBNL-42674, E.O. Lawrence Berkeley National Laboratory, Berkeley CA.

Van Loy, M.D.; Lee, V.C.; Gundel, L.A.; Sextro, R.G.; Daisey, J.M.; Nazaroff, W.W. 1997. Dynamic behavior of semivolatile organic compounds in indoor air, 1. Nicotine in a stainless steel chamber. Environ. Sci. Technol., 31(9):2554-2561.

Wald, N.J., K. Nanchahal, S.G. Thompson, and H.S. Cuckle (1986) "Does breathing other people's tobacco smoke cause lung cancer?" British. Medical. Journal, 293:1217-1222.

Wells, A.J. (1988) "An estimate of adult mortality in the United States from passive smoking," Environment International 14:249-265, 1988.Zhao, Y, Yoshino, H, and Okuyama, H. 1998. Evaluation of the COMIS model by comparing simulation and measurement of airflow and pollutant concentration. Indoor Air, 8(2):123-130.

Zhao Y.; Yoshino H.; Okuyama H. (1998). Evaluation of the COMIS Model by Comparing Simulation and Measurement of Airflow and Pollutant Concentration; *Indoor Air,* 8:123-130.

TABLES

Table 1. Instrumentation and methods used in the multizone chamber ETS experiments.

Parameter	Sampling Method	Sampling Duraton/ Flowrate	Analytical Method	Characteristics (measurement units)	Manufacturer/Model
Particle					
Mass	Filtration	0.25 – 4hr/ 63 L min^{-1}	Gravimetric	Particle Mass ($\mu g\ m^{-3}$)	Cahn Microbalance Model 21
	Impaction	0.25-20min/ 240 ml min^{-1}	Quartz Crystal Microbalance	Particle Mass 10 size bins 0.05 - 25 μm ($\mu g\ m^{-3}$)	California Measurements/ PC-2
Size	Differential Mobility	17 min/ 3 L min^{-1}	Condensation Nuclei Counting	Particle Number Counting, 0.01 to 0.45 μm, (Particles- cm^{-3})	TSI/Classifier 3071 Ultrafine Condensation Particle Counter 3025
	Optical Cavity	Continuous 2.7 L Min^{-1}	Laser Counting	Particle Number Counting, 0.01 to >3.0 μm, (Particles- cm^{-3})	Particle Measurements Systems/LAS-X
Chemistry	Filtration		Spectrophotometry/ HPLC[1]	Solanesol, UV Absorbing PM ($\mu g\ m^{-3}$)	Perkin-Elmer UV/Vis Lambda2 / HPLC, Hewlett Packard 1090M
Gas					
Nicotine	Tenax Sorbent Tube	1 – 10 min/ 2 L min^{-1}	Thermal Desorption - GC-NPD[2]	Time-averaged Nicotine Concentration ($\mu g\ m^{-3}$)	Hewlett Packard/ GC 5890 NPD Chrompack CP4020 TCT Injector
CO	Flow-Through	Continuous 1.0 L Min^{-1}	Gas Filter Correlation IR	Real-time Resolution (ppm)	Thermo-Environmental/Model 48
SF6	GC Trap	Continuous 1.0 L Min^{-1}	GC-ECD[2]	Near Real-time (ppb)	Hewlett Packard/ 5890
Temperature		Continuous	Thermocouple Array	Temperature (ºC)	LBNL
Humidity		Continuous	Capacitance Sensor	Relative Humidity (%)	General Eastern/MRH
ΔPressure		Continuous	Strain Gauge	Real-time pressure difference (Pa)	

[1] High Performance Liquid Chromatography; [2] Gas Chromatography/nitrogen phosphorous detection; [3] Gas Chromatography/electron capture detection

Table 2. Chamber door settings, inter-room transport, and Smoking Room pollutant decay rates

Test Name	Date	SR door setting	Flow Conditions	Inter-room Air Flow (m^3/h)	Standard Deviation	Gas Decay Rate (h^{-1})	Particle Decay Rate (h^{-1})	Particle Loss Rate (h^{-1})
MZ01	11/3/98	Sealed	Static	0		0.02	0.17	0.15
MZ02	11/5/98	Sealed	Static	0		0.04	0.15	0.10
Average:				0		0.03	0.16	0.12
MZ03	11/9/98	2.5 cm	Static	5.44	1.91	0.27	0.34	0.08
MZ04	11/11/98	2.5 cm	Static	6.03	3.09	0.21	0.38	0.16
MZ05	3/26/99	2.5 cm	Static	6.19	6.55	0.31	0.39	0.08
MZ07	4/8/99	2.5 cm	Static	4.37	4.07	0.13		
Average:				*5.51*		*0.23*	*0.37*	*0.11*
MZ06	4/1/99	Wide	Static	67.1	30.38	0.82	1.08	0.26
MZ08	4/12/99	Wide	Static	50.3	16.06	0.90	1.03	0.13
Average:				*58.7*		*0.86*	*1.06*	*0.20*
MZ09	4/19/99	1 cm	Static	0.79	3.97	0.06	0.14	0.08
MZ10	4/26/99	1 cm	Static	1.13	6.38	0.07	0.12	0.05
Average:				*0.96*		*0.07*	*0.13*	*0.06*
MZ11	5/3/99	1 cm	Forced	157.34		3.24	2.98	
MZ12	5/10/99	1 cm	Forced	138.35		2.85	2.50	
Average:				*147.84*		*3.04*	*2.74*	

Table 3. ETS tracer data for interroom transport experiments in the LBNL multizone environmental chamber.

Location/Time/Test Conditions	Just Before Smoking			Peak			Just After Smoking			4 Hours After Smoking			20 Hours After Smoking		
Test MZ01, Door Sealed, inter-room flowrate 0.0 m3/h	**SR**	**COR**	**NSR**	**SR**	**COR**	**NSR**	**SR**	**COR**	**NSR**	**SR**	**COR**	**NSR**	**SR**	**COR**	**NSR**
Nicotine (μg/m^3)	89.2			179.1			116.2			114.4					
UVPM (μg/m^3)	382	11	17	695			505						575		
FPM (μg/m^3)	297	18	22	835			319						447		
RSP (μg/m^3)	428	14	21	922			662								
Part. Size GM (GSD) (μm)	0.37 (2.8)	0.07 (2.0)	0.06 (2.3)	0.12 (1.8)	0.08 (2.0)	0.06 (2.0)	0.16 (1.7)	0.09 (2.0)	0.07 (2.1)	0.25 (1.9)	0.10 (1.9)	0.08 (2.1)			
RSP/Nicotine	4.8			5.1			5.7								
RSP/UVPM	1.1	1.3	1.2	1.3			1.3								
RSP/FPM	1.4	0.8	1.0	1.1			2.1								
Test MZ02, Door Sealed, inter-room flowrate 0.0 m3/h	**SR**	**COR**	**NSR**	**SR**	**COR**	**NSR**	**SR**	**COR**	**NSR**	**SR**	**COR**	**NSR**	**SR**	**COR**	**NSR**
Nicotine (μg/m^3)	119.9			185.9			127.9			132.8					
UVPM (μg/m^3)	468	13	8	828			509								
FPM (μg/m^3)	449	13	9	897			512								
RSP (μg/m^3)	368	20	10	845			527								
Part. Size GM (GSD) (μm)	0.31 (3.1)		0.08 (2.1)	0.09 (1.9)	0.09 (2.1)	0.10 (2.2)	0.15 (1.8)	0.10 (2.0)	0.07 (2.2)	0.16 (1.8)	0.11 (2.0)	0.08 (2.2)			
RSP/Nicotine	3.1			4.5			4.1								
RSP/UVPM	0.8	1.5	1.3	1.0			1.0								
RSP/FPM	0.8	1.5	1.1	0.9			1.0								
Test MZ03, Door Open 2.5 cm, inter-room flowrate 5.4 m3/h	**SR**	**COR**	**NSR**	**SR**	**COR**	**NSR**	**SR**	**COR**	**NSR**	**SR**	**COR**	**NSR**	**SR**	**COR**	**NSR**
Nicotine (μg/m^3)	77.1	9.6	7.4	83.4			81.2	15.0	8.8	80.8	7.2	7.0			
UVPM (μg/m^3)	13	16	23	577				110	104	121	172	118			
FPM (μg/m^3)	18	13	23	562				74	96	121	148	95			
RSP (μg/m^3)	17	11	24	465				61	124	141	176	126			
Part. Size GM (GSD) (μm)	0.10 (1.7)	0.10 (1.7)	0.06 (2.1)	0.12 (1.8)	0.12 (1.7)	0.11 (1.7)	0.16 (2.0)	0.12 (1.7)	0.12 (1.7)	0.22 (1.8)		0.13 (1.7)			
RSP/Nicotine	0.2	1.2	3.3	5.6				4.1	14.1	1.7	24.4	18.0			
RSP/UVPM	1.3	0.7	1.1	0.8				0.6	1.2	1.2	1.0	1.1			
RSP/FPM	1.0	0.9	1.0	0.8				0.8	1.3	1.2	1.2	1.3			

Table 3 (continued). ETS tracer data for inter-room transport experiments in the LBNL multizone environmental chamber.

Location/Time/Test Conditions	Just Before Smoking			Peak			Just After Smoking			4 Hours After Smoking			20 Hours After Smoking		
Test MZ04, Door Open 2.5 cm, inter-room flowrate 6.0 m3/h	**SR**	**COR**	**NSR**	**SR**	**COR**	**NSR**	**SR**	**COR**	**NSR**	**SR**	**COR**	**NSR**	**SR**	**COR**	**NSR**
Nicotine (μg/m^3)	113.3	8.0	10.2	139.0	12.0			11.4		83.0	12.5	10.6	57.0	11.0	
UVPM (μg/m^3)	521		24	859				26	130	253	84	159	46	42	69
FPM (μg/m^3)	337		38	736				27	109	258	75	135	35	35	70
RSP (μg/m^3)	495	17	36	930				30		228	87	194	62	58	81
Part. Size GM (GSD) (μm)		0.13 (1.7)	0.14 (2.0)	0.10 (1.8)	0.15 (1.7)	0.12 (1.7)	0.14 (1.8)	0.13 (2.0)	0.13 (1.7)	0.14 (1.9)		0.14 (1.8)	0.15 (2.0)		0.15 (2.0)
RSP/Nicotine	4.4	2.1	3.5	6.7				2.7		2.7	7.0	18.3	1.1	5.3	
RSP/UVPM	1.0		1.5	1.1				1.2		0.9	1.0	1.2	1.3	1.4	1.2
RSP/FPM	1.5		0.9	1.3				1.1		0.9	1.2	1.4	1.8	1.7	1.2
Test MZ05, Door Open 2.5 cm, inter-room flowrate 6.2 m3/h	**SR**	**COR**	**NSR**	**SR**	**COR**	**NSR**	**SR**	**COR**	**NSR**	**SR**	**COR**	**NSR**	**SR**	**COR**	**NSR**
Nicotine (μg/m^3)	34.6	0.2	0.1	257.1			70.4	5.9	3.4	97.1		2.4	45.9	2.6	2.1
UVPM (μg/m^3)	152	2	1	635			150	78	58	77	64	95	20	17	19
FPM (μg/m^3)	142	5	1	728			174	92	75	77	57	124	19	16	11
RSP (μg/m^3)	201	16	9	677			306	127	139	120	104	93	47	38	38
Part. Size GM (GSD) (μm)	0.10 (1.8)		0.12 (2.4)	0.12 (1.8)		0.12 (1.8)	0.12 (1.8)	0.11 (2.0)	0.13 (1.7)	0.15 (1.8)	0.14 (1.7)	0.14 (1.7)	0.17 (1.9)	0.14 (2.0)	0.10 (2.2)
RSP/Nicotine	5.8	83.4	91.9	2.6			4.3	21.7	41.0	1.2		37.8	1.0	14.9	17.8
RSP/UVPM	1.3	9.1	9.0	1.1			2.0	1.6	2.4	1.6	1.6	1.0	2.4	2.3	2.0
RSP/FPM	1.4	3.2	6.8	0.9			1.8	1.4	1.9	1.6	1.8	0.7	2.5	2.4	3.4
Test MZ06, Door Wide Open, inter-room flowrate 67.2 m3/h	**SR**	**COR**	**NSR**	**SR**	**COR**	**NSR**	**SR**	**COR**	**NSR**	**SR**	**COR**	**NSR**	**SR**	**COR**	**NSR**
Nicotine (μg/m^3)	85.8	0.3	0.1	244.8			47.9	15.7	10.2	36.6	12.3	8.1	23.4	7.4	6.3
UVPM (μg/m^3)	19	7	2	632			118	130	134	80	56	70	18	28	17
FPM (μg/m^3)	13	6	1	737			114	118	115	74	36	48	17	21	20
RSP (μg/m^3)	33	6	7	662			146	124	151	96	98	100	32	35	33
Part. Size GM (GSD) (μm)	0.37 (2.6)	0.09 (2.2)		0.11 (1.7)	0.12 (1.7)		0.13 (1.7)	0.14 (1.7)	0.13 (1.8)	0.15 (1.7)	0.14 (1.8)	0.15 (1.7)	0.16 (1.8)	0.14 (2.0)	0.18 (1.9)
RSP/Nicotine	0.4	19.9	68.5	2.7			3.0	7.9	14.8	2.6	8.0	12.5	1.4	4.8	5.2
RSP/UVPM	1.8	0.9	5.0	1.0			1.2	1.0	1.1	1.2	1.8	1.4	1.8	1.3	1.9
RSP/FPM	2.5	1.0	5.5	0.9			1.3	1.1	1.3	1.3	2.7	2.1	1.9	1.7	1.6

Table 3 (continued). ETS tracer data for inter-room transport experiments in the LBNL multizone environmental chamber.

Location/Time/Test Conditions	Just Before Smoking			Peak			Just After Smoking			4 Hours After Smoking			20 Hours After Smoking		
Test MZ07, Door Open 2.5 cm, inter-room flowrate 4.4 m3/h	**SR**	**COR**	**NSR**	**SR**	**COR**	**NSR**	**SR**	**COR**	**NSR**	**SR**	**COR**	**NSR**	**SR**	**COR**	**NSR**
Nicotine (μg/m^3)	101.6	0.4	0.2										53.6	1.6	1.5
UVPM (μg/m^3)				676											
FPM (μg/m^3)				715											
RSP (μg/m^3)				673											
Part. Size GM (GSD) (μm)	0.31 (1.4)	0.11 (2.3)		0.11 (1.8)			0.15 (1.7)	0.14 (1.7)		0.17 (1.8)	0.16 (1.8)	0.16 (1.7)	0.18 (1.8)	0.19 (1.9)	0.19 (1.9)
RSP/Nicotine															
RSP/UVPM				1.0											
RSP/FPM				0.9											
Test MZ08, Door Wide Open, inter-room flowrate 50.3 m3/h	**SR**	**COR**	**NSR**	**SR**	**COR**	**NSR**	**SR**	**COR**	**NSR**	**SR**	**COR**	**NSR**	**SR**	**COR**	**NSR**
Nicotine (μg/m^3)	75.5	0.5	0.3	171.4			50.7	11.8	4.8	37.4	9.3	4.1	24.1	6.6	4.0
UVPM (μg/m^3)	1	1	0	391			110	60	51	63	60	63	11	5	11
FPM (μg/m^3)	2	1	0	424			105	43	37	64	55	60	11	7	9
RSP (μg/m^3)	4	7	4	531		115	138	115	115	85	84	74	19	21	21
Part. Size GM (GSD) (μm)	0.05 (1.8)	0.06 (1.9)		0.11 (1.7)	0.11 (1.9)	0.03 (4.0)	0.13 (1.6)	0.12 (1.8)	0.12 (1.8)	0.14 (1.7)	0.13 (1.8)		0.16 (1.7)	0.15 (1.9)	0.15 (1.8)
RSP/Nicotine	0.1	14.2	15.1	3.1			2.7	9.8	24.2	2.3	9.0	18.0	0.8	3.2	5.2
RSP/UVPM	5.6	7.9	11.7	1.4			1.3	1.9	2.3	1.3	1.4	1.2	1.7	3.9	1.9
RSP/FPM	2.3	13.4	14.1	1.3			1.3	2.7	3.1	1.3	1.5	1.2	1.7	2.9	2.3
Test MZ09, Door Open 1.0 cm, inter-room flowrate 0.8 m3/h	**SR**	**COR**	**NSR**	**SR**	**COR**	**NSR**	**SR**	**COR**	**NSR**	**SR**	**COR**	**NSR**	**SR**	**COR**	**NSR**
Nicotine (μg/m^3)	68.1	0.7	0.0	172.3			101.6	0.7	0.7	98.1	0.7	0.5	78.1	0.8	0.7
UVPM (μg/m^3)	2	2	2	438			730	14	18	216	15	20	21	14	14
FPM (μg/m^3)	3	2	2	510			245	16	18	154	17	16	16	12	11
RSP (μg/m^3)	3	6	3	560			385	29	10	220		14	16	18	14
Part. Size GM (GSD) (μm)															
RSP/Nicotine	0.0	7.8	120.5	3.3			3.8	39.2	15.1	2.2		26.7	0.2	21.9	20.2
RSP/UVPM	1.2	3.6	1.5	1.3			0.5	2.1	0.5	1.0		0.7	0.8	1.3	1.0
RSP/FPM	1.0	3.5	1.6	1.1			1.6	1.8	0.5	1.4		0.9	1.0	1.5	1.2

Table 3 (continued). ETS tracer data for inter-room transport experiments in the LBNL multizone environmental chamber.

Location/Time/Test Conditions	Just Before Smoking			Peak			Just After Smoking			4 Hours After Smoking			20 Hours After Smoking		
Test MZ10, Door Open 1.0 cm, inter-room flowrate 1.1 m3/h	**SR**	**COR**	**NSR**	**SR**	**COR**	**NSR**	**SR**	**COR**	**NSR**	**SR**	**COR**	**NSR**	**SR**	**COR**	**NSR**
Nicotine (μg/m^3)	68.6	0.4	0.3	167.2			79.3		0.4	80.2	0.5	0.2	70.3	0.6	0.5
UVPM (μg/m^3)	3	1	1	508			561	16	13	275	10	14	26	12	24
FPM (μg/m^3)	4	2	2	585			426	15	16	232	14	16	21	13	15
RSP (μg/m^3)	7	6	3	540			408	28	22	263	33	14	27	30	18
Part. Size GM (GSD) (μm)	0.05 (2.1)	0.05 (2.0)		0.14 (1.8)	0.06 (1.8)	0.06 (2.0)	0.14 (1.8)	0.07 (1.7)	0.06 (2.1)	0.14 (2.0)	0.09 (2.0)	0.08 (2.0)	0.20 (1.7)	0.17 (1.8)	0.17 (1.9)
RSP/Nicotine	0.1	14.0	11.4	3.2			5.1		60.2	3.3	69.5	60.2	0.4	49.9	34.6
RSP/UVPM	2.2	4.3	2.9	1.1			0.7	1.8	1.6	1.0	3.4	1.0	1.0	2.6	0.8
RSP/FPM	1.9	3.5	2.0	0.9			1.0	1.9	1.4	1.1	2.3	0.8	1.3	2.4	1.2

Forced Flow Experiments Below:	Just Before Smoking			Peak			Just After Smoking			2 Hours After Smoking			3 Hours After Smoking			20 Hours After Smoking		
Test MZ11, Door Open 1.0 cm, inter-room flowrate 157.3 m3/h	**SR**	**COR**	**NSR**	**SR**	**COR**	**NSR**	**SR**	**COR**	**NSR**	**SR**	**COR**	**NSR**	**SR**	**COR**	**NSR**	**SR**	**COR**	**NSR**
Nicotine (μg/m^3)	107.2	0.4	0.0	237.1			70.1	13.1	6.4	38.3	13.9	5.8	18.7	1.2	1.0	73.5	0.2	0.6
UVPM (μg/m^3)	4	8	2	644			111	114	111	8	39	69	9	15	11	4	2	3
FPM (μg/m^3)	3	6	3	778			118	142	118	13	34	63	10	14	11	4	3	3
RSP (μg/m^3)	8	12	6	529			102	146	131	13	61	53	6	25	20	5	7	4
Part. Size GM (GSD) (μm)	0.06 (2.2)	0.05 (2.0)		0.10 (1.8)		0.07 (2.0)	0.11 (1.8)	0.11 (1.8)	0.12 (1.8)	0.03 (1.9)	0.12 (1.7)	0.12 (1.8)	0.04 (1.7)	0.09 (2.0)	0.10 (2.0)	0.08 (2.1)	0.08 (2.2)	0.07 (2.3)
RSP/Nicotine	0.1	29.7	309.2	2.2			1.5	11.2	20.6	0.3	4.4	9.2	0.3	21.5	19.6	0.1	27.5	6.7
RSP/UVPM	1.9	1.5	2.4	0.8			0.9	1.3	1.2	1.5	1.6	0.8	0.7	1.7	1.9	1.3	2.6	1.2
RSP/FPM	2.7	2.1	1.8	0.7			0.9	1.0	1.1	1.0	1.8	0.8	0.6	1.8	1.8	1.3	2.2	1.4
Test MZ12, Door Open 1.0 cm, inter-room flowrate 138.3 m3/h	**SR**	**COR**	**NSR**	**SR**	**COR**	**NSR**	**SR**	**COR**	**NSR**	**SR**	**COR**	**NSR**	**SR**	**COR**	**NSR**	**SR**	**COR**	**NSR**
Nicotine (μg/m^3)	83.6	0.3	0.2	254.8			74.8	5.5	3.5	56.4	4.6	2.1	23.1	1.6	0.8	64.9	0.2	0.2
UVPM (μg/m^3)	6	2	2	655			154	92	120	27	63	81	4	11	14	2	2	2
FPM (μg/m^3)	6	2	2	568			95	91	107	25	55	67	5	10	13	3	2	2
RSP (μg/m^3)	6	7	3	650			164	179	157	16	85	84	3	15	15	5	9	5
Part. Size GM (GSD) (μm)	0.07 (1.8)	0.06 (1.9)	0.06 (1.8)	0.13 (1.8)		0.07 (1.9)	0.15 (1.8)	0.14 (1.9)	0.15 (1.8)	0.11 (2.2)	0.15 (1.8)	0.14 (1.8)	0.07 (2.5)	0.15 (1.8)	0.09 (2.2)	0.09 (2.2)	0.09 (2.4)	0.09 (2.2)
RSP/Nicotine	0.1	20.2	15.0	2.6			2.2	32.6	44.9	0.3	18.4	40.4	0.1	9.5	17.7	0.1	35.6	22.5
RSP/UVPM	1.0	4.3	2.0	1.0			1.1	2.0	1.3	0.6	1.4	1.0	0.7	1.4	1.0	2.0	4.5	2.6
RSP/FPM	1.1	3.8	2.1	1.1			1.7	2.0	1.5	0.6	1.5	1.3	0.5	1.6	1.1	1.8	4.1	2.7

Table 4. SAS General Linear Models Procedure output. This model explores the association between time series of log-measured SR nicotine concentrations and the smoking and ventilation sequence during the conditioning phase of the multi-zone ETS experiments. The regression coefficients and their probabilities are given for the statistically significant ($p<0.15$) model parameters.

General Linear Models Procedure

Dependent Variable: LOGE [ln(nic)]

Source	DF	Sum of Squares	Mean Square	F Value	Pr > F
Model	7	103.26794889	14.75256413	95.29	0.0001
Error	184	28.48692019	0.15482022		
Corrected Total	191	131.75486908			

R-Square	C.V.	Root MSE	LOGE Mean
0.783788	8.331600	0.3934720	4.72264651

Parameter	Parameter Estimate	T for H0: Parameter=0	Pr > |T|	Std Error of Estimate
INTERCEPT	5.3698	32	0.0001	0.1657
Elapsed Time since first cig	-0.0127	-5.1	0.0001	0.0025
(Elapsed Time since first cig)^2	0.00004	5.0	0.0001	0.00001
Time since last cigarette	-0.0036	-5.5	0.0001	0.0007
Number of Cigs smoked in last 4 hrs	0.0411	11	0.0001	0.0037
Avg. vent rate last 24 hrs	-0.2366	-7.7	0.0001	0.0309
Number of cigs smoked last 24-168 hrs	0.0048	4.0	0.0001	0.0012
Avg. vent. rate last 24 - 168hrs	-0.0224	-1.5	0.1307	0.0147

Figures

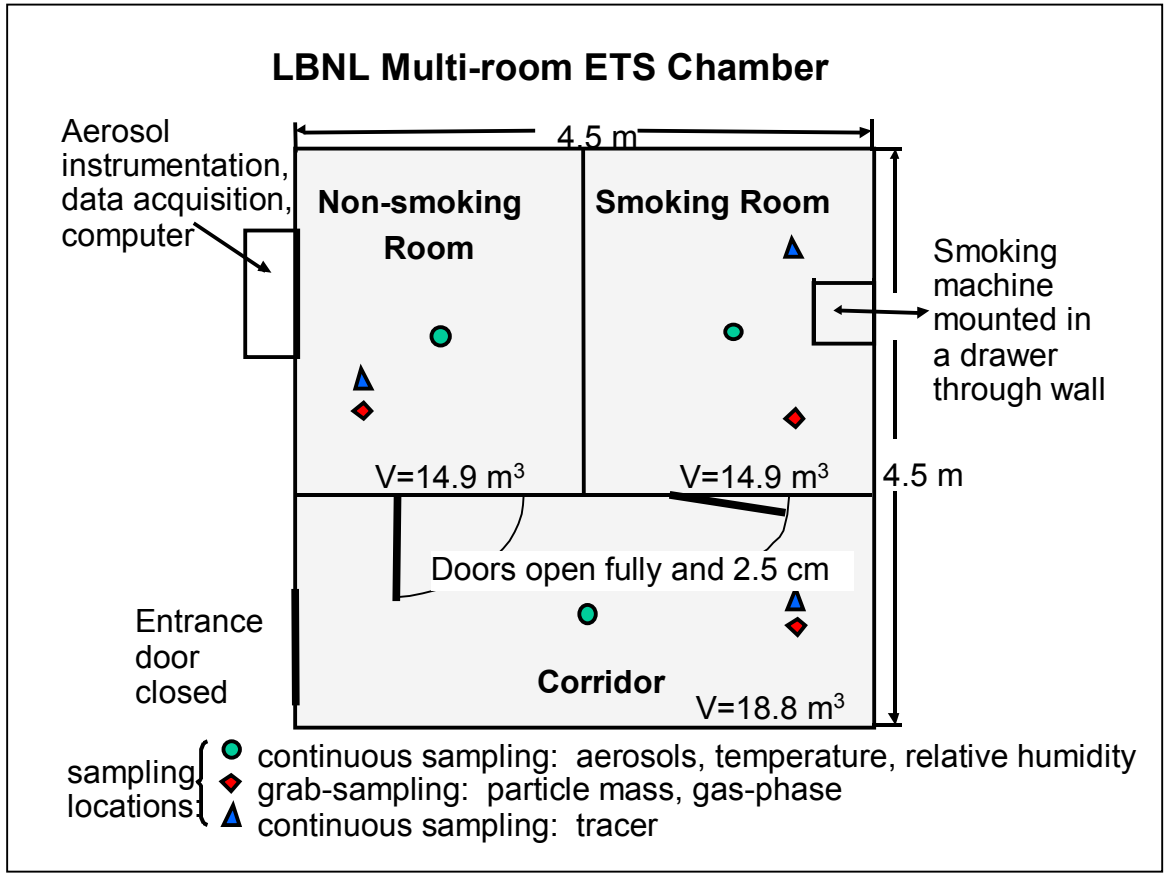

Figure 1. Schematic of the LBNL multi-room environmental chamber.

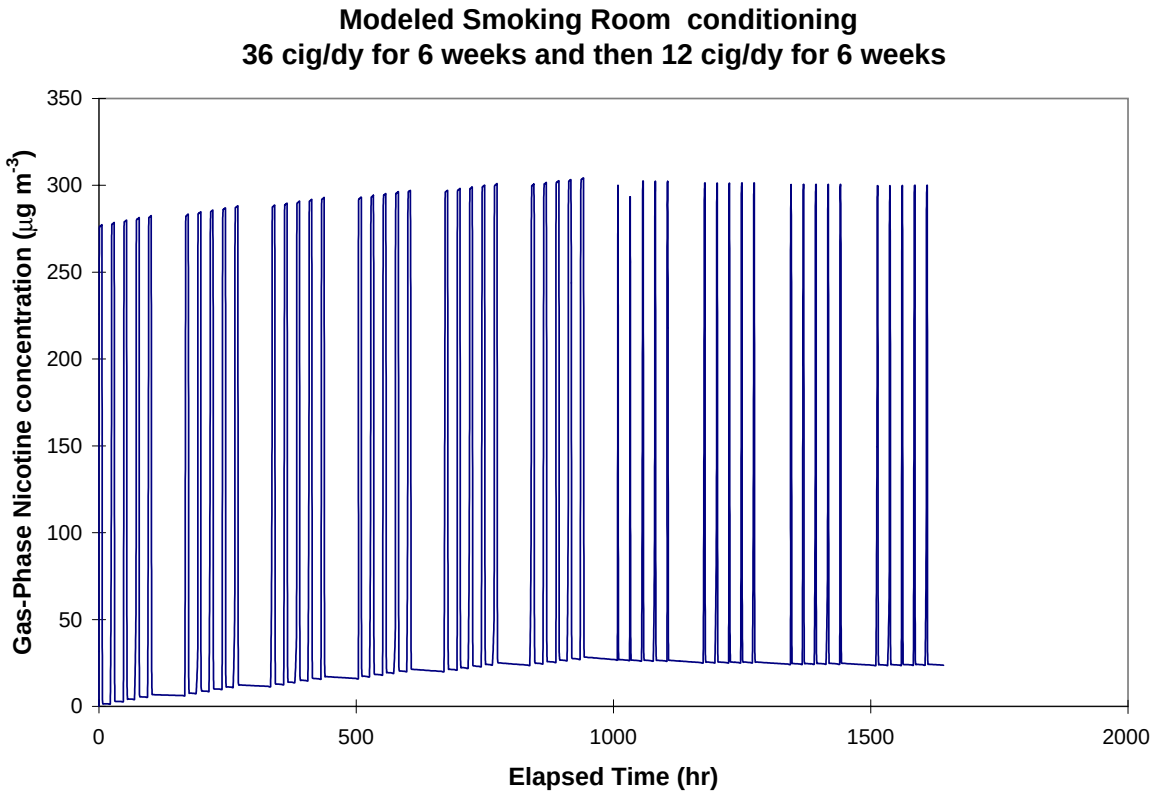

Figure 2. Predicted Smoking Room nicotine concentrations using the Van Loy model assuming a nicotine emission rate of 5.0 mg cig^{-1}, and a SR volume of 14.9 m^3. The particles are based on smoking 36 cigarettes sequentially on each weekday with no smoking during the weekend. After 1000 hours, the assumed daily smoking rate was reduced to 6 cigarettes per day.

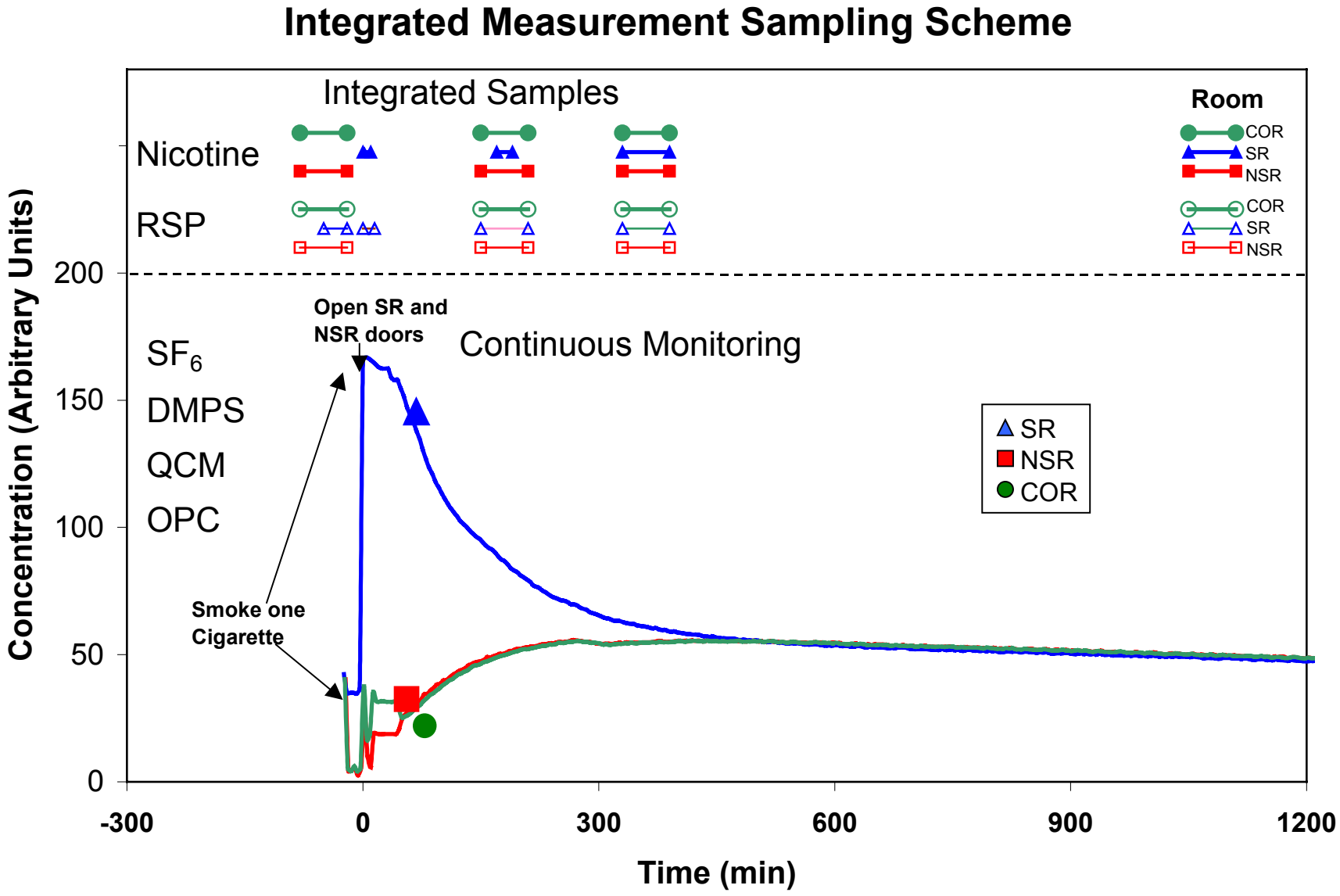

Figure 3. Inter-room ETS transport experimental protocol and measurement schedule. The triangles denote smoking room concentrations, while the circles and squares denote corridor and non-smoking rooms, respectively.

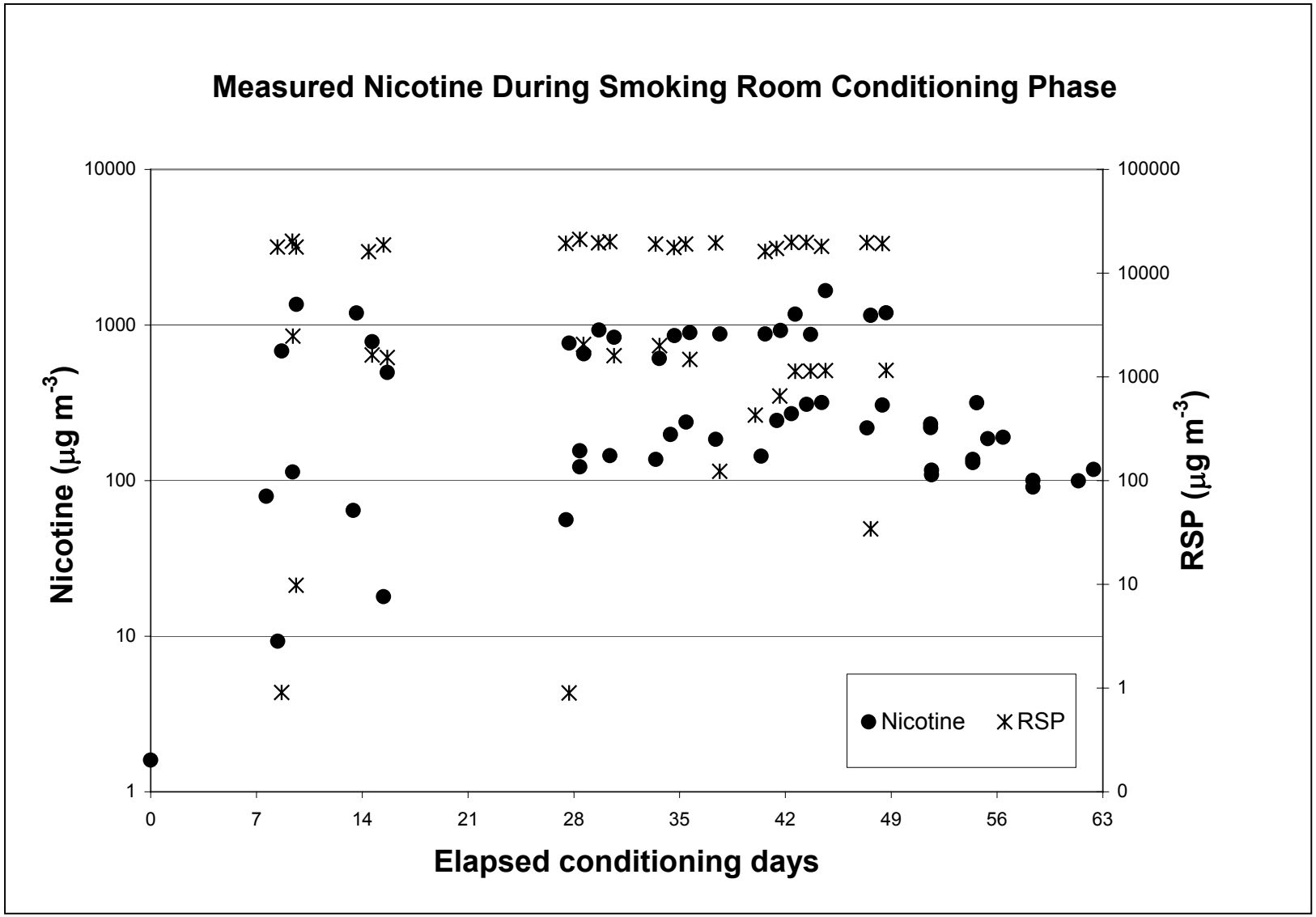

Figure 4. Nicotine and RSP concentrations in the smoking room during the conditioning phase. Note that measurements were taken prior to and just after smoking during each smoking day.

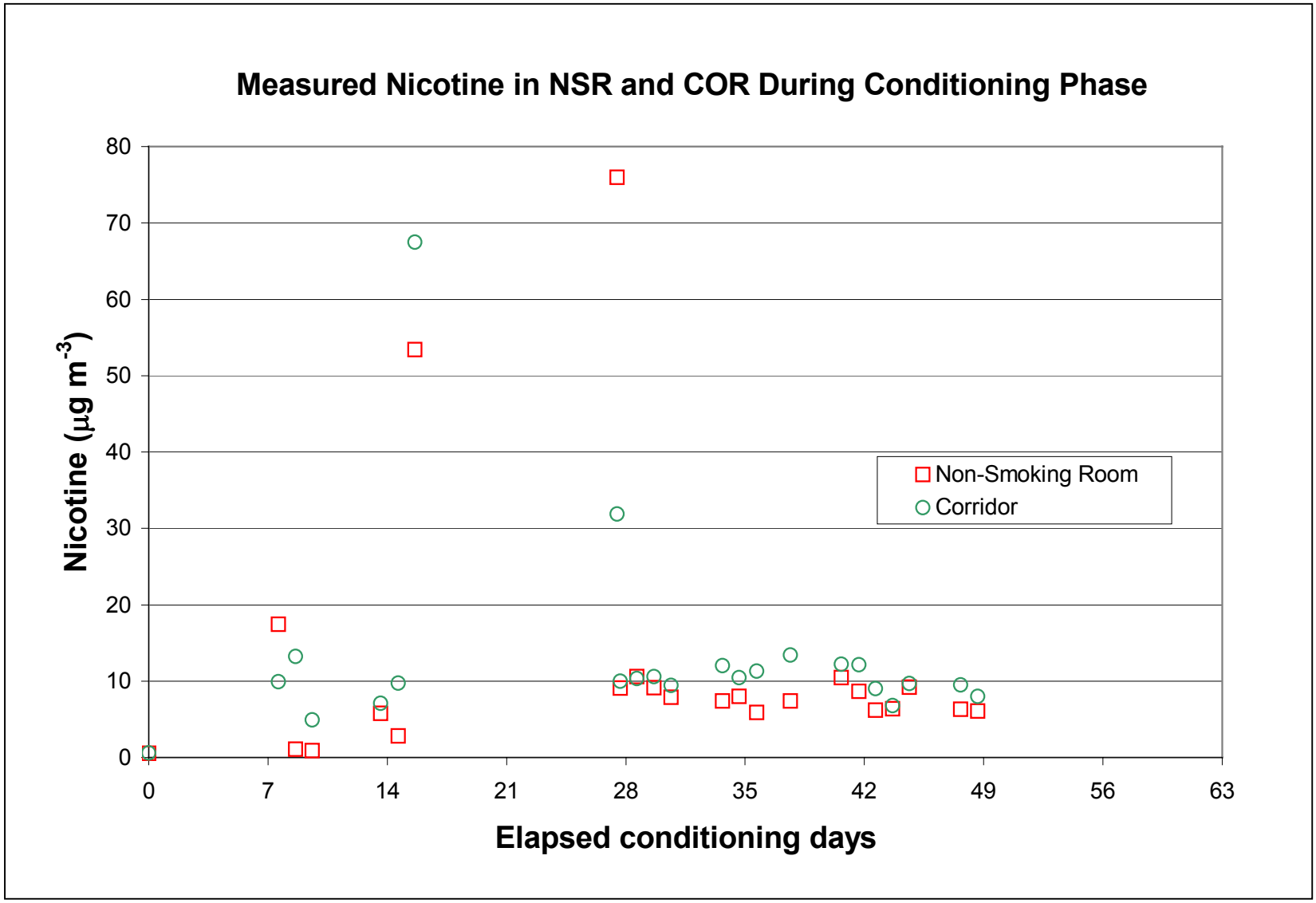

Figure 5. Nicotine concentrations in the Non-Smoking Room and Corridor during the SR conditioning phase.

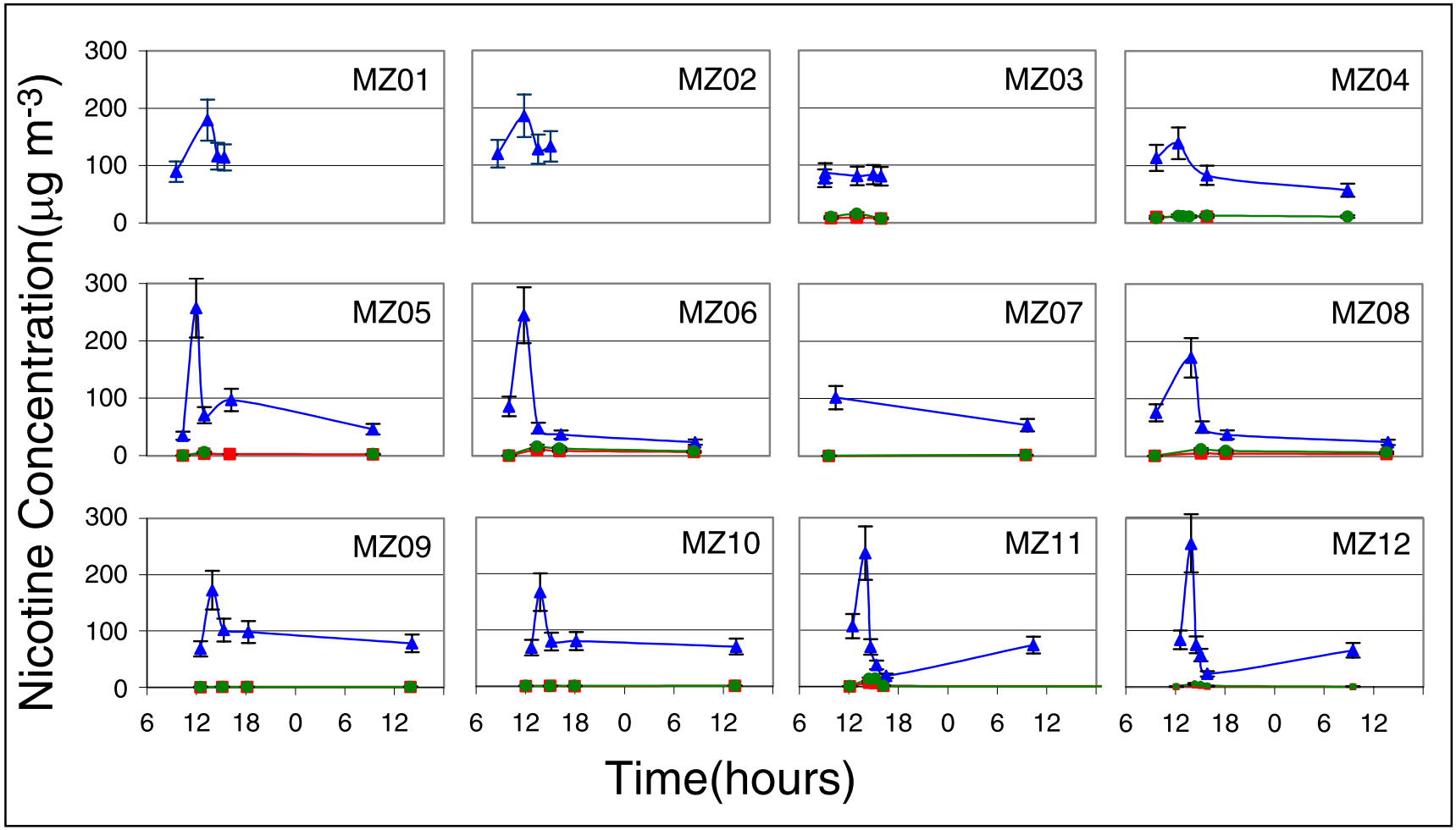

Figure 6. Nicotine concentrations in the SR (triangles), COR (squares), and NSR (circles) during multizone ETS experiments. Note that error bars represent estimates of error in quantitation of nicotine concentrations.

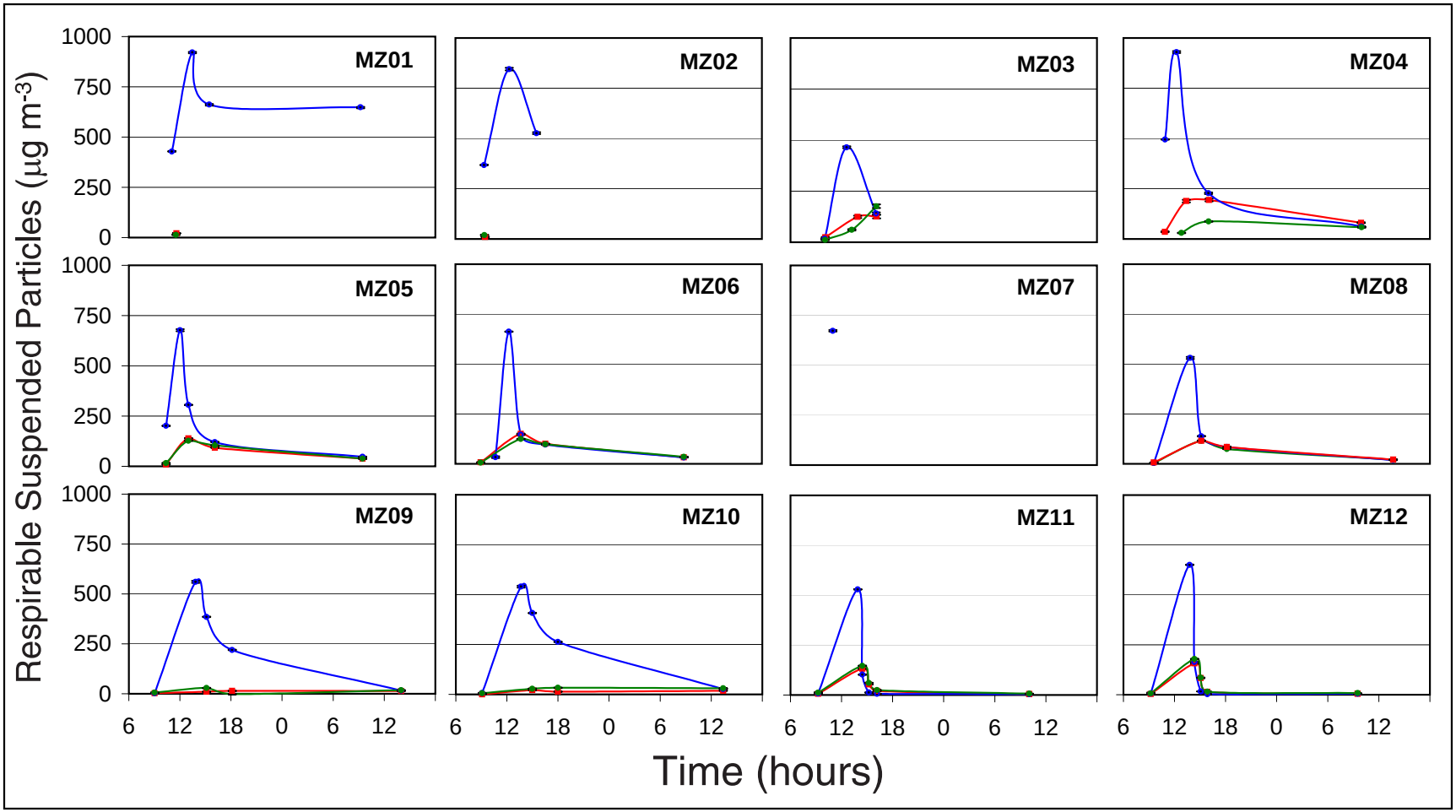

Figure 7. Respirable suspended particle (RSP) concentrations in the SR (triangles), COR (squares) , and NSR (circles) during multizone ETS experiments. Note that error bars represent estimates of error in quantitation of RSP concentrations. RSP error is typically on the order of a few percent.

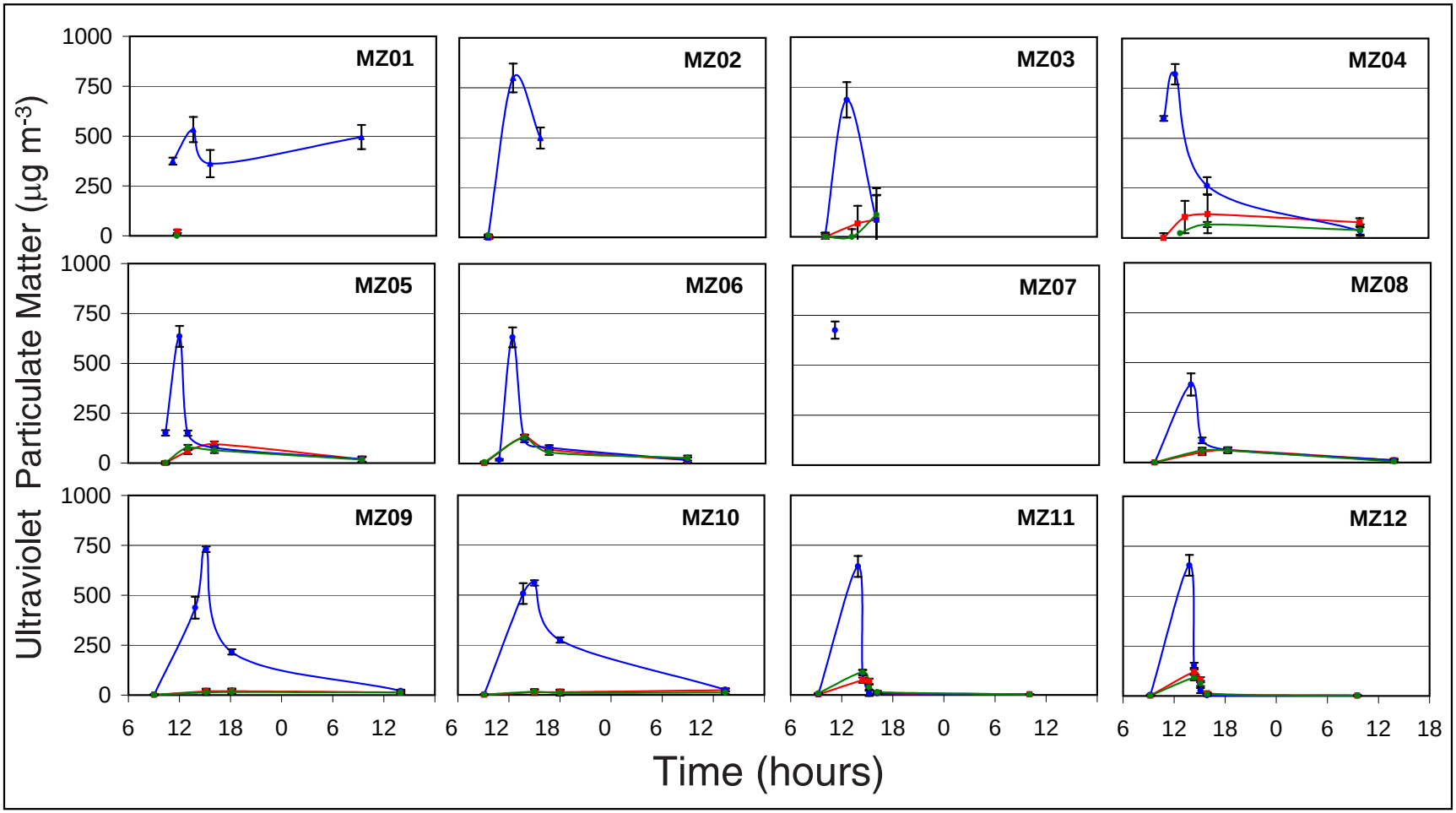

Figure 8. Ultraviolet particulate matter (UVPM) concentrations in the SR (triangles), COR (squares) , and NSR (circles) during multizone ETS experiments. Note that error bars represent estimates of error in quantitation of UVPM concentrations. UVPM error is typically on the order of a few percent.

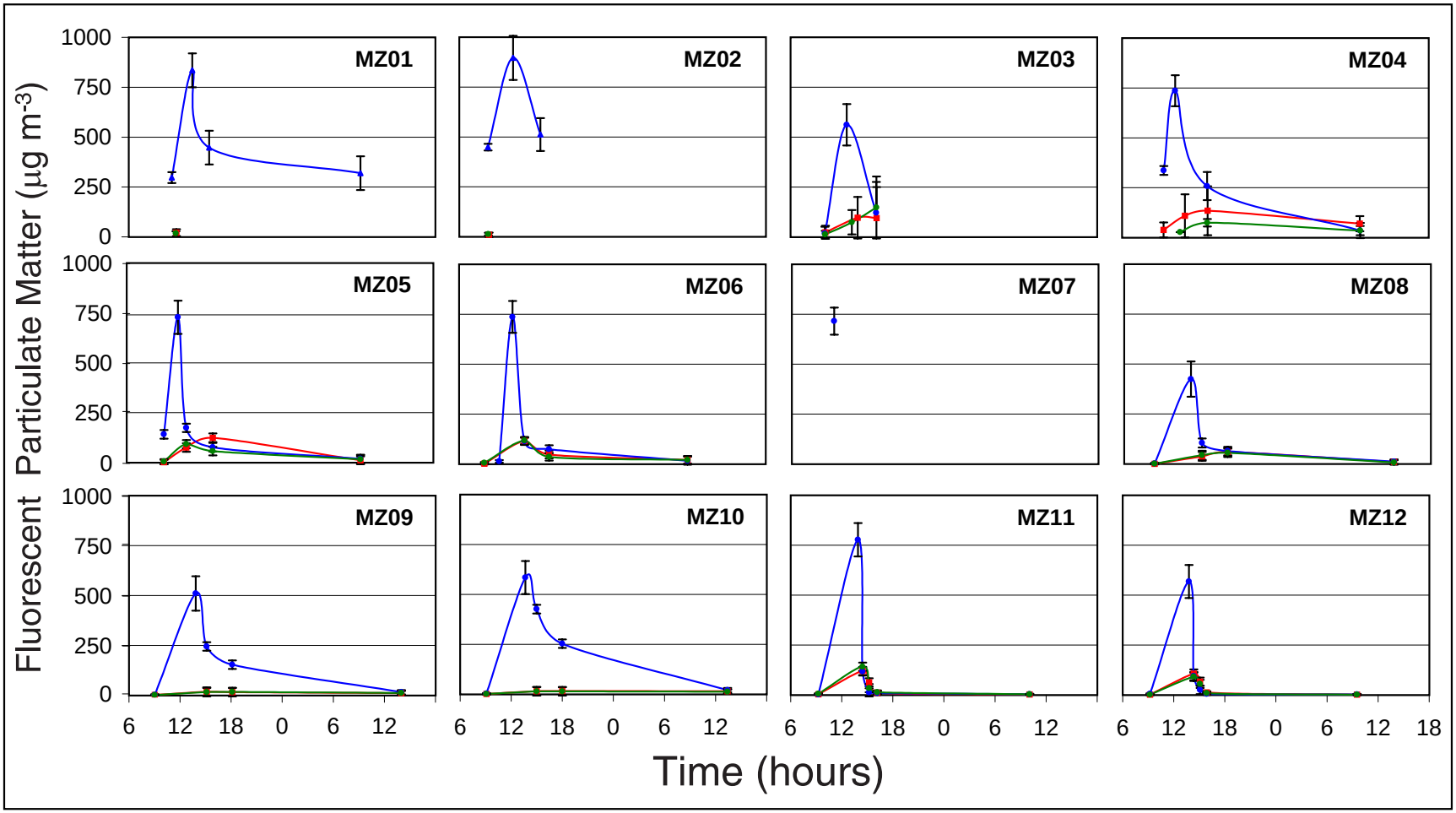

Figure 9. Fluorescent particulate matter (FPM) concentrations in the SR (triangles), COR (squares), and NSR (circles) during multizone ETS experiments. Note that error bars represent estimates of error in quantitation of FPM concentrations. FPM error is typically on the order of a few percent.

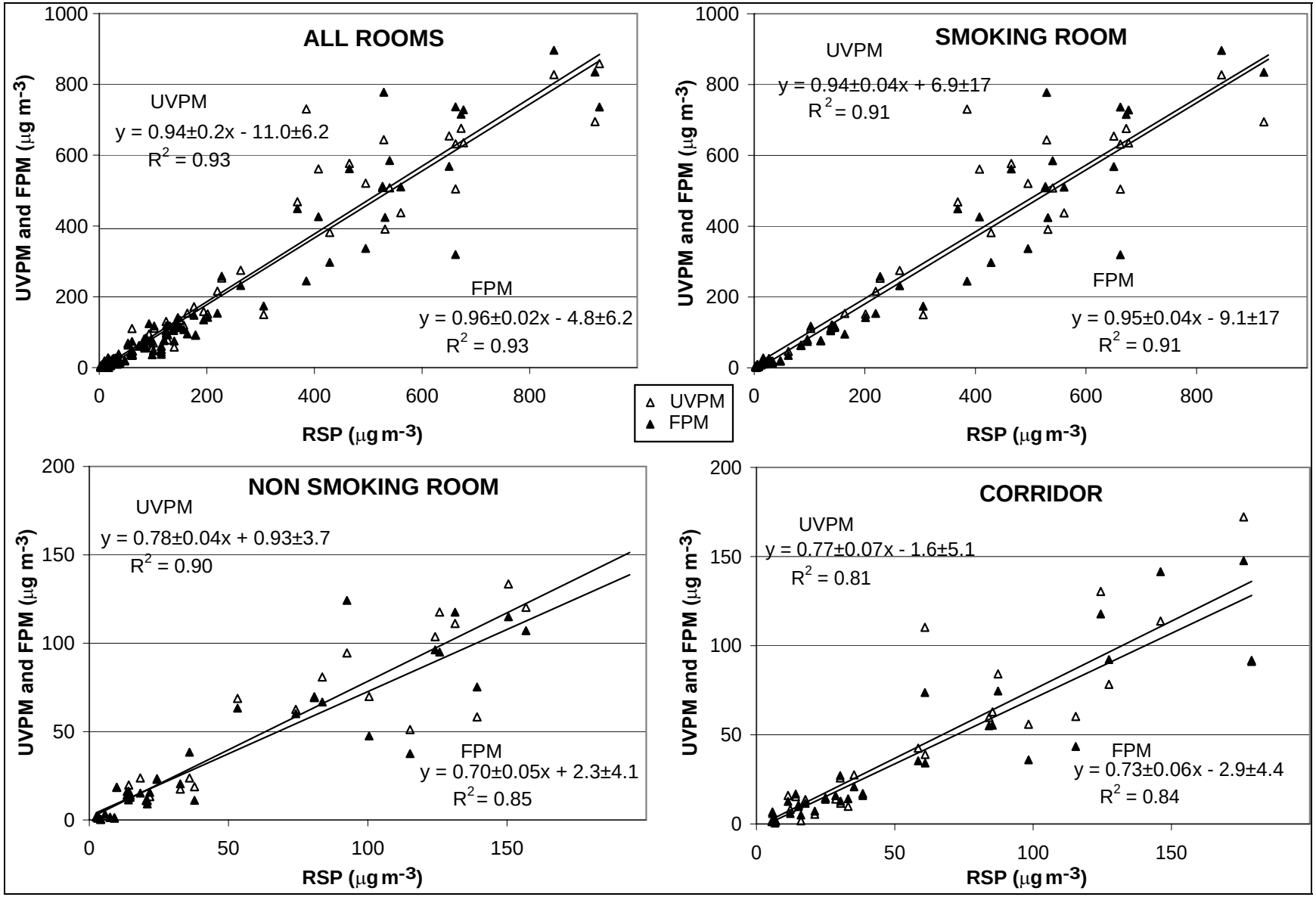

Figure 10. Smoking Room measured particulate matter concentration (RSP) vs. UVPM and FPM concentrations measured in the SR, COR, and NSR, and all data combined. Regression coefficients include estimates of standard error.

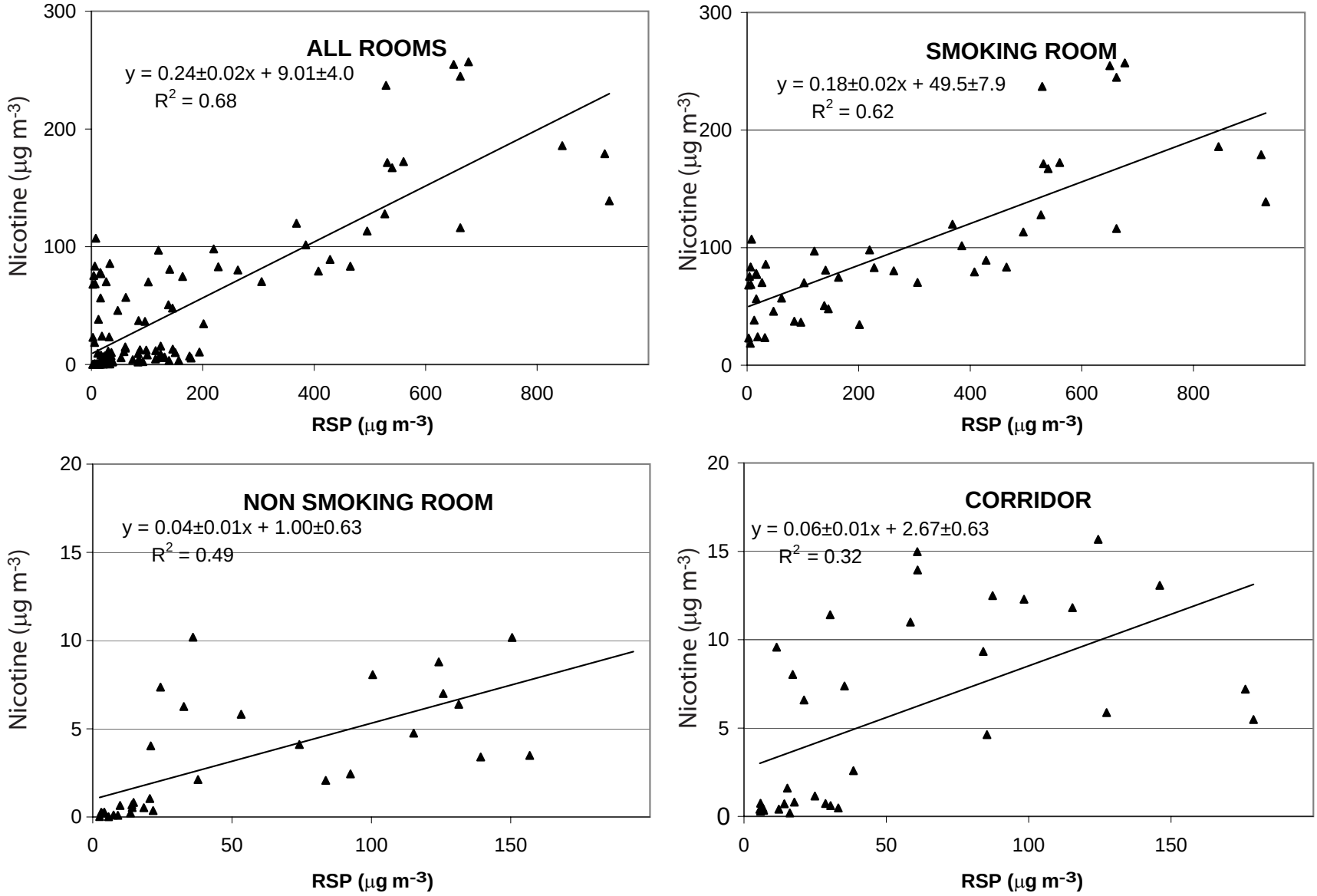

Figure 11. Nonsmoking Room (SR) measured particulate matter concentration (RSP) vs. nicotine concentrations measured in the SR, COR, and NSR, and all data combined. Regression coefficients include estimates of standard error.

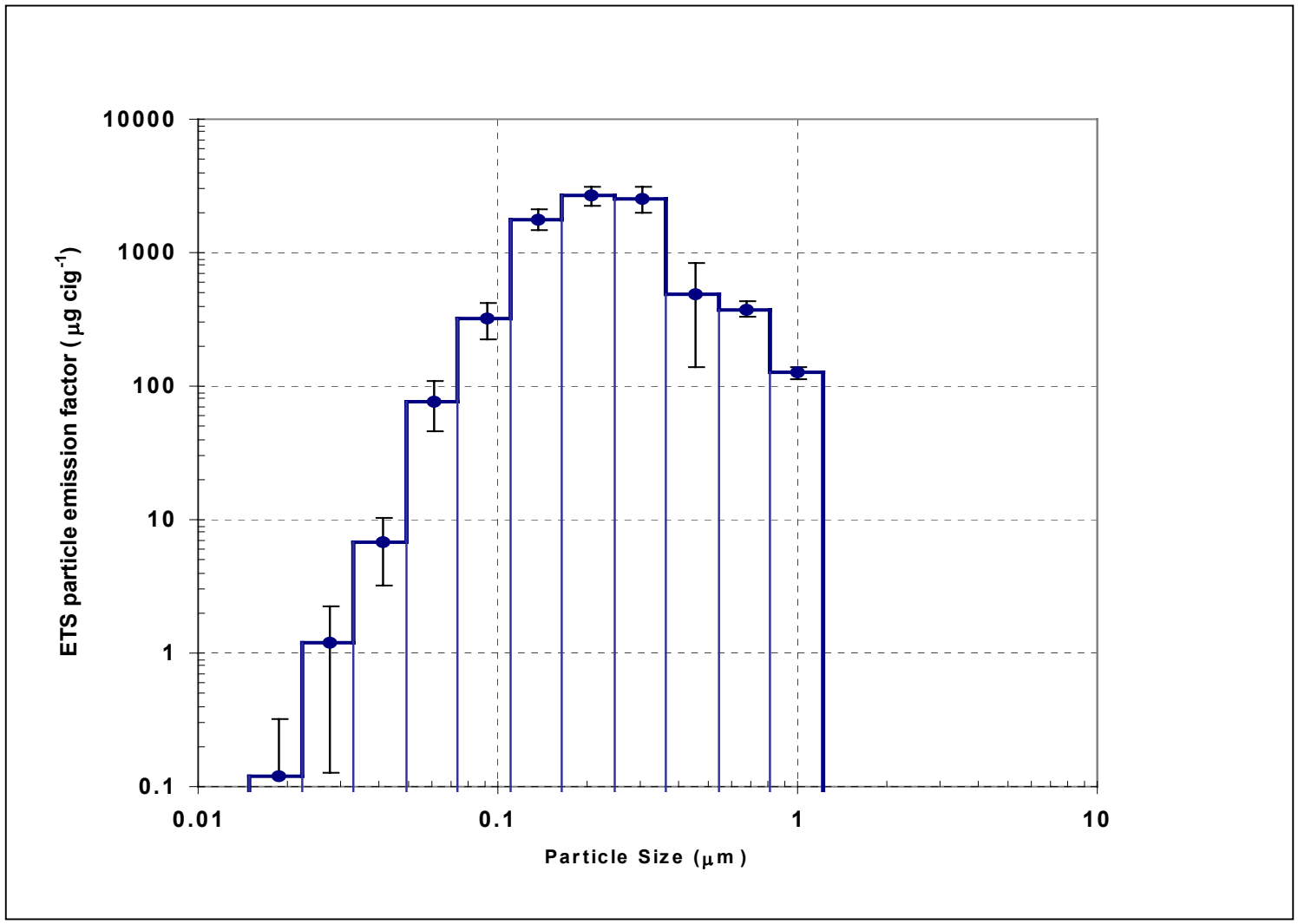

Figure 12. Average ETS per-cigarette, size-resolved, sidestream-only particle mass emission rates. These data represent the average of 12 experiments where one cigarette was smoked in the smoking room of the multizone environmental chamber. Error bars represent ± 1 standard deviation about the average emission rate in each size bin.

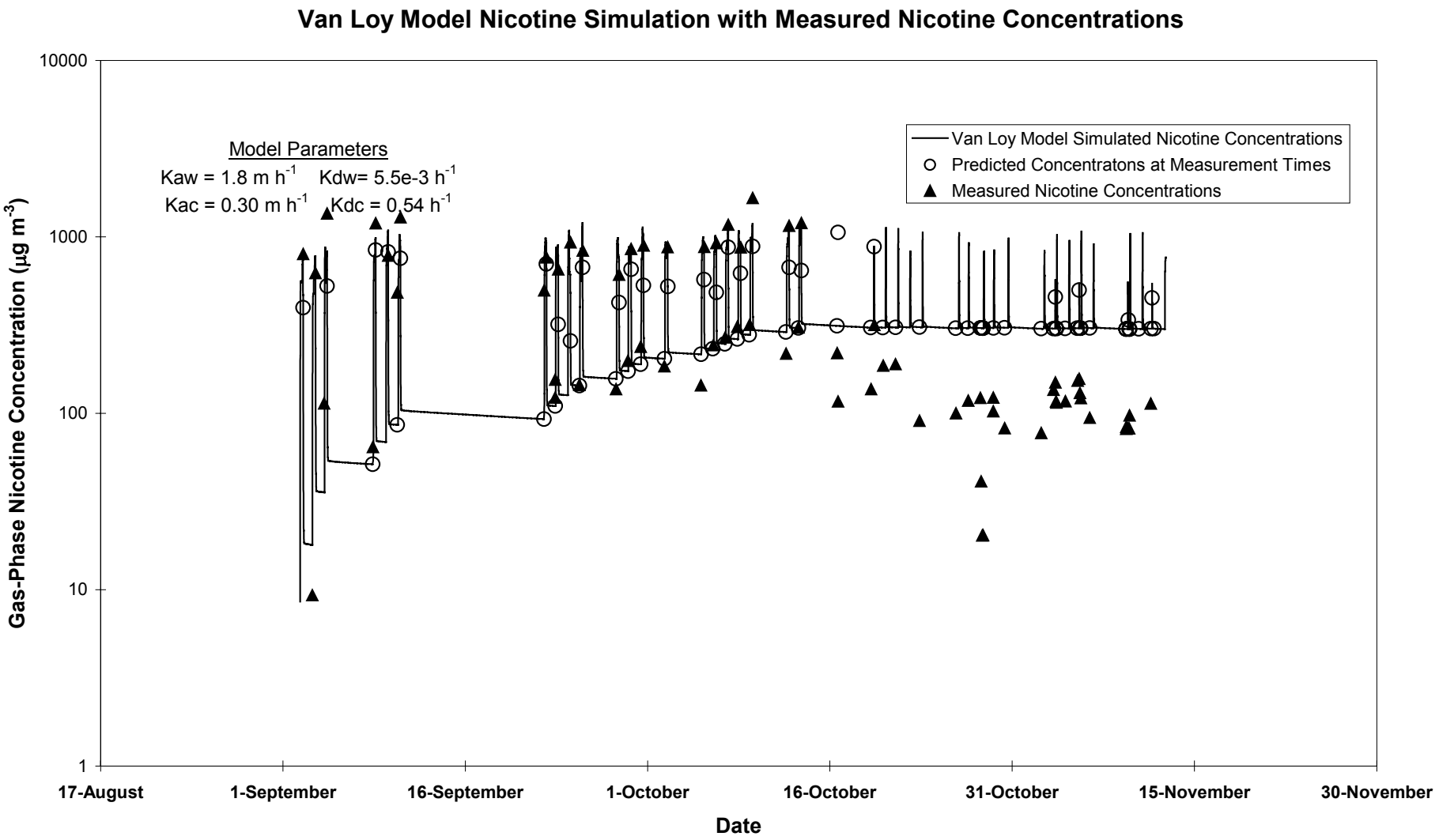

Figure 13. Measured and Van Loy Model-predicted nicotine concentrations in the SR during the conditioning phase of the multi zone ETS experiments. Solid triangles indicate measured SR nicotine concentrations, the line indicates model predictions, and the open circle represents the predicted nicotine concentration at the time measurements were made. The model parameters shown represent optimal values from fitting the model to the measured data. Overall uncertainty in the nicotine measurements is approximately ±20%.

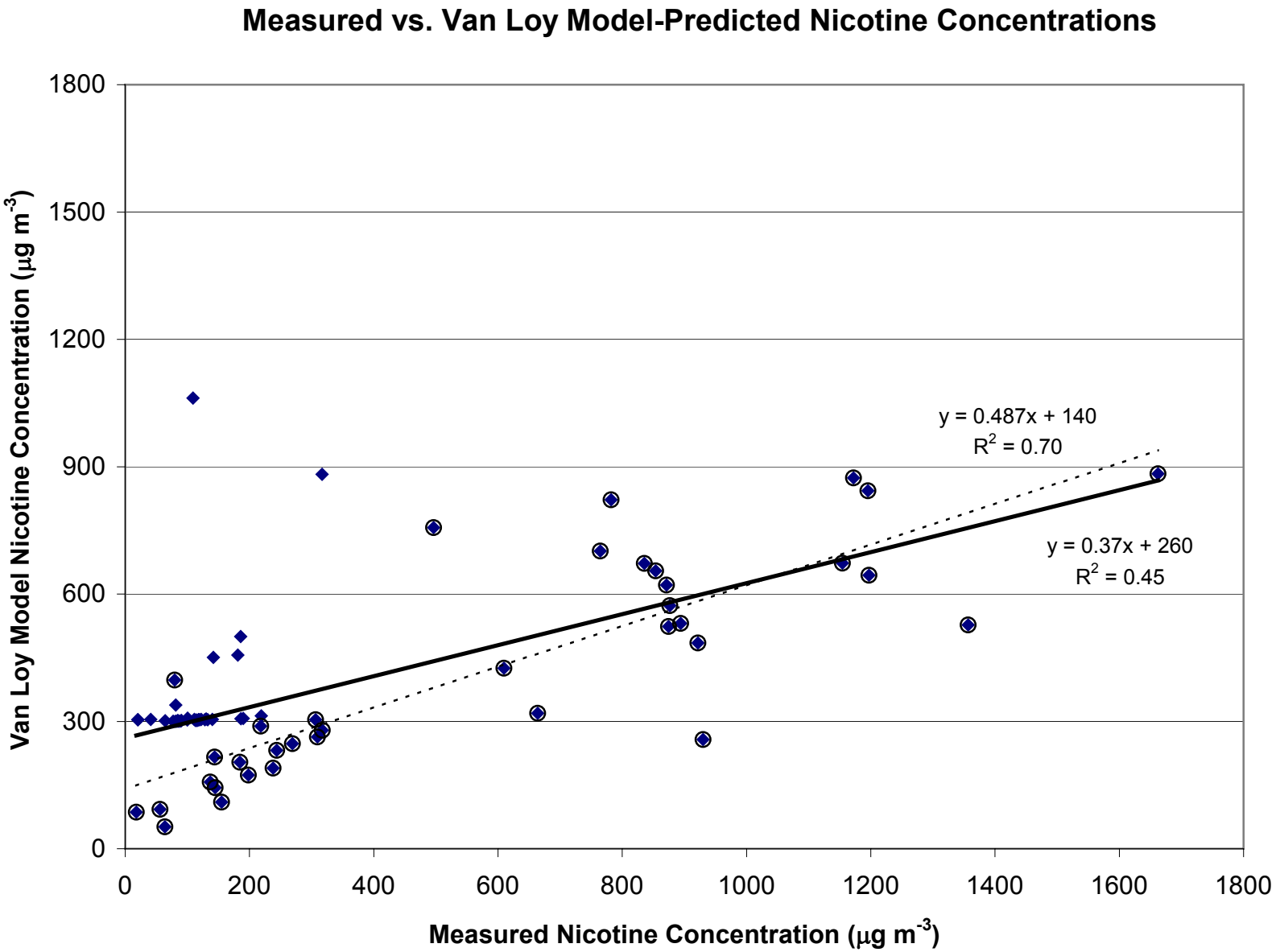

Figure 14. Measured vs. Van Loy Model-predicted SR nicotine concentrations (see Figure 13) during the conditioning phase of the multi-zone ETS experiments. Note that the solid line indicates a least-squares regression fit (R^2=0.57) to the entire dataset (all data points) while the dashed line is a fit to the data for the initial 6 weeks of conditioning at 36 cigarettes per weekday (depicted with encircled data points).

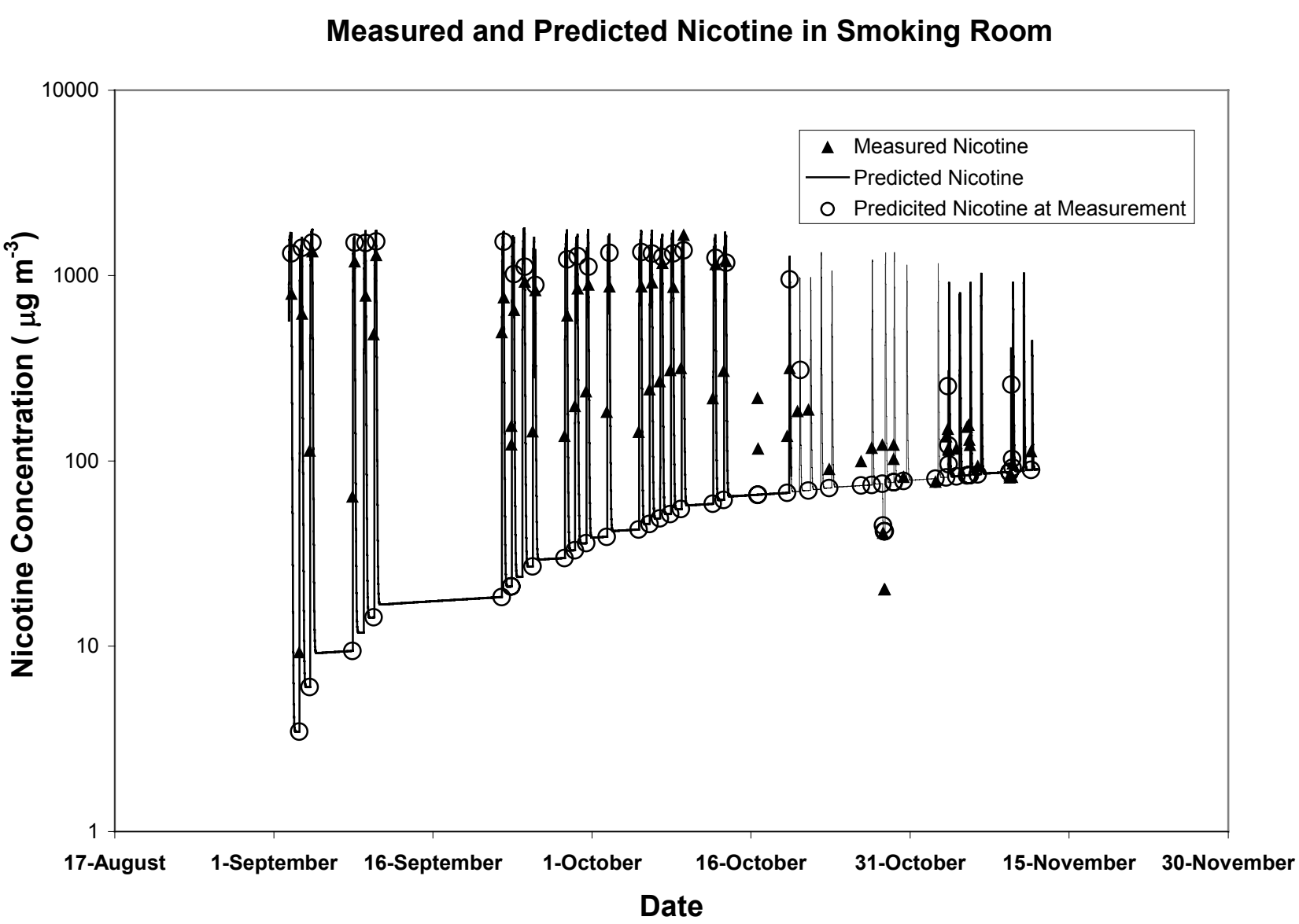

Figure 15. Measured and linear/lumped surface sorption model parameter-predicted nicotine concentrations in the SR during the conditioning phase of the multi-zone ETS experiments. Solid triangles indicate measured SR nicotine concentrations, the line indicates model predictions, and the open circles represent the predicted nicotine concentration at the time measurements were made. Optimal values for k_{an} and k_{dn} were found to be 0.5 m h^{-1} and 1.0 x 10^{-5} h^{-1}, respectively. Overall uncertainty in the nicotine measurements is approximately ±20%.

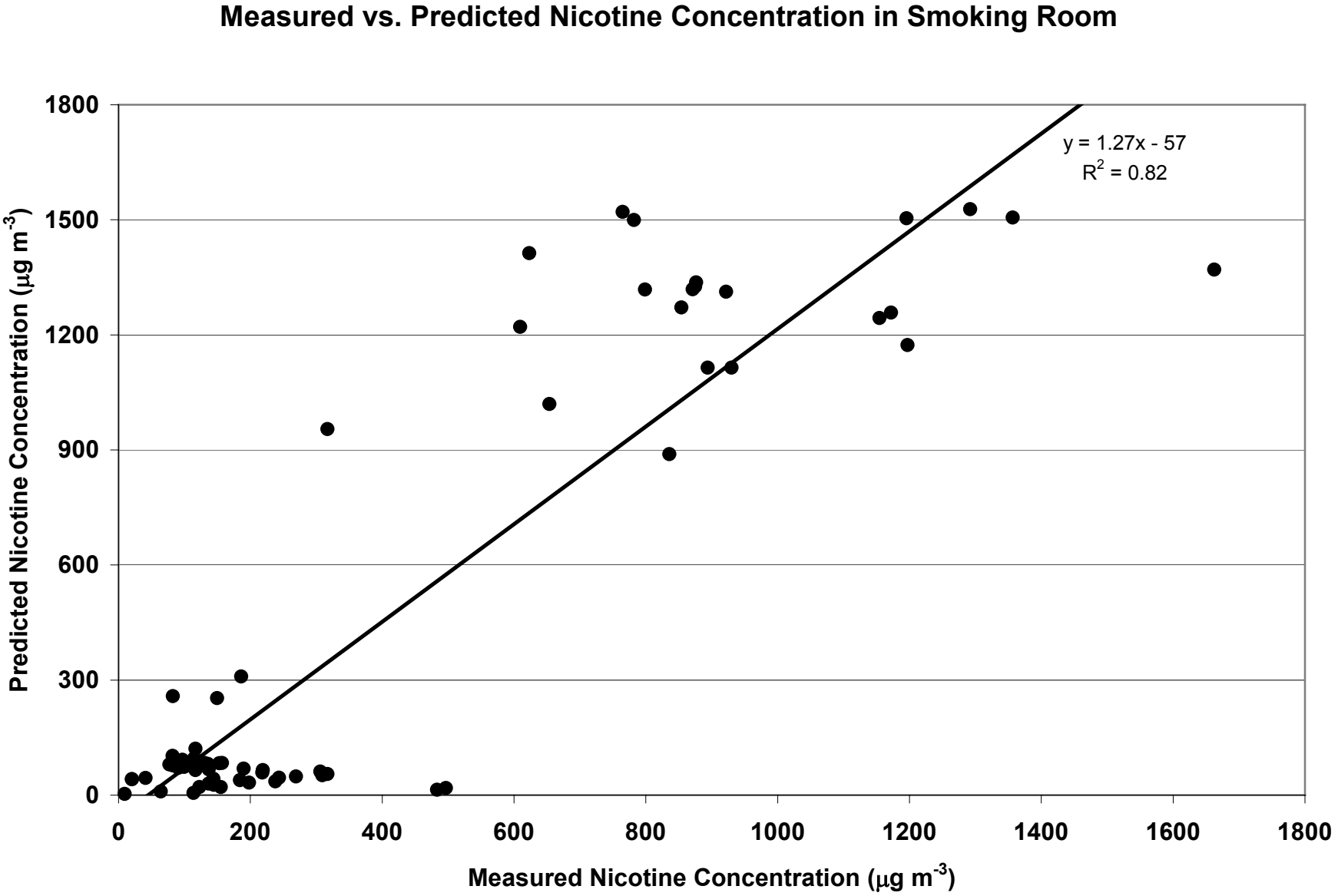

Figure 16. Measured vs. linear/lumped surface sorption parameter model-predicted SR nicotine concentrations (see Figure 15) during the conditioning phase of the multi-zone ETS experiments.

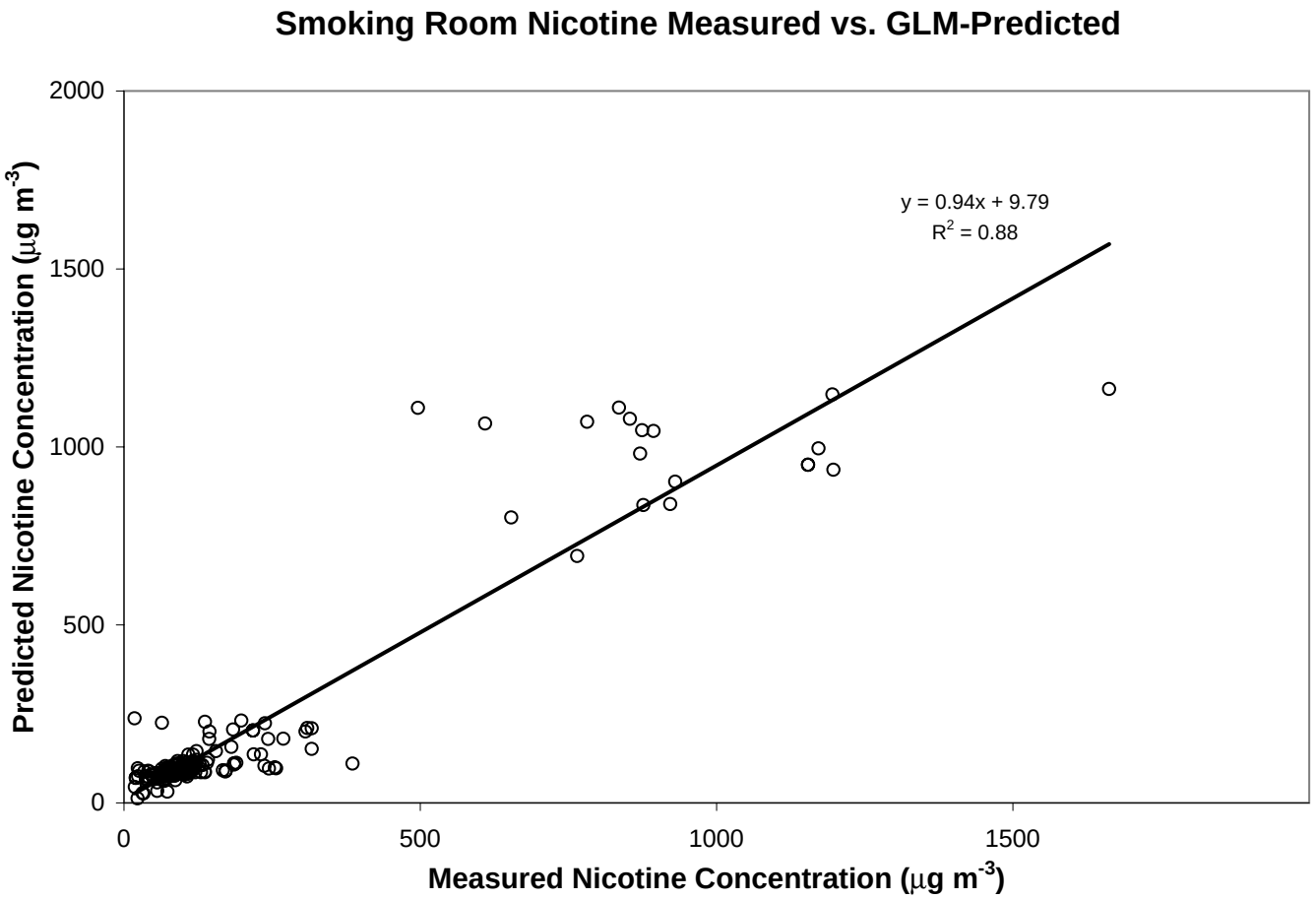

Figure 17. Measured vs. GLM regression model-predicted SR nicotine concentrations during the conditioning phase of the multi-zone ETS experiments.

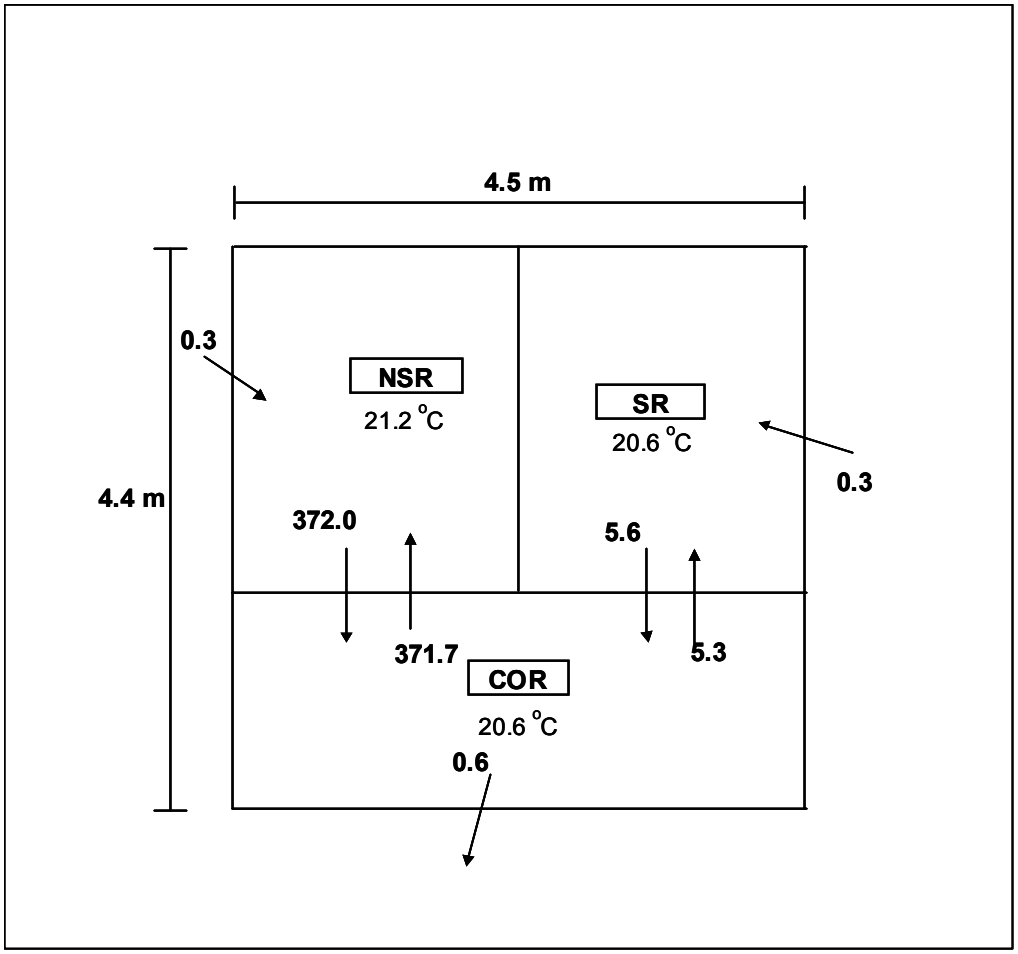

Figure 18. Predicted average airflow between rooms in the MZ04 experiment. The door between the non-smoking room and the corridor is open; the door between the corridor and the smoking room is open 2.5 cm. The units are in m^3h^{-1}. Average room temperatures during the experiment are shown and the average temperature outside the multizone chamber was 19.5°C.

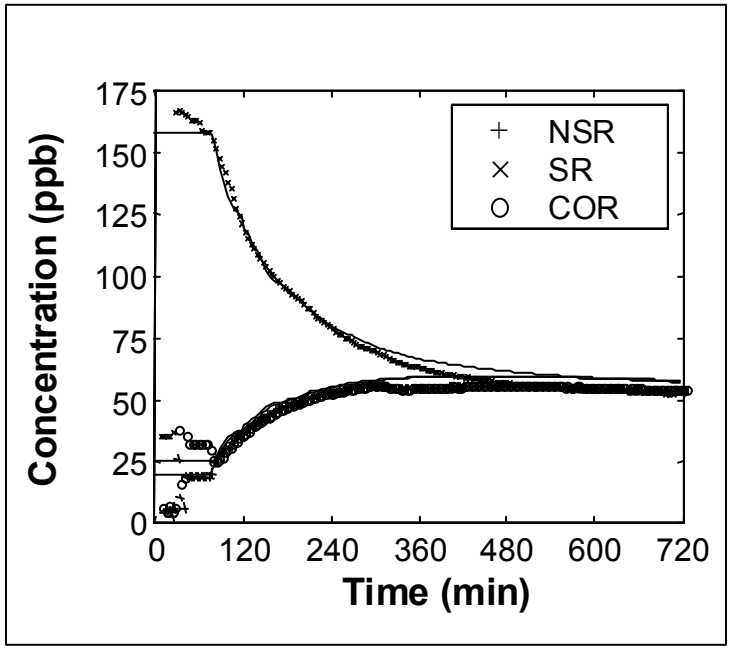

Figure 19. SF_6 concentrations measured and predicted from the MZ04 experiment. The upper curve represents the SR data while the lower two sets of curves represent the COR and NSR data.

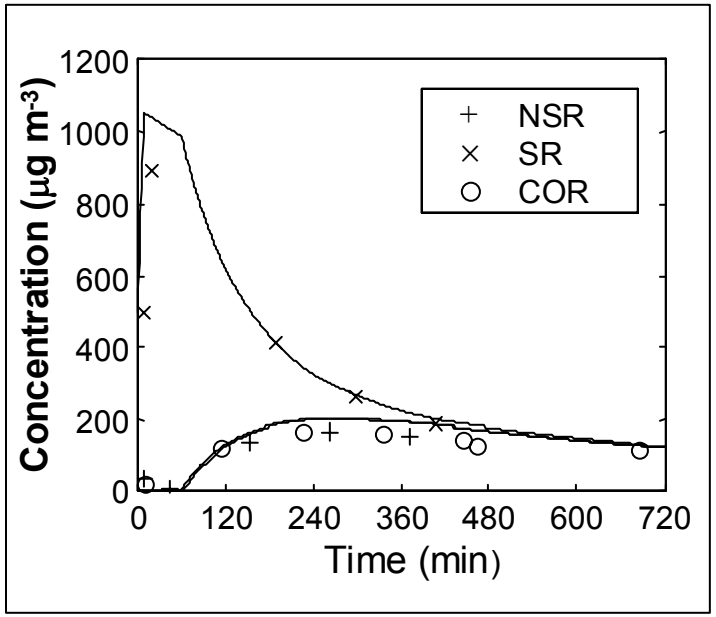

Figure 20. ETS concentrations measured and predicted using COMIS and MIAQ4 from the MZ04 experiment. The upper curve represents the SR data while the lower two sets of curves represent the COR and NSR data.

Appendix A

Third-year Research Results: A Three-home Pilot Study of ETS Tracer Behavior During a Smoking Intervention.

Introduction

A small pilot field study was conducted to evaluate the results of the multi-zone environmental chamber studies in a real environment. We studied three single-smoker residences during five one-week periods while each household's smoker was enrolled in a six-week smoking cessation program. The objectives of the pilot field study were to: (1) examine in actual homes the laboratory observations regarding the reliability of various ETS particle tracers; ·(2) estimate potential bias of nicotine-based exposure assessments due to nicotine sorption and re-emission behavior; (3) estimate potential bias of particle-mass based exposure assessments due to interference from other particle sources; and, (4) quantify non-smoker ETS residential exposure reduction due to smoking cessation.

Methods

Study organization

Three houses were selected in collaboration with a six-week-long smoking cessation class conducted by the Berkeley Department of Health and Human Services, Tobacco Prevention Program, in Berkeley, CA. We solicited study participants from the class. A monetary reward was offered to participants who allowed environmental monitoring to be conducted in their household during the entire 6-weeks of the study. Each participant was to be the only smoker in his or her household. Weekly smoking rate was monitored by butt-count – the participants were given a specially prepared metal container in which to deposit their cigarette butts. Houses were monitored during weeks 1, 2, 3, 4 and 6. The smoking cessation class encouraged participants to quit smoking at the start of week 3.

Measurements and analyses

The five one-week integrated measurements included nicotine, particle mass, and time averaged whole-house ventilation rate. PM 3.5 (respirable suspended particulates) was sampled at 1.7 L min^{-1} and collected on pre-weighed, pre-cleaned filters. Unlike the laboratory particle sampling, a 10 mm nylon cyclone was used to limit the aerodynamic diameter of the particles collected to ≤ 3.5 μm in diameter (50% cut-point = 3.5μm). The homes were visited weekly to recover the particle filter samples, the passive nicotine samplers, the tracer gas sampling bags and the cigarette butts and to deploy the new sampling media.

The various samples were returned to the laboratory for analysis. The collected particle mass was determined gravimetrically. Ultraviolet particulate matter (UVPM) and fluorescent particulate matter (FPM) concentrations were analyzed from extracts of the PM 3.5 particle filter

samples, following the procedures described in the laboratory experimental section. Although solanesol analyses were conducted, quantitation was not feasible for one-week samples in this study due to instability of the analyte. Particle and nicotine samples were collected indoors in the rooms identified as the main smoking room and the non-smoking room. Outdoor particle filter samples were also collected at each home. These outdoor samples were used to correct for any infiltrating particles or particle-bound tracers; we assumed that other indoor sources of PM or PM tracers are negligible during the course of these experiments.

Whole-house air exchange rate was measured using a continuous sulfur hexafluoride injection (SF_6) system. Suitcases containing multi-layer tedlar gas bags, and equipped with either peristaltic injection pumps (q ~ 6.5 cm^3 h^{-1}) or peristaltic sampling pumps (q = 60 cm^3 h^{-1}) were deployed in the homes. One injection suitcase supplying pure SF_6 was deployed in a central (non-smoking) room about 1-2 m above the floor. These injection suitcases incorporated small mixing fans to help disperse the pure SF_6. Two sampling suitcases were used, one in the smoking room and one in the non-smoking room. Weekly-average indoor SF_6 concentrations ranged from 3.0 to 130 parts per billion by volume (18 to 780 μg m^{-3}) in the homes during the study.

Mass balance concepts were used to analyze the results of the study. Although an exact smoking time and emission rate profile would be needed to correctly model the true week-average ETS concentrations, the steady-state mass balance model can be used to compare, on an equivalent basis, the measured ETS particle and particle tracer concentrations across study weeks and between houses. The steady-state form of the mass balance equation, repeated from Traynor et al, (1989), is:

$$C_{ss} = \frac{Pa\,C_o + S/V}{(a+k)}, \qquad \text{(A2-1)}$$

where
C_{ss} = the steady-state particle or particle tracer concentration (μg m^{-3}),
P = penetration fraction of particles from outdoors (0-1, unitless),
C_o = the outdoor concentration of particles or particle tracers (μg m^{-3}),
S = the ETS particle or particle tracer source strength (μg h^{-1}),
V = the house volume (m^3),
a = the whole-house air exchange rate (h^{-1}), and
k = the particle deposition decay rate (h^{-1}).

For the purposes of normalizing the field data, we have used weekly cigarette butt count as a surrogate for S, under the assumption that this count will be proportional to the weekly average ETS particle emission rate. We have assumed a typical value of 0.08 h^{-1} for k, the particle deposition rate loss term (Traynor et al, 1989). Although k is particle size dependent, we did not make particle size measurements in the pilot field study, hence we have used a value that represents particle sizes typical of ETS (i.e., particle mass dominating in the aerodynamic diameter range of 0.1 to 1.0 μm). Measured house volume and weekly average air exchange rate values were used for V and a, respectively.

In order to adjust indoor particle and particle-bound tracer concentrations accurately for penetration of particles from outside air it is necessary to consider the value of the penetration factor in the mass balance model. Traynor et al, 1989 present a geometric mean value of 0.7 (geometric standard deviation 1.28) for P, based upon measurements of penetration of outdoor particles into residences conducted over a one-year period. In the following analyses the indoor PM 3.5 and PM tracers have been adjusted by subtracting $PaC_o/(a+k)$ where P and k are 0.7 and 0.08 h^{-1}, respectively.

House characteristics

The data in Table 2 summarize the residence type and smoking characteristics of the participant's households. As with the lab-based measurements, where we established a distinct smoking room (SR) and non-smoking room (NSR), with the assistance of the study participants we identified rooms in each study house in which smoking did or did not occur and designated them as the SR and NSR, respectively.

In House 1, a single story, single family residence, the smoker was accustomed to limiting smoking to the kitchen, and stated that it was typical to open the back door during smoking. This kitchen did not have an exhaust fan. For the purposes of this study the NSR was chosen to be the living room, which was centrally located in the house and communicated directly with the SR via one doorless portal. The occupants stated that this room was off limits to smoking during regular daily routines. The NSR communicated to two bedrooms via closable doors. The outdoor measurements were collected in the back yard of this home. Our impression of the house is that it was operated to have a lot of ventilation; the data in Table 2 support this impression. House 1 was located in an urban neighborhood within four blocks (~300 m) of a major road, and within about 0.5 km of a major freeway.

House 2 was a large two-story wooden structure with a flat on both floors. The smoker and family occupied the second story flat. The living room of this household was stated to be the SR. The smoker typically sat next to a small open window to smoke. The flat had three bedrooms, and one of these, occupied by two children, was used as the NSR. The smoker claimed not to smoke in the children's bedrooms. The living room did not have a door, but communicated to the bedrooms and kitchen via a long hallway. The NSR was mid-way down this hallway. Bedroom doors in the flat were often found closed during the field visits. Our impression of the house operation was that it was typically kept closed with the exception of two or three small windows that were regularly open. Outdoor sampling was conducted through a sampling line inserted through a window on the second floor (the gap in the window caused by insertion of the sampling line was taped closed), protruding out about 10 cm from the outside wall, and 10 cm below the window opening. House 2 was located in a dense urban neighborhood within two blocks of a major road, and within about 0.5 km of a major freeway.

House 3 was a small two-story wooden structure with a flat on both floors. The smoker and family occupied the second story flat. The SR was identified as the smoker's bedroom, and the smoker stated that this was the only room that was used for smoking on a regular basis. The other bedroom in the flat was not suitable for study as a heavy chain smoker had recently lived in the room, and it had a very strong tobacco smell. The laundry room, equivalent in size to the

bedroom was used as the NSR. This room was located off the kitchen and was indirectly connected to the SR, via two often open doorways, to the kitchen. The house was operated without much ventilation – during field visits the doors and windows were typically all closed. Outside samples were collected through a sampling line inserted through a window in the NSR; as in House 2, protruding out about 10 cm from the outside wall, and 10 cm below the window opening, the gap in the window was taped closed. House 3 was located in a dense urban neighborhood within two blocks of a major road, and within about 0.5 km of a major freeway.

Results and Discussion

Figure 1 depicts the measured weekly smoking room and nonsmoking room indoor PM 3.5 concentrations (adjusted for infiltrating outdoor PM 3.5) for the three study households. The clear downward trends in adjusted indoor PM 3.5 during the course of the smoking intervention reflects the attempts of the smokers to reduce their smoking rate. Weekly smoking rates in the houses are presented in Table 2. The non-zero adjusted PM 3.5 values for weeks when butt counts were zero indicates the likely presence of other particle sources in the homes. The PM 3.5 respirable particle size cut includes particles large enough that they could be from non-combustion, re-suspended aerosols. It is likely that this re-suspension of larger particles may be responsible for the elevated concentrations.

The limit of detection (LOD) of the nicotine concentrations presented below, based upon nicotine passive sampler field blanks, is estimated to be about 0.07 $\mu g\ m^{-3}$. Likewise, roughly estimated uncertainty based upon duplicate measurements is about ±10% for nicotine concentrations greater than 0.15 $\mu g\ m^{-3}$ (LOD*2) and ±50% for those less than 0.15 $\mu g\ m^{-3}$. As discussed in the laboratory section of this report, the estimated uncertainty for UVPM measurements ranged from approximately ±30% to ±50% depending upon the concentration range. Similarly, uncertainty estimates for FPM ranged from ±40% to ±80%. Uncertainty in the PM 3.5 measurements is estimated to be less than ±10%.

Figures 2, 3, and 4 present the relationship between one-week average nicotine and ambient-adjusted PM 3.5, UVPM, and FPM concentrations for both smoking and non-smoking rooms across all study weeks in the pilot study homes. These data are shown organized by household. Note that compared to the SR, PM tracer and nicotine levels in the NSR are a factor of two to three and approximately an order of magnitude lower, respectively.

Figures 2-4 indicate that the correlation between nicotine and the PM tracers was variable depending upon the household. For SR measurements the PM 3.5 correlated well with nicotine in Houses 2 and 3, but not in House 1. UVPM was moderately correlated with nicotine in all three houses, while FPM was well correlated with nicotine in houses 1 and 3.

Figures 5 and 6 present the adjusted PM 3.5 relationships to adjusted UVPM and FPM in the SR and the NSR, respectively. The correlation coefficients of fitted least-square regression lines to these data indicate relatively poor relationships between adjusted PM 3.5 and the PM tracers. Additionally, the slopes of these fits indicate that the adjusted PM 3.5 is not characterized well by the PM tracers. No doubt, this can be explained partially by the large uncertainty of the UVPM and FPM quantitations, however, other reasons could include the presence of indoor sources of non-UV absorbing and non-fluorescing respirable particles. It is also possible that the

dynamic, long-term behavior of the semivolatile components of ETS may lead to surface losses and selected sample blow-off. The same issues were observed in the relatively short-term samples collected in the SR and COR/NSR samples in the chamber study, although the relationships correlated better in the laboratory study.

The NSR data in Figures 2-4 also indicate a great inter-house variability in the correlation between PM tracers and nicotine. Note that the week 1 nicotine measurement in the NSR (0.003 $\mu g\ m^{-3}$) has been removed from these figures, as it is an extreme outlier, inconsistent, and likely to be faulty. Although quite noisy, the relationship between tracers behaved with fair consistency. House 3 nicotine values in the NSR appear to be virtually independent of the PM 3.5 and UVPM concentrations, showing a moderate correlation with FPM. The average NSR nicotine levels in House 3 appear to be about 0.8 $\mu g\ m^{-3}$.

Figures 7 and 8 present the nicotine and ambient-adjusted PM 3.5, UVPM, and FPM indoor tracer concentrations from all three houses for the SR and NSR, respectively. Based upon the discussion of the uncertainty of the PM tracer data and the limited data on only three houses, these figures should be considered indicative of ETS behavior, but not conclusive. In these figures the tracer concentrations are plotted against the household ETS source strength calculated from the weekly butt-count - and ventilation rate data. This normalization allows us to examine the tracer behavior across the three houses. After normalization, it is clear that the PM tracers and nicotine perform similarly in predicting weekly smoking rates (and thus ETS emission rates) in ETS-conditioned spaces in real homes – the correlations between butt-count based source strengths and both PM and nicotine tracers have R^2 values from 0.6 to 0.7.

In the NSR case the relationship between the tracer concentrations and the ETS source strength is much less clear. Nicotine and FPM have poor predictive ability when data from all houses are considered together. Note again that the spurious nicotine value from House Three has been removed. If this data point were included nicotine would have no predictive value (R^2 =0.03, slope=0.70). UVPM, with an R^2 of 0.5 appears to do the best at predicting NSR ETS concentrations, while adjusted PM 3.5 had much lower R^2 values, possibly due to other indoor sources of respirable particles. Overall, none of the ETS tracers appear to have been able to provide strong predictive power for ETS in the NSR.

Concluding Comments

This pilot study was conducted to (1) evaluate in actual homes the laboratory observations regarding the reliability of various ETS particle tracers; (2) estimate potential bias of nicotine-based exposure assessments due to nicotine sorption and re-emission behavior; (3) estimate potential bias of particle-mass based exposure assessments due to interference from other particle sources, and; (4) quantify non-smoker ETS residential exposure reduction due to smoking cessation. The three home set was also intended to be a pilot study and thus, in part, to examine how to conduct a study in a larger number of houses. Three homes do not provide sufficient statistical certainty that we can address these objectives definitively. Nevertheless, the data collected provide the basis for an initial assessment.

After adjustment for infiltration of outdoor PM, UVPM and FPM do perform as ETS tracers in both smoking and non-smoking rooms, however, their performance was not particularly good. Improved effectiveness may be possible with further calibration. These tracers have more than sufficient sensitivity for residential exposure assessment, however the uncertainty in quantitation of the PM tracers reduces their utility.

Interestingly, in the SR, after adjustment, PM 3.5 tended to provide the most consistent and highest correlation with ETS source strength as estimated through butt-count (Equation A2-1). This condition is not likely to occur in all cases, especially if significant indoor sources of PM 3.5, such as combustion-generated particles from a fireplace, cooking, or other sources exist in study homes.

Nicotine traced ETS well in the smoking areas of all three houses, but was inconsistent in the non-smoking rooms where surfaces were presumably not saturated with nicotine. These results indicate that in areas with unknown smoking histories nicotine will not trace ETS reliably.

Inter-room transport of ETS can be observed in this study. Based upon Figures 7 and 8, across houses, for every 0.1 Cig-h-m^{-3} of smoking in a house about 17 μg m^{-3} of elevated respirable suspended particles (RSP) can be expected in the SR, and 4.1 μg m^{-3} in the NSR. Similarly, predicted increases in nicotine concentrations at the same normalized smoking rate would be 21 μg m^{-3} and 0.27 μg m^{-3}, respectively. Thus, it was seen in these houses that the concentration of ETS particulate matter in non-smoking rooms was about 25% of that in the SR, while on average, only about 13% of the nicotine was transported and in air of the NSR. An estimate of ETS particle exposure in a non smoking room (such as a child's bedroom) might be biased low by a factor of two if nicotine were used as the tracer. If the additional nicotine datum that was removed from the above analyses is included, the underestimate of ETS exposure based upon average nicotine measurements could be as much as 800%.

Sorption and/or re-emission phenomena may have contributed background nicotine of about 0.8 μg m^{-3} to the non-smoking area of the home with highest smoking rate (house 3). The other homes showed no background nicotine (zero intercept in regression of nicotine vs. indoor PM 3.5 and nicotine vs. UVPM). However these data are extremely limited and should be interpreted with caution.

The pilot field study did not uncover significant bias from other ambient particle sources during spring weather in residential neighborhoods. Evaluation of the selectivity of UVPM for ETS compared to other particle sources requires supplementary measurements of ETS in the presence of wood smoke and diesel exhaust (Alevantis and Fisk, 2001, Gundel et al. 2000).

An initial premise in this study was that indoor respirable particle sources would be negligible compared to the ETS source. In fact, indoor sources of respirable particles without a UV absorbing or fluorescing component may have been present in concentrations similar to the ETS particles. It is possible that there were also some sources of UV absorbing and fluorescing PM in the houses, however, they would likely have been at much lower concentrations during times when smoking was occurring. Certainly, as the smoking behavior declined with the cessation efforts, indoor sources would be likely to become more dominant. Additionally, the actual smoking rates experienced in Houses 1 and 2 were uniformly lower than expected.

Based on this pilot study, indoor PM 3.5, UVPM, and FPM and nicotine correlated well with ETS emission rates (calculated from cigarette butt counts and ventilation measurements as discussed above) in household smoking rooms. UVPM tracked ETS emission rates with modest reliability in non-smoking rooms after all three smokers reduced their smoking rate by at least half during the six-week program. Additional method development is necessary to reduce the uncertainty in the PM tracer quantitations. Furthermore, a larger sample size of households would be necessary to make any clear conclusions from this study design.

With respect to the feasibility of studying the reliability of various ETS tracers in a larger set of homes, no major problems were encountered in the three pilot homes. It is clear that additional homes need to be studied in-order-to better quantify the relationship between ETS tracers and ETS concentrations. This is especially evident for situations where there are distinct smoking and non-smoking areas. It appears, based in both the pilot study and the more extensive laboratory chamber studies, that nicotine may not a very reliable tracer for situations where the smoking history is unknown.

On the other hand, the use of UVPM and FPM may need additional development work to improve their reliability. Unfortunately, the more tobacco-specific tracer, solanesol, appears to degrade substantially and thus have almost no utility.

References

Alevantis, L. and Fisk, W.J. 2001. Effectiveness of Smoking Rooms in Relation to AB13, Progress Report to TRDRP, Year 2, 2001.

Gundel, L.A., Fisk, W.J., Apte, M.G.; Sullivan, D.; Faulkner D.; Shpilberg, V. 2000. Real-time monitoring of environmental tobacco smoke in the presence of other combustion sources, presented at the annual meeting of the International Society for Exposure Analysis, Asilomar, CA, October 2000.

Hammond, S.K. and Leaderer, B.P. 1987. "A diffusion monitor to measure exposure to passive smoking." *Environmental Science and Technology*, **21**: 494-497.

Traynor, G.W., J.C. Aceti, M.G. Apte, B.V. Smith, L.L. Green, A. Smith- Reiser, K.M. Novak, and D.O. Moses, 1989. Macromodel for Assessing Residential Concentrations of Combustion-Generated Pollutants: Model Development and Preliminary Predictions for CO, NO2, and Respirable Suspended Particles,. LBL-25211. Lawrence Berkeley Laboratory, University of California, Berkeley, CA 94720.

Tables

Table 1. Instrumentation and measurement methods for 3 home ETS pilot field study.

Parameter	Sampling Method	Instrumentation (field)	Analytical Method (laboratory)
Nicotine	Passive diffusion onto sodium bisulfite treated filter	Hammond Passive Sampler	Gas Chromatography (see Hammond and Leaderer, 1987)
PM 3.5	Gravimetric air sampling with cyclone inlet. Flow = 1.7 $L \cdot min^{-1}$	LBNL Particle Sampler, 10mm Nylon Cyclone, Teflon Coated Glass Fiber Filter, Microbalance	Gravimetry
Ultraviolet and Fluorescent PM	As PM 3.5	Analysis of PM 3.5 filter	High Performance Liquid Chromatography
Ventilation Rate	Peristaltic pump and tedlar source and sample collection bags	LBNL infiltration rate system, continuous injection and sampling of SF_6	Gas Chromatography with electron capture

Table 2. Housing characteristics of the ETS field study houses including measured ventilation rates and unadjusted ETS tracer concentrations.

House	Residence Type	Number of occupants[1]	Volume (m^3)	Smoking Rate[2] (Cig $week^{-1}$)	Ventilation Rate (h^{-1})	Sampling Location	Nicotine ($\mu g\ m^{-3}$)	PM 3.5 ($\mu g\ m^{-3}$)	UVPM ($\mu g\ m^{-3}$)	FPM ($\mu g\ m^{-3}$)
1	Single Family	4	194							
Week 1				48	1.38					
						SR	1.82	25.2	11.0	7.6
						NSR	0.13	11.1	1.9	1.6
						Outdoor	-	7.6	0.7	1.5
Week 2				49	2.98					
						SR	2.65	13.7	5.9	3.6
						NSR	0.44	19.1	7.4	3.7
						Outdoor	-	5.9	1.1	0.2
Week 3				0	2.75					
						SR	0.16	25.1	2.0	1.3
						NSR	0.09	20.5	2.2	1.1
						Outdoor	-	16.3	1.5	1.2
Week 4				0	2.97					
						SR	0.11	19.1	2.2	2.0
						NSR	0.09	13.9	1.4	2.4
						Outdoor	-	12.2	1.6	1.2
Week 6				0	2.52					
						SR	0.27	7.5	2.3	1.9
						NSR	0.13	8.8	1.8	1.8
						Outdoor	-	8.1	0.9	0.8

[1]The participant was the only smoker in each household.
[2]Based on butt count.

Table 2. Housing characteristics of the ETS field study houses including measured ventilation rates and unadjusted ETS tracer concentrations (continued).

House	Residence Type	Number of occupants[1]	Volume (m^3)	Smoking Rate[2] (Cig $week^{-1}$)	Ventilation Rate (h^{-1})	Sampling Location	Nicotine ($\mu g\ m^{-3}$)	PM 3.5 ($\mu g\ m^{-3}$)	UVPM ($\mu g\ m^{-3}$)	FPM ($\mu g\ m^{-3}$)
2	Duplex	8	425							
Week 1				15	0.64					
						SR	2.17	26.6	4.3	3.0
						NSR	0.5	17.6	4.5	3.4
						Outdoor		7.6	0.7	1.5
Week 2				6	1.05					
						SR	1.87	19.2	7.1	5.4
						NSR	0.3	10.6	3.1	1.7
						Outdoor		6.0	0.8	0.6
Week 3				4	0.99					
						SR	0.78	21.1	4.5	2.9
						NSR	0.2	13.4	0.2	0.0
						Outdoor		16.6	1.7	1.7
Week 4				7	1.06					
						SR	0.30	16.5	1.8	5.0
						NSR	0.1	13.1	1.3	0.8
						Outdoor		10.9	0.8	1.6
Week 6				7	1.51					
						SR	0.84	12.3	3.4	2.4
						NSR	0.2	12.2	2.9	2.1
						Outdoor		9.6	1.0	1.0

[1]The participant was the only smoker in each household.
[2]Based on butt count.

Table 2. Housing characteristics of the ETS field study houses including measured ventilation rates and unadjusted ETS tracer concentrations (continued).

House	Residence Type	Number of occupants[1]	Volume (m^3)	Smoking Rate[2] (Cig $week^{-1}$)	Ventilation Rate (h^{-1})	Sampling Location	Nicotine ($\mu g\ m^{-3}$)	PM 3.5 ($\mu g\ m^{-3}$)	UVPM ($\mu g\ m^{-3}$)	FPM ($\mu g\ m^{-3}$)
3	Duplex	2	217							
Week 1										
						SR				
						NSR				
						Outdoor				
Week 2				122	1.21					
						SR	6.29	67.4	19.9	27.2
						NSR	0.0034	30.8	11.9	3.9
						Outdoor	-	18.0	1.7	1.8
Week 3				65	1.11					
						SR	4.08	65.0	7.0	4.8
						NSR	0.88	40.0	9.0	6.6
						Outdoor	-	40.0	1.6	1.7
Week 4				57	1.54					
						SR	3.22	45.0	17.1	9.5
						NSR	0.54	25.8	7.5	2.3
						Outdoor	-	28.4	2.4	0.9
Week 6				45	1.29					
						SR	1.31	26.9	10.4	6.9
						NSR	0.92	17.3	3.0	3.6
						Outdoor	-	20.5	1.6	1.4

[1]The participant was the only smoker in each household.
[2]Based on butt count.

FIGURES

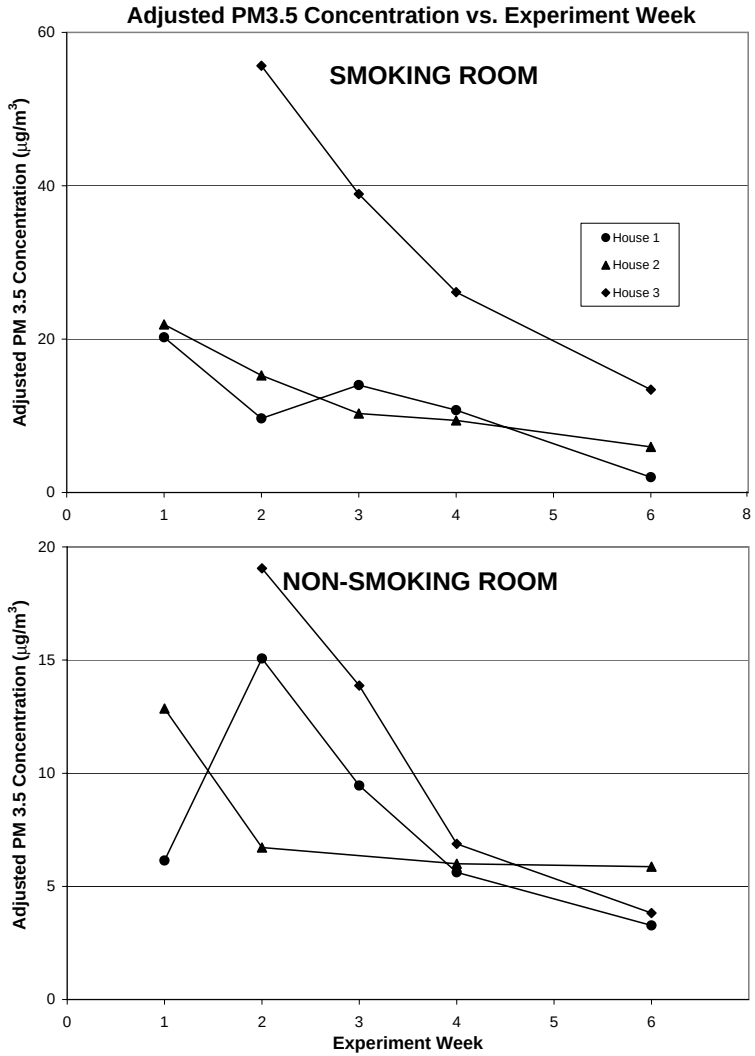

Figure 1. Ambient-adjusted indoor PM3.5 in smoking and non-smoking rooms by study week.

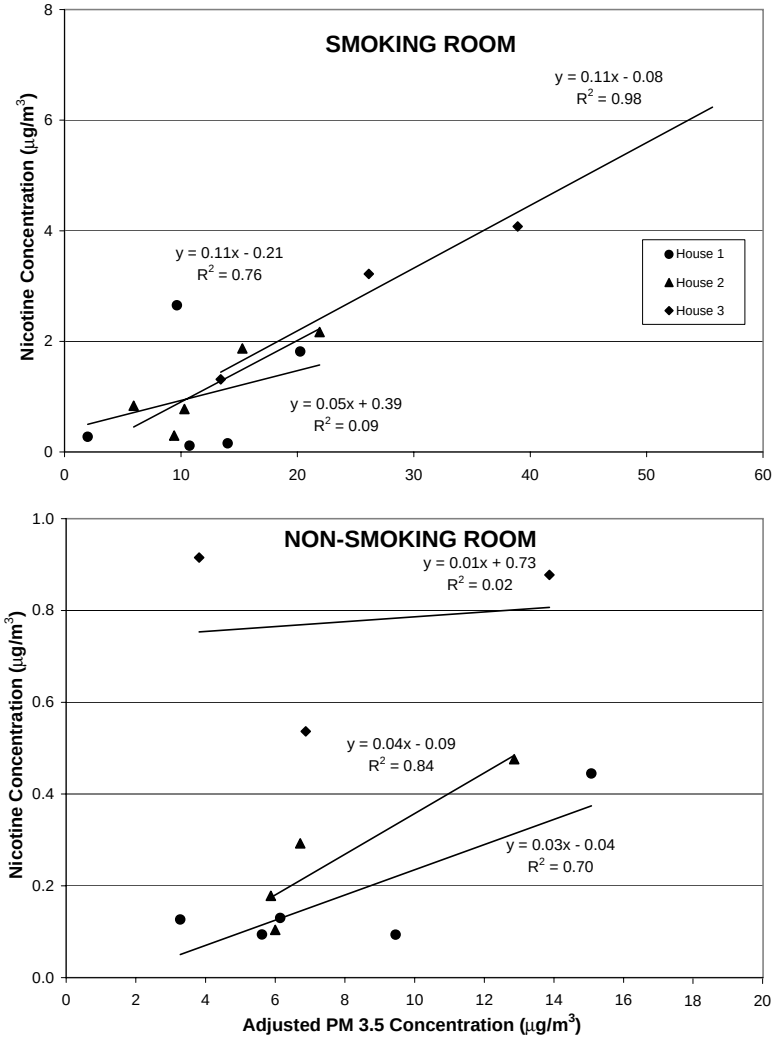

Figure 2. Indoor nicotine concentrations vs. ambient-adjusted PM 3.5 in smoking and non-smoking rooms of pilot study residences for all study weeks.

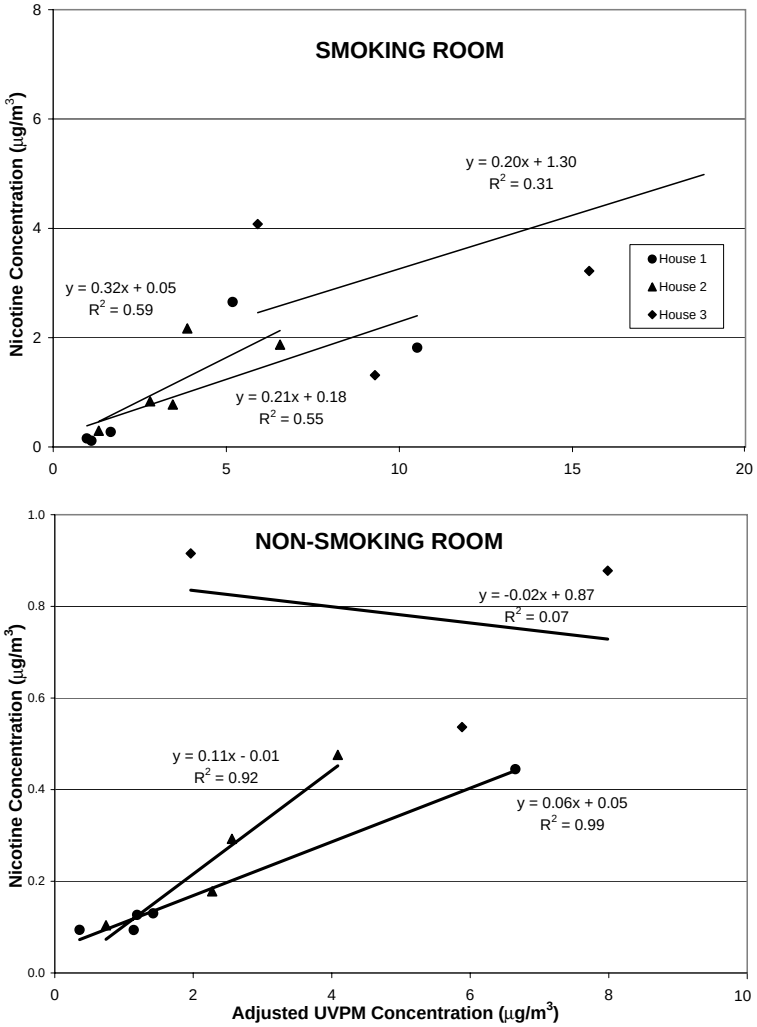

Figure 3. Indoor nicotine concentrations vs. ambient-adjusted UVPM in smoking and non-smoking rooms of pilot study residences for all study weeks.

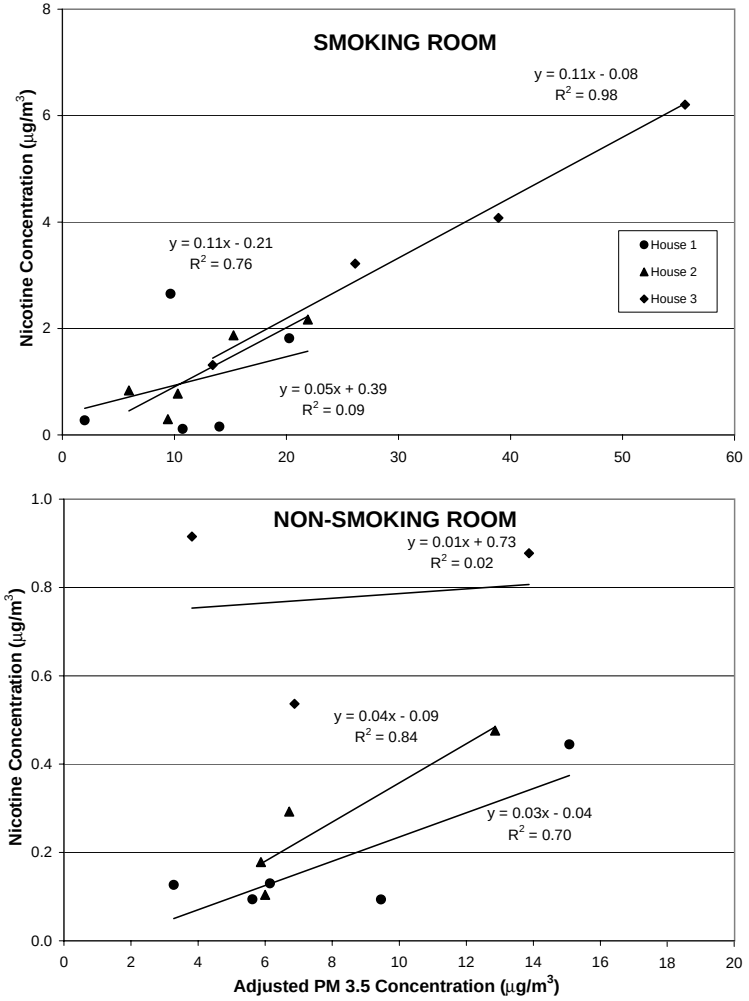

Figure 4. Indoor nicotine concentrations vs. ambient-adjusted FPM in smoking and non-smoking rooms of pilot study residences for all study weeks.

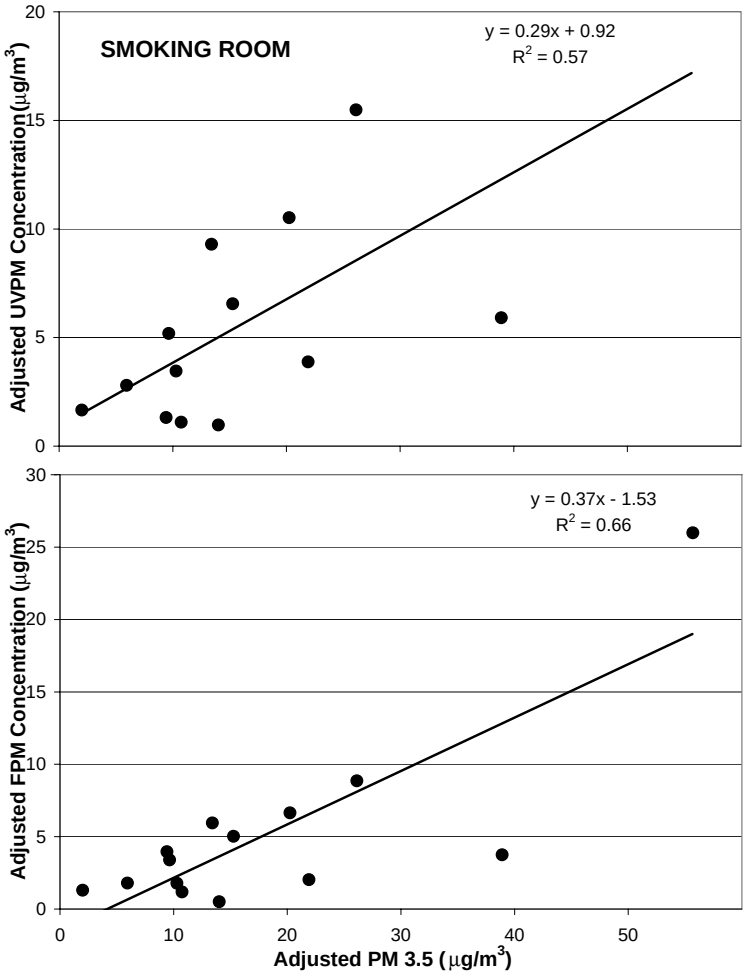

Figure 5. All Adjusted UVPM and FPM smoking room data vs PM 3.5. Concentrations are adjusted for penetration of ambient particle tracer concentrations. The indoor particle deposition rate (k) is assumed to be 0.8 h^{-1}. Week-average indoor ventilation rates were measured each week in each house. Regression lines and associated statistics indicate the least-squares best fit to the data.

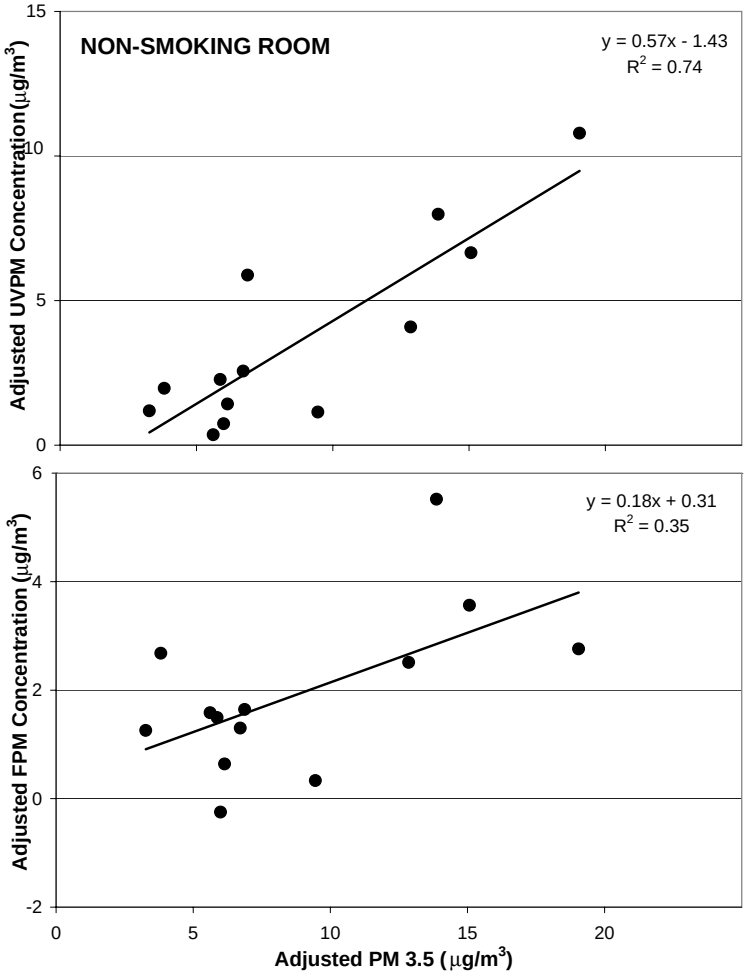

Figure 6. All Adjusted UVPM and FPM non-smoking room data vs PM 3.5. Concentrations are adjusted for penetration of ambient particle tracer concentrations. The indoor particle deposition rate (k) is assumed to be 0.8 h^{-1}. Week-average indoor ventilation rates were measured each week in each house. Regression lines and associated statistics indicate the least-squares best fit to the data.

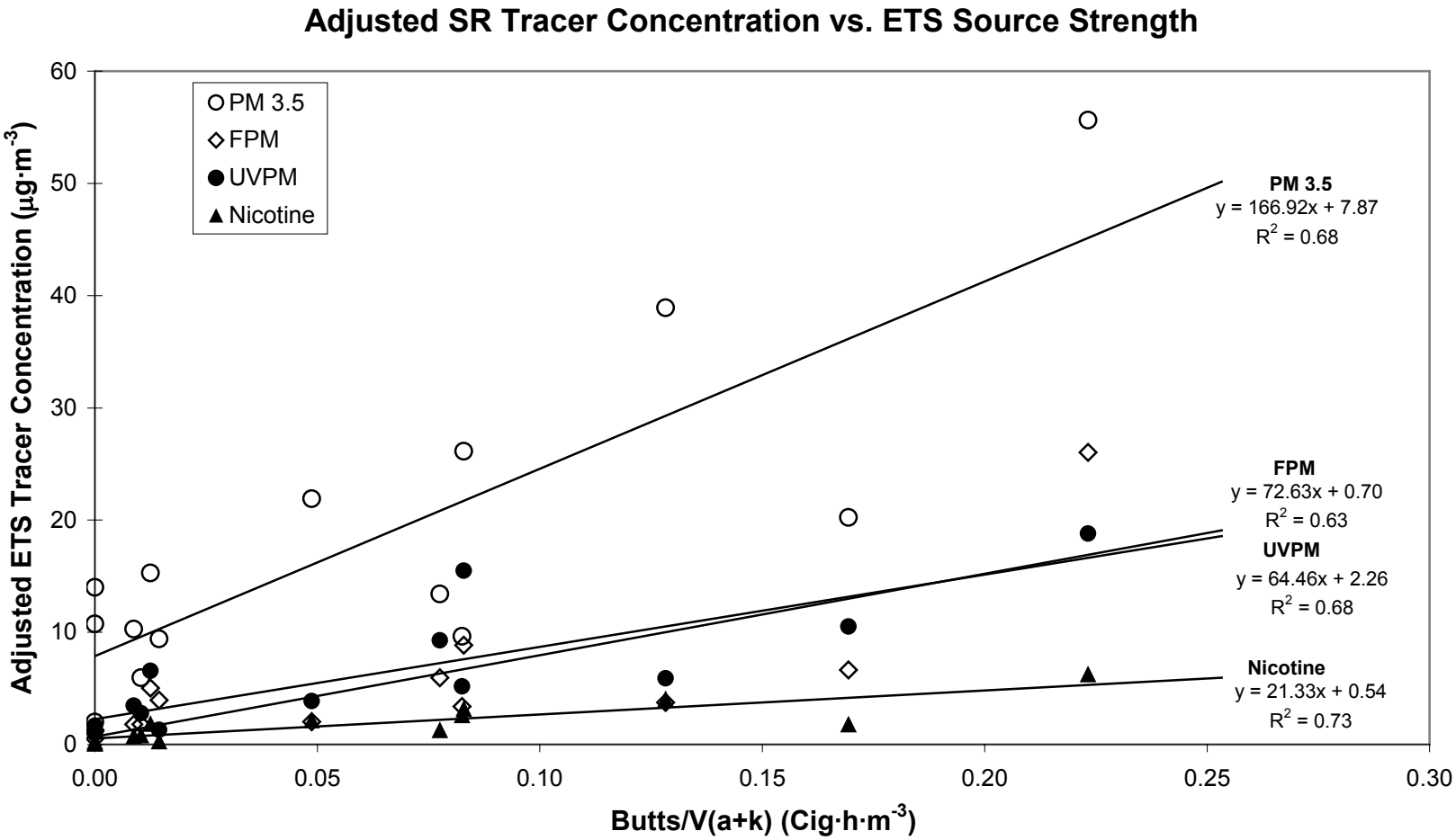

Figure 7. Indoor ETS tracer concentrations in the smoking room (SR) vs, butt-count based source strength for all three study homes. Indoor particle tracer concentrations are adjusted for penetration of ambient particle tracer concentrations. The indoor particle deposition rate (k) is assumed to be 0.8 h^{-1}. Week-average indoor ventilation rates were measured each week in each house. Regression lines and associated statistics indicate the least-squares best fit to the data.

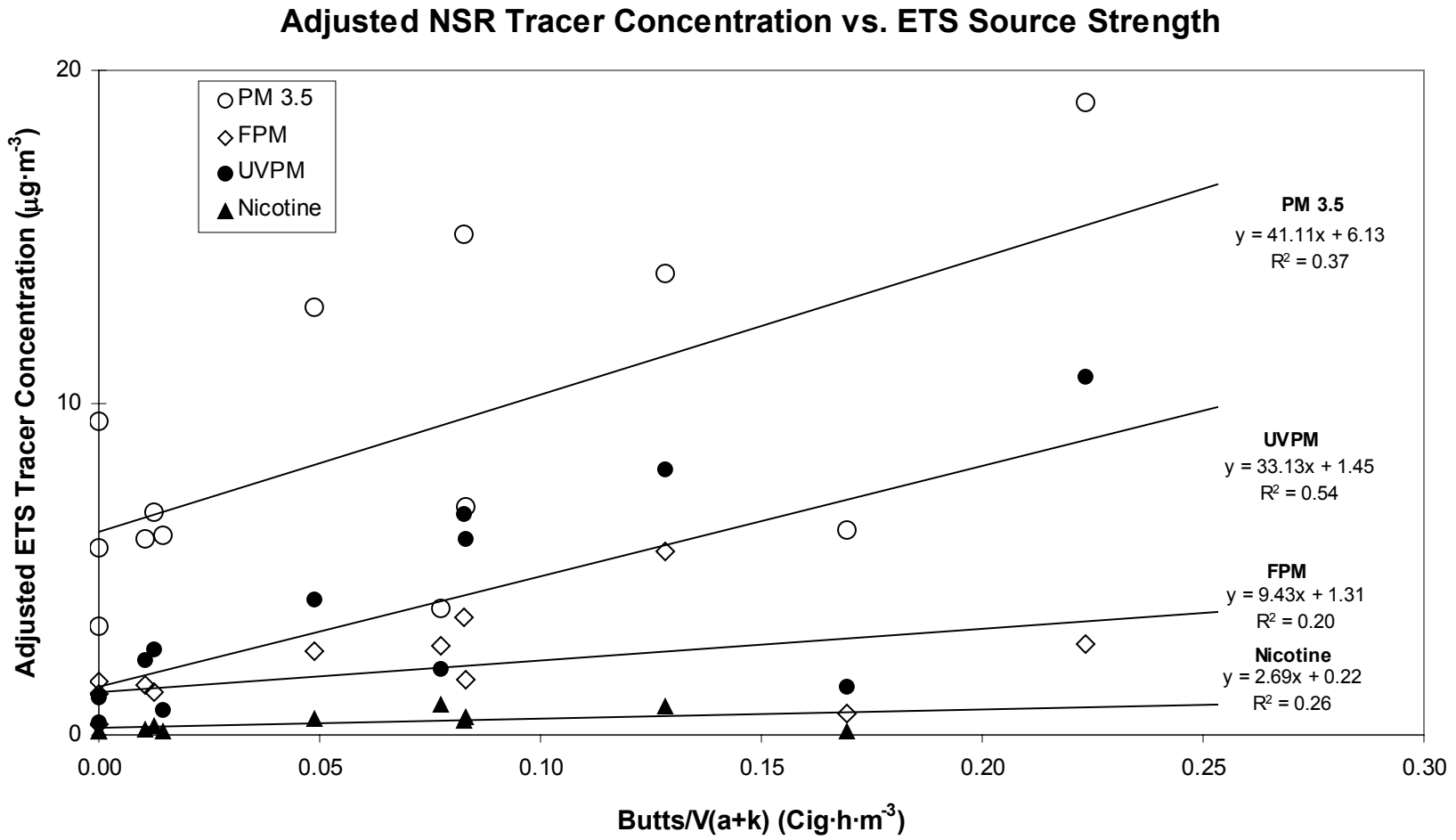

Figure 8. Indoor ETS tracer concentrations in the non-smoking room (NSR) vs, butt-count based source strength for all three study homes. Indoor particle tracer concentrations are adjusted for penetration of ambient particle tracer concentrations. The indoor particle deposition rate (k) is assumed to be 0.8 h^{-1}. Week-average indoor ventilation rates were measured each week in each house. Regression lines and associated statistics indicate the least-squares best fit to the data.